ELECTROCHEMISTRY AND ENZYMES
ON-LINE WITH MASS SPECTROMETRY

By

KEVIN JOHN VOLK

A DISSERTATION PRESENTED TO THE GRADUATE SCHOOL
OF THE UNIVERSITY OF FLORIDA
IN PARTIAL FULFILLMENT OF THE REQUIREMENTS FOR THE
DEGREE OF DOCTOR OF PHILOSOPHY

UNIVERSITY OF FLORIDA

1989

To my loving and devoted wife, Linda.

ACKNOWLEDGEMENTS

I wish to express my sincere gratitude to Dr. Richard A. Yost and Dr. Anna Brajter-Toth for their guidance, friendship, and direction during the completion of this work. The success of this work was dependent on their willingness to work together on a joint project. The past four years were made more enjoyable by their presence. I would also like to acknowledge and thank the members of my graduate committee, Dr. James Winefordner, Dr. James Deyrup, and Dr. Raymond Bergeron.

I would also like to acknowledge the U. S. Army Chemical Research, Development, and Engineering Center and National Institutes of Health for their financial support of this work.

I thank my fellow group members, especially Mike Lee for his assistance with the TQS45, Todd Gillespie, Dave Berberich, Jodie Johnson, Jody Freeman, and Mark Hail.

Sincere thanks go to my parents for their continued support, both emotional and financial. Thanks go to my mother who taught me "how to smell the roses" during the busy times of my life. I would also like to thank my brother, Brian, and brother-in-law, Bill Sagues, for the many weekend fishing adventures. Without such trips, I would have surely lost my perspective.

Finally, I would like to thank my wife, Linda, who was always there to provide support and encouragement with a warm heart and a warm meal. I cannot fully express the gratitude that I feel for Linda. She was

always there when I needed her most. As a result of our shared experiences (both good and bad) during the past fours years, I feel a bond has been forged that will never break.

TABLE OF CONTENTS

page

ACKNOWLEDGEMENTS iii

ABSTRACT vii

CHAPTERS

1 INTRODUCTION 1

Previous Studies Combining Electrochemistry or Enzymes On-Line With Mass Spectrometry 2
  Electrochemistry 2
  Enzymes 5
Thermospray Ionization 6
Electrochemical Investigations of Small Biological Molecules 11
Overview of Thesis 23

2 CHARACTERIZATION OF ON-LINE ELECTROCHEMISTRY/THERMOSPRAY/TANDEM MASS SPECTROMETRY FOR STUDYING REDOX REACTIONS 24

Introduction 24
Experimental 25
  Samples and Reagents 25
  Mass Spectrometry 26
  Electrochemical 27
Uric Acid as a Model Compound 29
On-Line Electrochemistry/Thermospray Mass Spectra 34
Mass Spectrometric Hydrodynamic Voltammograms 49
Time Resolution of EC/TSP/MS 52
Identification of Electrochemically Generated Intermediates and Products by Tandem Mass Spectrometry 56
Conclusions 66

3 CHARACTERIZATION OF ELECTROCHEMICAL OXIDATION PATHWAYS VIA ON-LINE CHROMATOGRAPHIC SEPARATION 68

Introduction 68
Experimental 70
  Samples and Reagents 70
  Spectroelectrochemistry 70
  HPLC Procedures 71
  Mass Spectrometry 74
Detection by UV-Vis Spectrophotometry 77

6-Thiopurine 77
2-Thiopyrimidine 98
Detection by Thermospray/Mass Spectrometry 110
  6-Thiopurine 110
    Mass Spectrometric Hydrodynamic Voltammograms 123
  2-Thiopyrimidine 131
    Mass Spectrometric Hydrodynamic Voltammograms 139
Conclusions 142

4 CHARACTERIZATION OF SOLUTION-PHASE AND GAS-PHASE REACTIONS IN ON-LINE ELECTROCHEMISTRY/THERMOSPRAY/TANDEM MASS SPECTROMETRY 144

Introduction 144
Experimental 145
  Samples and Reagents 145
  Mass Spectrometry 145
Tip Temperature and Source Temperature Studies 148
  Oxidation of Uric Acid 148
  Oxidation of 6-Thiopurine 159
Mobile-Phase and Gas-Phase Studies 165
  Methylamine 165
  Ammonia 168
Conclusions 169

5 CHARACTERIZATION OF THERMOSPRAY/TANDEM MASS SPECTROMETRY FOR STUDYING ENZYMATIC OXIDATION PATHWAYS 171

Introduction 171
Experimental 172
  Samples and Reagents 172
  Enzyme Binding Procedure 172
  Mass Spectrometry 175
Uric Acid 176
Conclusions 188

6 CONCLUSIONS AND FUTURE WORK 190

LITERATURE CITED 195

BIOGRAPHICAL SKETCH 200

Abstract of Dissertation Presented to the Graduate School of the
University of Florida in Partial Fulfillment of the Requirements for
the Degree of Doctor of Philosophy

ELECTROCHEMISTRY AND ENZYMES ON-LINE WITH MASS SPECTROMETRY

by

Kevin John Volk

August 1989

Chairman: Richard A. Yost
Major Department: Chemistry

Interfacing an electrochemical cell on-line with tandem mass spectrometry (MS/MS) via a thermospray liquid/chromatography interface, demonstrated for the first time in this work, can provide important information about electrochemically generated species. This on-line technique offers the ability to directly monitor reactants, short-lived intermediates, and products of electrochemical reactions as a function of electrode potential. Because molecular weight information alone is not always convincing evidence for compound identification, MS/MS makes it possible to determine the structure of each of the mixture components, which produce only molecular ions in thermospray.

This thesis emphasizes the investigation of electrochemical and enzymatic redox reactions by the combination of electrochemistry and enzymes on-line with MS/MS. Uric acid served as a model compound and was used to demonstrate the feasibility and capabilities of these techniques. The use of high performance liquid chromatography to separate electrochemical oxidation products prior to detection by mass spectrometry and by UV-Vis absorption spectrophotometry has also been demonstrated. It was shown that unique insights into reaction pathways of thiols could be obtained as a function of electrode potential. In addition, it was determined that nucleophilic reactions of reactive species (e.g. intermediates and unstable compounds) in the thermospray process occur in the solution phase in the heated capillary, not in the gas phase in the ion source.

The utility of combining enzymes on-line with mass spectrometry was also demonstrated. Products and intermediates formed as a result of an enzymatic-catalyzed reaction were monitored on-line with mass spectrometry. The enzymatic and electrochemical oxidation pathways of uric acid determined on-line with thermospray/mass spectrometry were compared. In the enzymatic oxidation of uric acid with peroxidase and H_2O_2, the same intermediates and products were observed as in the electrochemical oxidation.

CHAPTER 1
INTRODUCTION

In this dissertation the concepts of combining an electrochemical cell or an enzyme reactor on-line with tandem mass spectrometry (MS/MS) via a thermospray liquid chromatography/mass spectrometry (LC/MS) interface are described. This combination allows the electrochemical and enzymatic oxidation pathways of polar compounds not normally amenable to mass spectrometry to be determined. The inherent speed and selectivity of this on-line technique permits electrochemically generated species to be monitored as a function of electrode potential. A comparison of the electrochemical results with off-line cyclic voltammetry is also presented. The use of high performance liquid chromatography (HPLC) to separate electrochemically generated species prior to mass analysis will be discussed. Finally, results obtained when an enzymatically catalyzed reaction is monitored on-line with mass spectrometry will be presented and compared to the electrochemical results.

This introductory chapter describes previous studies which have combined electrochemistry or enzymes on-line with mass spectrometry. In addition to providing background on the thermospray ionization process, information on previous off-line electrochemical and enzymatic investigations of purines and purine drugs are discussed, followed by an overview of the thesis organization.

Previous Studies Combining Electrochemistry or Enzymes On-Line With Mass Spectrometry

Electrochemistry

Determining the origin of products isolated after bulk electrolysis is often a difficult and complicated process due to chemical reactions which may occur between electrochemical intermediates and other species in solution. To minimize these problems, it is preferable to identify the electrochemically generated species as soon as possible after their production at the electrode surface. Bruckenstein was the first to combine electrochemistry on-line with mass spectrometry (1). A porous membrane made of Teflon acted as the inlet by allowing volatile components to pass through it while acting as a barrier to the liquid phase. Since small molecules such as CO_2 and methane permeate the Teflon membrane more readily than larger molecules such as the solvent or larger organics, enrichment of lower molecular weight components was achieved. In this work, mass spectrometry was used to monitor the electrochemical generation of oxygen from 0.1 M $HClO_4$ (1). These experiments indicated that 36% of the electrochemically generated oxygen enters the vacuum system of the mass spectrometer. In later work, Bruckenstein and co-workers monitored the formation of methanol during the oxidation of methoxyphenols (2), ammonia production via electrochemical reduction of nitrate (3), and the electrochemical generation of CO_2 from the oxidation of adsorbed CO at a platinum electrode (4). Bolzan and co-workers used a similar system for studying the electrochemical oxidation of glucose, with production of CO_2 monitored during a potential scan (5).

Anderson and co-workers used a similar approach to study the reduction of dibromocylcohexane to cyclohexane (6). In this work, the Teflon membrane was replaced by a semipermeable silicon membrane. Since silicone membranes have been applied to separating permeable organics from the impermeable carrier gas in gas chromatography/mass spectrometry (GC/MS) (7), it was assumed that the electroactive reactants and products would be partitioned into and diffuse through the membrane and be detected by mass spectrometry (6). However, due to the selective nature of the silicone membranes, only certain reactants and products permeated through the membrane (6,8). Since the analysis of only the volatile components of electrochemical reactions severely limits the number of systems that can be studied, these methods have not been actively pursued.

It was not until the invention of thermospray by Vestal (9) that mass spectrometry could be routinely used for the analysis of polar and involatile compounds such as electrochemical oxidation products in solution. Hambitzer and Heitbaum (10) were the first to successfully combine electrochemistry on-line with mass spectrometry via a thermospray LC/MS interface. These experiments demonstrated the potential for direct detection of electrochemically generated products by monitoring the formation of dimers and trimers upon the electrooxidation of N,N dimethylaniline at a Pt electrode. The system developed by Heitbaum had several limitations such as a large ohmic drop and dead time of ca. 10 s between generation in the electrochemical cell and detection by mass spectrometry.

Electrochemistry has recently been used on-line with mass spectrometry for enhancing the thermospray mass spectra of difficult to ionize compounds (11). In this work, an electrochemical cell was used to chemically transform a compound via oxidation to a species which was more amenable to analysis by thermospray.

We have recently demonstrated (12) the utility of on-line electrochemistry/thermospray/tandem mass spectrometry (EC/TSP/MS/MS) for elucidating redox reactions of biologically important compounds. This was the first instance of using EC/TSP/MS/MS for biooxidation studies. In this work, tandem mass spectrometry played an important role in determining the structures of electrochemically generated intermediates and products.

Getek and Korfmacher have used a similar approach to study acetaminophen conjugate formation upon electrooxidation (13). In this study, the reaction of acetaminophen after electrochemical oxidation with glutathione was monitored by TSP/MS. Mixing of glutathione with electrolyzed acetaminophen resulted in the formation of the acetaminophen glutathione conjugate on the time scale of one second.

Bartmess (14) has recently introduced electrochemically assisted fast atom bombardment (FAB) in an attempt to overcome the compound-dependent nature of static FAB. This process makes the analyte more amenable to FAB by ionizing the sample on the probe tip via electrolysis. However, in the present two-electrode configuration, there is very little control of the working electrode potential. Since very large potentials (±15 V) are applied, virtually all analytes will undergo electron transfer, making it difficult to interpret the results of the electrochemical process.

Enzymes

On-line mass spectrometric procedures using columns containing immobilized enzymes coupled via thermospray to a mass spectrometer have been recently described (15-17). The combination of thermospray HPLC/MS and immobilized enzyme hydrolysis can be very useful in peptide identification and sequencing. In this work, Vestal and coworkers have used immobilized enzyme columns containing carboxypeptidase Y and trypsin for on-line peptide sequencing. This system used a combination of immobilized enzymes, liquid chromatographic columns, and a thermospray mass spectrometer (15,16). A column containing immobilized trypsin was used to cleave the peptide being analyzed into primary fragments. Next, an HPLC column separated these primary fragments. A second enzyme column containing immobilized carboxypeptidase Y then digested each fragment as it emerged from the HPLC column. Finally, thermospray mass spectrometry was used to identify the fragment molecules (15,16). Voyksner (17) has also used a series of enzyme columns on-line with HPLC/MS to identify and determine the amino acid sequence of endorphins.

The development of fast atom bombardment (FAB) by Barber (18) as a method for the analysis of ionic and non-volatile compounds has led to a variety of applications in the biological sciences. For example, Caprioli has shown that the liquid matrix used in FAB can be used to maintain enzymatic activity in order to follow the course of a reaction (19). In this work, Caprioli demonstrated that for a number of proteases, hydrolysis reactions could be followed in real time with a single sample inside the mass spectrometer. In addition the enzymatic hydrolysis reaction rates could also be measured in real time by monitoring the reaction as it proceeded on the FAB probe tip inside the mass spectrometer.

However, peptide sequencing by enzymes/FAB did not gain tremendous popularity until the development of a continuous-flow (CF) FAB probe by Caprioli (20). Since this discovery, CFFAB has been used for the analysis of peptide mixtures which were obtained from enzymatic digests of proteins (20-22). Microbore gradient techniques are often used with CFFAB since it provides separation of individual components of a mixture and as a result, minimizes ion suppression effects (23). Unfortunately, this is time-consuming with separations ranging from 20-40 min for a typical gradient separation (23).

Thermospray Ionization

Due to the basic incompatibilities of liquid chromatography and mass spectrometry, the development of a practical LC/MS interface has been difficult to achieve. Only recently did Blakely and Vestal (9,24-26) progress from their early attempts to rapidly volatilize LC eluent with lasers to simple direct resistive heating of a metal capillary. Figure 1.1 illustrates a diagram of a commercially available thermospray source. In order to accommodate the high flow rates (1-2.0 mL/min) used in high performance liquid chromatography (HPLC), a 300 L/min mechanical vacuum pump together with a liquid nitrogen cold trap is directly coupled to the ion source and provides additional pumping to remove the excess vapor delivered to the source. In addition to providing extra pumping speed, the cold trap prevents the contamination of the mechanical pump oil by serving as an efficient method of trapping the mobile phase solvents.

The primary functions of the thermospray ion source shown in Figure 1.1 are to provide additional heat downstream from the thermospray probe tip and to serve as a pressure reduction stage. The source is heated to continue droplet evaporation which was initiated in the thermospray probe and to prevent condensation. Since operating pressures in the source are typically in the range of 10 to 20 Torr (25), a sampling cone with a 500μm aperture reduces the gas load entering the mass analyzer region of the instrument.

When this vaporization process occurs in the vacuum of a mass spectrometer, a supersonic jet of vapor is created which consists of a mist of fine particles and solvent droplets. In their early pioneering work, Blakely and Vestal discovered that ionization can occur without the use of an external source of electrons (filament) if the mobile phase contains a volatile electrolyte such as ammonium acetate.

Although the fundamental processes of thermospray ionization are not completely understood, at least two different mechanisms, direct ion evaporation of preformed ions from the droplets and chemical ionization of neutral sample molecules by the ammonium acetate buffer, may be responsible for ion formation (27-29). Direct ion evaporation may occur for any molecule which is ionized in aqueous solution. However, the conditions required to produce ions by direct ion evaporation may be different than those conditions which favor chemical ionization (CI). Because gas-phase ion/molecule reactions such as CI have been shown to influence the thermospray process (30-33), the production of sample ions

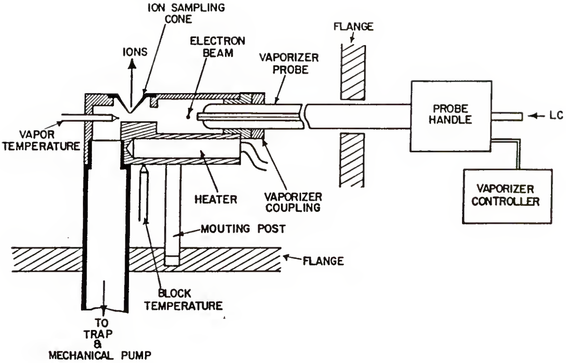

Figure 1.1. Schematic diagram of the thermospray LC/MS interface (24).

will depend on experimental parameters which affect the vaporization process. These parameters include capillary diameter, tip temperature, and flow rates. The CI process will additionally be affected by gas-phase proton affinities, concentrations of various reagent ions, temperatures, and ion/molecule kinetics. Stainless steel capillaries with diameters of 150μm are typically used as vaporizer probes.

Recently, Vestal and co-workers have demonstrated that ion evaporation processes are affected by the size of the exit aperture of the thermospray vaporizer probe (34). In this work, replaceable vaporizer tips with 100 micron and 50μm tip sizes were used. Restriction of the vaporizer tip decreases droplet size and results in increased analyte evaporation and consequently an increase in the mass spectrometric signal (34). The thermospray interface which was used in these studies was an early model and used standard vaporizer probes with 150μm stainless steel capillaries.

In the thermospray process, CI can produce sample ions via gas-phase reactions with reagent ions produced from the ammonium acetate buffer (without filament) if the conditions are favorable for gas-phase proton transfer. This process is illustrated in Figure 1.2. Hence, if ammonium acetate buffer is used, any compound (uncharged in solution) with a proton affinity less than that of NH_3 will not be observed as a protonated molecular ion $(M+H)^+$; in negative ion thermospray, any compound with higher gas-phase proton affinities than that of the acetate ion will not form an $(M-H)^-$ ion. In addition, hydrogen-bonded adduct or cluster ions such as $[M+NH_4]^+$ and $[M+CH_3COO]^-$ can also form and provide useful molecular weight information. Indeed, the addition of chloroacetonitrile promotes the production of $[M+Cl]^-$ ions and has been shown to improve the detection

Reagent Ion Formation

$$NH_4^+CH_3COO^- \longrightarrow NH_4^+ + CH_3COO^-$$

Chemical Ionization Reactions

$$M + NH_4^+ \longrightarrow (M+H)^+ + NH_3$$

$$M + NH_4^+ \longrightarrow (M+NH_4)^+$$

$$M + CH_3COO^- \longrightarrow (M-H)^- + CH_3COOH$$

$$M + CH_3COO^- \longrightarrow (M+CH_3COO)^-$$

Figure 1.2. Formation of chemical ionization reagent ions from the ammonium acetate buffer. Gas-phase ion molecule reactions with reagent ions produce analyte ions.

limits for many compounds which do not otherwise efficiently produce negative ions during by thermospray (35).

Many thermospray interfaces are also equipped with an external filament and discharge electrode which can used to enhance ionization when buffer ionization is ineffective (36). Due to the presence of large amounts of water vapor in the source, filament ionization requires a rugged emitter. Thoriated iridium filaments are commonly used in order to achieve long operating lifetimes. In addition, at least 600-800V electron energy is required to obtain effective penetration of the electrons into the high pressure source (36). When the filament is used, electron ionization of the solvent produces reagent ions which can result in CI of the sample molecules. Finally, application of a high voltage to an electrode placed into the source results in a stable discharge due to the high operating source pressures, producing reagent ions for CI.

Electrochemical Investigations of Small Biological Molecules

During the past fifteen years, the redox chemistry of many natural and synthetic compounds including purines has been investigated using electrochemical methods, frequently in combination with other analytical techniques (37-48). The premise of this work has been that the mechanisms observed electrochemically can provide insight into the biological redox reactions of these molecules and is based on the fact that both electrochemical and biological redox (oxidation or reduction) reactions involve heterogeneous electron-transfer processes (37). As is evidenced by the work of Adams and his co-workers on the electrochemistry of catecholamine neurotransmitters (49,50) and of McCreery and co-workers on the electrochemical oxidation of phenothiazine tranquilizer drugs (51-54), electrochemical methods are well suited to provide insight into redox and related chemical reactivity of compounds of biological interest.

The studies by Adams have provided some insights into the ways in which catecholamines and the intermediates formed upon electrooxidation might be involved in certain types of neurochemical behavior. The work of McCreery and co-workers indicated that the decay rate of phenothiazine radical cations formed upon electrooxidation was dependent on the structure of the radical (51). Since the radical cation has been proposed as an intermediate in phenothiazine metabolism, these results give definite insights into the mechanism and structural factors which might influence metabolite formation from the radical (51-54).

In electrochemical studies of biological molecules, an electrode is poised at a suitable potential and is used to simulate the redox enzyme. Obviously, the unique selectivity associated with enzymes cannot be precisely duplicated using this method. However, in analogy to the active site of an enzyme, the substrate molecule must be properly orientated before an electron transfer reaction can occur at the electrode surface. As a result, the electrode material and its surface characteristics can play an important role in this process. Carbon electrodes are commonly used in the electrochemical investigations of biological oxidations because of the large potential range (+1.2 to -1.7 V versus SCE) and low background in aqueous solutions (55-57).

Because of their importance in biological systems, the electrochemistry of a large number of purine derivatives has been intensively investigated using off-line methods (37-48). As can be seen in Figure 1.3, purine

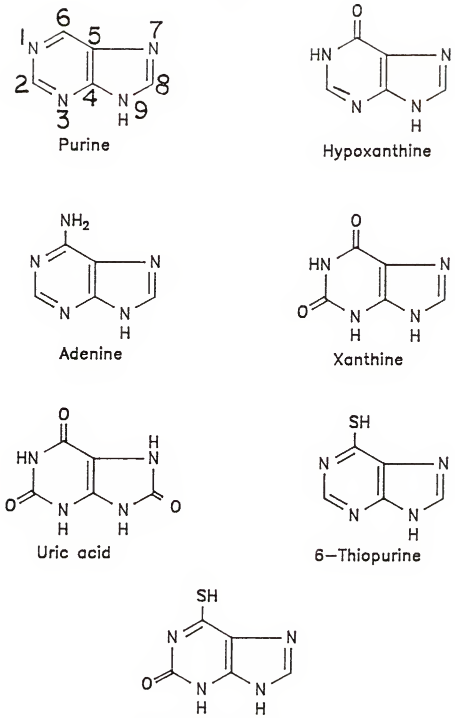

Purine

Hypoxanthine

Adenine

Xanthine

Uric acid

6–Thiopurine

6–Thioxanthine

Figure 1.3. Structure of Purines.

itself consists of fused pyrimidine and imidazole rings. Included in Figure 1.3 are the structures of other important purines such as hypoxanthine, xanthine, uric acid, 6-thiopurine, 6-thioxanthine, and adenine and the Beilstein numbering convention for purines (58). Adenine is the most abundant purine found in ribonucleic acid (RNA) and deoxyribonucleic (DNA) (58). In higher animals, nucleotides undergo enzymatic hydrolysis to yield free purine and pyrimidine bases (58). If these bases are not salvaged and reused, they are enzymatically degraded and the end products excreted (58). In man, an enzyme called xanthine oxidase is involved in the degradation of purines to the end product, uric acid (58). This process has been extensively studied in man and other animals (58,59).

Both the electrochemical and enzymatic oxidation pathways of uric acid have been extensively studied (37,46). Dryhurst and co-workers have found that at pH 7.0 uric acid (37,40,46,47) undergoes a $2e^-,2H^+$ electrochemical oxidation at ca. +0.40 V vs SCE to form an unstable intermediate with a proposed quinonoid diimine structure (Figure 1.4). Evidence supporting the diimine structure includes its reduction peak in cyclic voltammetry (40,60), intermediates detected by thin-layer spectroelectrochemistry (47), and the identification of its partial hydration product, the imine alcohol by GC/MS (47). Kinetic studies indicate that the imine alcohol has a half-life of ca. 2 minutes in solution at room temperature (47). Trapping of the imine alcohol intermediate (47) was accomplished by carrying out a spectroelectrochemical experiment to the point where the UV-absorbing intermediate reached a maximum concentration. The solution in the thin-layer cell was then collected by rapidly ejecting the contents

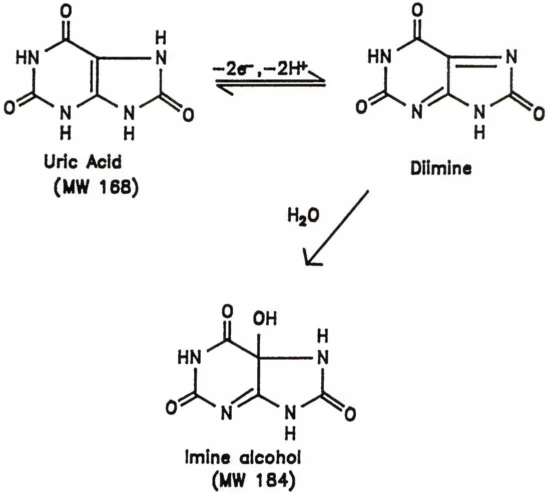

Figure 1.4. Formation of the primary oxidation intermediate of uric acid, which further reacts by nucleophilic addition of water to form an imine alcohol.

into a vial maintained at -78 C. These low temperatures presumably slow further hydration reactions (47). The frozen mixture was then lyophilized and derivatized prior to analysis by gas chromatography/mass spectrometry (GC/MS) (47). The resulting mass spectral information indicated that the isolated compound had a molecular weight of 184. The molecular weight and number of silyatable sites was in exact agreement with the proposed structure of the imine alcohol intermediate (Figure 1.4). This trapping procedure was indeed novel and proved successful. However, the conditions and the time required for derivatization severely limit the use of GC/MS for the identification of electrochemically generated intermediates. In other words, only electrochemically generated compounds of sufficient stability can be analyzed by GC/MS (46,47).

The mechanism proposed by Goyal and co-workers (40) for the electrochemical oxidation of uric acid can be seen in Figure 1.5. Between pH 3 and 5.6, the final products of uric acid oxidation were determined to be allantoin, urea, 5-hydroxyhydantoin-5-carboxamide, and alloxan (46). Much of the pathway shown in Figure 1.5 has been derived via rationalization of end reaction products. Accordingly, presence of alloxan and 5-hydroxyhydantoin-5-carboxamide indicated that the imine alcohol intermediate can decay by two different mechanisms. Goyal (40) has proposed that the main mechanism for the decomposition of the imine alcohol intermediate involves contraction of the imidazole ring followed by hydration and decarboxylation resulting in the formation of allantoin (Figure 1.5). However, the imine alcohol can decay via a second mechanism which involves further hydration of the imine alcohol to form a diol (Figure 1.5). The diol is too unstable and has never been detected (46).

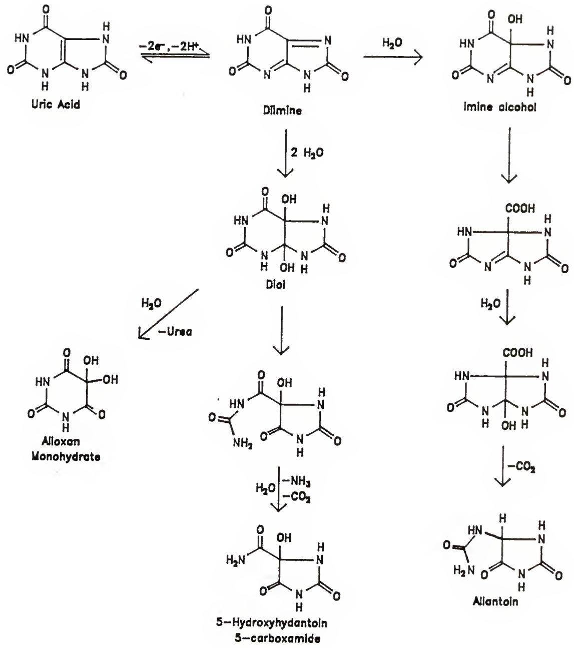

Figure 1.5. Electrochemical oxidation pathway of uric acid proposed by Goyal and co-workers (46).

Hydrolysis of the diol followed by opening of the pyrimidine ring produces alloxan and urea (Figure 1.5). 5-Hydroxyhydantoin-5-carboxamide (Figure 1.5) is produced when the imidazole ring opens during decomposition of the diol.

The pathway shown in Figure 1.5 is based on the information obtained from a variety of analytical techniques such as cyclic voltammetry, double-potential-step chronoamperometry, spectroelectrochemistry, and GC/MS (46). Although tremendous amounts of important information were obtained in these studies, a combination of these techniques was required because each technique provided only limited information. Hence, any instrumental method which can provide more selectivity or sensitivity during electrochemical studies can make an important contribution. The oxidation pathway of uric acid determined by on-line electrochemistry/ thermospray/tandem mass spectrometry (EC/TSP/MS/MS) will be discussed in Chapter 2.

Although uric acid is the final product of purine metabolism in man, in many other organisms further degradation of the purine molecule can occur. For example, in certain mammals, reptiles, and mollusks, the end product is allantoin (58). Uricase, one of the important enzyme systems involved in uric acid oxidation, catalyzes the transfer of two electrons from uric acid to oxygen resulting in the formation of allantoin (61).

Unlike uricase, various peroxidases and H_2O_2 can oxidize uric acid as well as its N-methyl derivatives. Peroxidases are relatively rare in the animal world, but are more common in plants (46). The enzymatic oxidation of uric acid and its N-methyl derivatives has been extensively studied by Dryhurst and co-workers (46) using horseradish peroxidase/H_2O_2. The results of the enzymatic studies have been compared to the electrochemical oxidation (46,62). In these studies it was found that the spectral properties of intermediates generated electrochemically and enzymatically were the same; the final products in both reactions were also identical. In addition, kinetic studies indicated that the electrochemical and enzymatic intermediates monitored by UV-Vis have almost the same rate constants. Hence the data obtained during the enzymatic studies was virtually indistinguishable from the electrochemical data. Since the same intermediate (imine alcohol) and final product (allantoin) are generated electrochemically during the oxidation of uric acid as during the enzymatically catalyzed reaction with horseradish peroxidase, this evidence supports the conclusion that the electrochemical and enzymatic reactions proceed, in a chemical sense, by an identical mechanism (46).

Because electrochemical methods provide a much greater degree of control of the redox process via control of electrode potential, modern electroanalytical techniques are able to provide valuable probes into both electrochemical and enzymatic processes. The enzymatic oxidation pathway of uric acid determined on-line with TSP/MS via an enzyme reactor will be discussed in Chapter 5.

The electrochemical oxidations of a large number of purines besides uric acid have been studied with off-line electrochemical methods. These include adenine (63), guanine (64), 6-thiopurine (65), xanthine (60), 1,3 dimethylxanthine (60,66), 2,6 dithiopurine (36), hypoxanthine (67), 6-thioxanthine (38), and caffeine (68). In many of these studies, both the electrochemical and enzymatic oxidations were carried out. In general, there was a correlation between the products observed electrochemically and enzymatically. Dryhurst and co-workers have made a number of general conclusions about the ease of oxidation of purines (37):

1. The more highly oxygenated the purine ring, the more easily oxidized the purine. Purine itself is not oxidizable.
2. In all cases examined, the initial oxidation process of purines proceeds at any unoxidized and unsubstituted N=C bond. When all unblocked N=C bonds are oxidized, the C-4=C-5 bond is oxidized.
3. Oxidation of the C-4=C-5 bond results in the formation of some type of unstable diimine which can sometimes be detected via the reduction step during cyclic voltammetry.
4. Hydration reactions of the diimine appear to lead to the production of the final products.
5. Many purines are adsorbed at carbon electrodes.

The generalizations made by Dryhurst and co-workers appear to apply to all purine derivatives except those containing an exocyclic sulfur atom (37).

Several purine derivatives such as 6-thiopurine and caffeine are known to undergo oxidation in vivo (69). It appears likely that xanthine oxidase which normally interacts with hypoxanthine and xanthine participates in these reactions (69). Other structurally similar purines such as 6-thioxanthine are known substrates of xanthine oxidase and 6-thiouric acid is a product of the enzymatic oxidation (70).

The degradation pathways of thiopurines are of intense interest because of their use as antineoplastic agents. Antineoplastic agents are used for suppressing the growth and spread of malignant cells by interfering with DNA and RNA synthesis in proliferating cells. The most important purine antagonist, 6-thiopurine, acts by several mechanisms (71). First it is converted to the active form of the drug, the ribonucleotide. In this form, it competes with enzymes that convert hypoxanthine ribonucleotide to adenine and xanthine ribonucleotides (71). It is metabolized to 6-thioxanthine nucleotide, 6-thioguanine nucleotide, and 6-thiouric acid (71). Incorporation of thiopurines into DNA as fraudulent bases may lead to DNA strand breaks and mutations (72,73). In addition, 6-thiopurine can be converted to 6-methyl thiopurine and its ribonucleotide (71). These metabolites tie up the enzyme that synthesizes phosphoribosylamine which is required for RNA and DNA synthesis (71).

Since 6-thiopurine is also a potent immunosuppressive agent, it is used extensively in the prevention of organ rejection (72). However, its use has been restricted in some patients because of hepatotoxicity associated with the drug (72). The mechanism by which 6-thiopurine changes immune responses is still largely unknown (73). It has been suggested that metabolic activation of 6-thiopurine by the liver results in the formation of highly reactive metabolites which may explain the hepatotoxic effects associated with the drug (72,73). Hyslop and Jardine have recently studied the irreversible binding of a metabolite of 6-thiopurine to mammalian hepatic protein (72,73). In this work, they describe a previously unknown oxidation pathway of 6-thiopurine which involves activation by cytochrome P-450 to produce a highly reactive intermediate, proposed to be purine-6-sulfenic acid. Subsequent binding of purine-6-sulfenic acid to protein thiols would result in mixed disulfide bonds and liver impairment (74).

In order to further study the metabolic activation of 6-thiopurine, Jardine and co-workers synthesized purine-6-sulfenic acid via chemical oxidation of the parent thiol (74). After determining the pH stability and half-life of this compound, radiolabeled purine-6-sulfenic acid was used to demonstrate that this species directly binds with hepatic microsomal protein (74). Hence, these results suggest that purine-6-sulfenic acid may be the highly reactive metabolite responsible for both the immunosuppressive activity as well as hepatic necrosis (74).

Dryhurst has characterized the electrochemical oxidation pathway of 6-thiopurine with cyclic voltammetry, polarography, and coulometry (65). Photo-oxidation studies of 6-thiopurine have also been performed (75). Irradiation of 6-thiopurine with near-UV light produces purine-6-sulfinic acid as the primary product (75). In the electrochemical work, it was found that the oxidation of 6-thiopurine appears to follow a pathway quite different from the major enzymatic oxidative route (65). In other words, electrochemical oxidation of 6-thiopurine does not produce 6-thioxanthine or 6-thiouric acid.

At low potentials, the electrochemical oxidation of thiols usually leads to the corresponding disulfide (76). This has been shown for 6-thiopurine and structurally similar 6-thioxanthine (38,65). The first step in disulfide formation proceeds by a one-electron transfer mechanism, most probably via thiyl radicals (76). It has been shown that at high potentials, the purine ring of 6-thioxanthine undergoes oxidation resulting in the formation of allantoin (38). However, since 6-thiopurine does not contain any electronegative oxygen substituents, the purine ring is not vulnerable to oxidation. As a result, at high potentials, the thiol group may be further oxidized to oxygen containing compounds such as sulfinic or sulfonic acids (65,76). Dryhurst (65) determined that bulk electrolysis of 6-thiopurine produces bis(6-purinyl) disulfide, purine-6-sulfinic acid, and small amounts of purine-6-sulfonic acid. New insights into the electrochemical oxidation of 6-thiopurine provided by on-line EC/TSP/MS will be discussed in Chapter 3.

Overview of Thesis

This thesis represents studies to characterize the use of on-line electrochemistry/thermospray/tandem mass spectrometry for studying redox reactions. The following chapters provide a detailed description of the electrochemical and enzymatic results obtained during these studies. Chapter 2 will describe the electrochemical and mass spectrometric instrumentation that was used in these studies. In order to characterize our on-line system, uric acid was chosen as a model compound. The results obtained for the on-line electrochemical oxidation of uric acid will also be discussed in Chapter 2. The electrochemical oxidation pathways of thiols determined by using HPLC prior to UV-Vis and mass spectrometric analysis will be discussed in Chapter 3. A systematic study to characterize the decomposition reactions of electrochemically generated intermediates and products during the thermospray process will be discussed in Chapter 4. The ability of thermospray/tandem mass spectrometry to characterize enzymatic oxidation pathways will be discussed in Chapter 5. The last chapter of this thesis (Chapter 6) contains conclusions and suggestions for future studies which combine electrochemistry on-line with mass spectrometry.

CHAPTER 2
CHARACTERIZATION OF ON-LINE ELECTROCHEMISTRY/THERMOSPRAY/TANDEM MASS SPECTROMETRY FOR STUDYING REDOX REACTIONS

Introduction

When electrochemical methods are used in combination with mass spectrometry (1-6,8,10-13,38,40,41), high performance liquid chromatography (42,43), or molecular spectroscopy (37,38,46,48), important information about the structure of electrochemical intermediates, products, and the chemical reactions which may occur following electrooxidation can be obtained. Electrochemistry on-line with mass spectrometry has provided a powerful tool which allows fast identification of electrochemically generated species as a function of electrode potential where hydrodynamic EC/MS results can be obtained and compared with off-line cyclic voltammetry (1-6,8,10-13). While chemical information, in addition to that obtained by electrochemistry, may be obtained by other spectroscopic techniques such as on-line UV-Vis absorption spectrophotometry (spectroelectrochemistry) (37,46,48), the inherent selectivity and sensitivity of mass spectrometry allows the monitoring and identification of individual species.

Since the introduction of thermospray as a viable LC/MS interface (9,24-26), this technique has gained popularity as a soft ionization technique that gives primarily molecular weight information. Interfacing an electrochemical cell with mass spectrometry via a thermospray LC/MS interface generally provides only molecular weight information about electrochemically generated species (10-13). Because molecular weight information alone is not always convincing evidence for compound identification, the use of a mass spectrometer specifically designed to perform MS/MS experiments can provide important structural evidence (12). In addition, the use of tandem mass spectrometry allows identification of intermediates and products in a mixture based on their characteristic daughter spectra, a feature important to the identification of structurally related metabolites (77,78). As will be demonstrated in this chapter, the ability to obtain structural information on each component in an electrolysis mixture without chromatographic separation is a unique feature of EC/TSP/MS/MS. This chapter describes the studies which were carried out to determine the capabilities of EC/TSP/MS/MS for on-line characterization of redox reactions.

Experimental

Samples and Reagents

Uric acid, 9-methyl uric acid, allantoin, alloxan monohydrate, urea, and parabanic acid were obtained from Sigma (St. Louis, MO). All reagents were analytical grade. Analytical grade ammonium acetate was obtained from Mallinckrodt (St. Louis MO). The compounds were dissolved in, and then injected into, a mobile phase which consisted of 0.1 M ammonium acetate (pH ~ 7). Twenty-five microliters of a 100 ppm solution were typically injected.

Mass Spectrometry

A Finnigan triple stage quadrupole (TSQ45) mass spectrometer was used. Nitrogen was used as the collision gas at pressures ranging from 1.5 to 2.0 mTorr. Collision energies of 25 to 30 eV were used. The electron multiplier was typically operated at -1000 V for full scan mass spectra and -1800 V to -2000 V for MS/MS spectra. Both positive ion and negative ion thermospray mass spectra were obtained by pulsed positive ion/negative ion chemical ionization (PPINICI). Typical scan conditions for TSP/MS were scan range m/z 125 to 300 in 0.3 s.

A Vestec thermospray (TSP) LC/MS interface (Vestec Corp., Houston, TX) was used in all studies. A schematic representation of the Vestec interface is shown in Figure 1.1. In our interface, the vapor temperature thermocouple was replaced with a 1 mm i.d. tube which was connected to a Granville-Phillips thermogauge for monitoring source pressure. Two temperatures were monitored in the experiments: the vaporizer exit temperature (tip temperature) and the source block temperature. At a flow rate of 2.0 mL/min, the typical operating temperatures were tip, 240 C, and source, 290 C. However, when 0.1 M ammonium acetate/methanol (pH 6.9 80/20, v/v) was used, the optimum operating temperatures were tip, 220 C, and source, 290 C.

Since the mass spectrometer used in these studies was not a dedicated LC/MS instrument, normal electron impact (EI) tuning was performed on a standard EI/CI source with the standard calibration compound perflourotributylamine (PCR Research Chemicals, Inc., Gainesville, FL) on the TSQ45 prior to installation of the TSP source. After installation of the TSP source, the lens voltages were optimized by injecting a solution containing polyethylene glycol (PEG 200) obtained from Sigma. The mobile phase was delivered by a LC-2600 syringe pump (ISCO, Inc., Lincoln, NE) at flow rates ranging from 1.5 to 2.0 mL/min. All solutions were filtered through a 0.45μm filter before use. Samples were injected with a Rheodyne (model 7410) injector fitted with a 25μL loop.

Electrochemical

The results reported in this chapter were obtained with an ESA coulometric electrochemical cell (ESA, Inc., Bedford, MA). The coulometric cell (model 5020) has a cell volume of 5μL, a reticulated vitreous carbon working electrode with a surface area of 12-cm^2, and palladium counter and reference electrodes (Figure 2.1). The large ratio of the working electrode surface area to cell volume provides for high electrochemical conversion efficiencies. In addition, the cell is capable of withstanding pressures greater than 6000 psi. Although the palladium reference electrode is a quasi-reference, the peak potential (E_p) of uric acid vs. the palladium reference electrode corresponds within 50 mV to the E_p vs. a SCE reference electrode under the conditions employed in these studies (0.1 M ammonium acetate supporting electrolyte). A model 173 Potentiostat (EG&G Princeton Applied Research, Princeton, NJ) was used with the on-line electrochemical cell.

Double potential step chronoaperometry was performed in the time resolution studies using a model 175 Universal Programmer (EG&G Princeton Applied Research, Princeton, NJ). In these studies, a solution of 9-methyluric acid was continuously introduced into the EC/TSP/MS system.

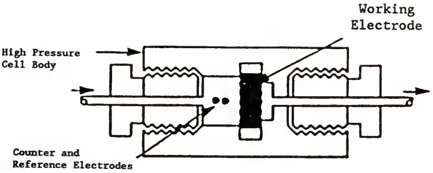

Figure 2.1. Diagram of high pressure electrochemical cell used in on-line studies.

A square wave potential-step, from an initial potential of -250 mV to a final potential of +800 mV, was applied for a duration of 500 ms. After 500 ms, the potential was stepped back to the initial potential of -250 mV. By using the mass spectrometer to trigger the waveform generator, application of the square waveform occurred simultaneously with the start of the acquisition of the mass spectrometer. Since the acquisition sequence and the potential pulse were synchronized, time delay measurements could be obtained by monitoring the formation of specific electrochemical intermediates.

All off-line cyclic voltammetric experiments were carried out using a BAS-100 electrochemical analyzer (Bioanalytical Systems, Inc., West Lafayette, IN). The working electrode used in cyclic voltammetric experiments was pyrolytic graphite (PG) with an area of ca. 0.05 cm^2. The PG electrode was prepared by sealing a piece of PG (1.5 mm x 10 mm) into glass tubing with inert epoxy (1C white, Dexter Corp.). Platinum and palladium wires served as counter and reference electrodes, respectively. The surface of the PG working electrode was resurfaced prior to each measurement by grinding the electrode on 600 grit silicon carbide paper (Mark V Laboratory, East Granby, CT) using a Beuhler Ecomet 1 Polisher-Grinder (Evanstown, IL). After grinding, the electrode was rinsed with distilled water and wiped with soft tissue paper.

Uric Acid as a Model Compound

Because the electrochemical oxidation of uric acid has been extensively studied using off-line methods (37,40,78), uric acid served as an ideal model and test system. The information provided by the previous studies included half-lives of proposed intermediates, identity of the final products confirmed by derivatization GC/MS, and a reaction pathway which accounts for the formation of the final products (Figure 1.5).

Before on-line electrochemical studies could be performed, experiments were conducted to determine the thermospray mass spectral characteristics of the starting material, uric acid. Unfortunately, preliminary observations indicated that ions indicative of uric acid were not present in the thermospray mass spectrum. In order to determine if uric acid decomposed during the thermospray ionization process, the lower scan limit of m/z 120 which is normally used to avoid major background ions was reduced to m/z 25. Using this lower mass limit, no ions above the normal background ion intensities were observed when a solution containing 2.5 μg of uric acid was injected. These results were totally unexpected since uric acid exists predominately as an anion at pH 7 (27,46). According to Vestal (9,24-26), if a compound exists as a preformed ion in solution, it should form an ion during the thermospray process. Obviously, other factors are involved in direct ion evaporation processes during thermospray ionization.

However, these results appear to be affected by the particular vaporizer probe used in the study. Four thermospray vaporizer probes were obtained from Vestec and compared. Although the stainless steel capillaries inside the vaporizer probes are claimed by the manufacturer to be identical, only one of the vaporizer probes was capable of producing $[M-H]^-$ ions of uric acid at m/z 167. Figure 2.2 illustrates the negative ion thermospray mass spectrum of uric acid when its $[M-H]^-$ ion was observed. Since the mass spectra obtained in this study were obtained

Figure 2.2. Negative ion full scan thermospray mass spectrum of 2.5 μg of uric acid obtained at 2.0 mL/min of 0.1 M ammonium acetate. Tip temperature and source temperature 240 C and 295 C, respectively.

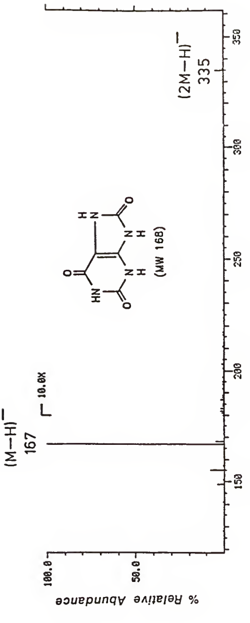
% Relative Abundance
100.0
50.0
150
200
250
300
350
(M—H)⁻
167
10.0X
(2M—H)⁻
335
HN
NH
O
O
O
N H
N H
(MW 168)

under identical thermospray conditions (flow rate, vaporizer and source temperatures), the lack of reproducibility indicates there are significant differences between the vaporizer probes used in the study. Indeed, the formation of the $[M+H]^+$ and $[M-H]^-$ ions of uric acid was found to be very sensitive to thermospray conditions. The procedure used to promote the production of $[M+H]^+$ and $[M-H]^-$ ions of uric acid is as follows: 1) After normal thermospray operation, the flow of the mobile phase is stopped, and the inlet of the vaporizer probe is fitted with a vacuum-tight plug. 2) The power applied to the vaporizer probe is reduced to zero, but the thermospray probe is allowed to remain inside the heated thermospray source to maintain thermal contact. 3) After about 1 hour, the tip temperature is increased to its normal value and the flow is resumed. The pseudo-molecular ions of uric acid can then often be observed for about 30 minutes. It is important to note that when the $[M+H]^+$ and $[M-H]^-$ ions of uric acid are observed in this manner, the total reconstructed ion current (RIC) has increased as well. In other words, the overall sensitivity of thermospray has increased well above the level which was observed before shutting down. Unfortunately, this enhanced sensitivity gradually disappears (< 30 minutes).

When the procedure described above is used, it is reasonable to propose that the inside diameter of the capillary is reduced by partial clogging due to the deposition of involatile residue from the mobile phase or uric acid which itself has low solubility. Although no significant increase in pump back-pressure is observed when the procedure described is followed, it is not unreasonable to propose that the reduction of the inside diameter of the capillary produces smaller droplets which evaporate more efficiently. As discussed in Chapter 1, recent results with replaceable vaporizer tips of various diameters indicate that the inside diameter of the capillary plays an important role in the ionization process (34).

On-Line Electrochemistry/Thermospray Mass Spectra

A diagram of the on-line EC/TSP/MS/MS system used to investigate the electrochemical oxidation of uric acid is shown in Figure 2.3. The delay time between electrochemical generation and detection by mass spectrometry can be minimized by reducing the length of HPLC tubing which connects the electrochemical cell and the thermospray vaporizer probe. To prevent contamination of the electrochemical cell from particulate matter, an in-line filter (not shown in Figure 2.3) was positioned between the injector and the electrochemical cell.

Optimum conditions for the operation of the thermospray interface, such as tip temperature, are traditionally obtained by maximizing the solvent-buffer ion intensities for a given flow rate (80-82). Under the conditions employed in the these studies, a maximum solvent-buffer ion intensity is obtained at a tip temperature of ca. 240 C for a flow rate of 2.0 mL/min. As expected, this tip temperature also produces the most intense reconstructed ion current for samples in EC/TSP/MS. However, ions which have maximum responses at lower tip temperatures have been identified. At tip temperatures lower than 240 C, additional ions such as 158^+, 184^+, and 182^- are observed in the EC/TSP mass spectra of uric acid, which correspond to intermediates formed from amination reactions.

Figure 2.3. Diagram of on-line electrochemistry/thermospray/tandem mass spectrometry system.

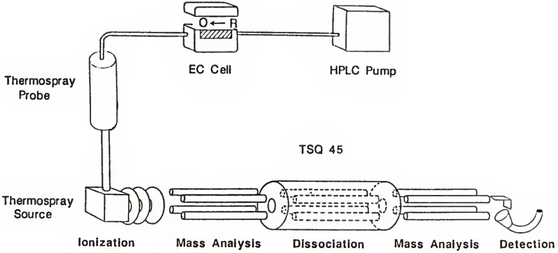
O ← R
EC Cell
HPLC Pump
Thermospray
Probe
TSQ 45
Thermospray
Source
Ionization
Mass Analysis
Dissociation
Mass Analysis
Detection

The relative mass spectral abundances of the ions corresponding to the amination products vary dramatically over a 20 C range in tip temperature from 230 C to 250 C. The positive ion full scan mass spectra of the oxidation products of uric acid at tip temperatures of 240 C and 220 C can be seen in Figure 2.4. The negative ion full scan mass spectra of the oxidation products of uric acid at tip temperatures of 240 C and 220 C can be seen in Figure 2.5. Interpretation of the spectra shown in Figures 2.4 and 2.5 is relatively simple since most of the ions observed in thermospray are pseudo-molecular ions ($[M+H]^+$ or $[M-H]^-$).

The results of the positive ion and negative ion thermospray mass spectra of the oxidation products of uric acid (tip temperature 238 C) when the lower scan limit was reduced to m/z 25 are summarized in Table 1. As can be seen in Figure 2.6 and Table 1, all of the secondary intermediates and final products of uric acid oxidation arise from the product of nucleophilic attack on the imine double bonds of the primary diimine intermediate. The electrochemical oxidation pathway of uric acid determined by on-line EC/TSP/MS/MS at a tip temperature of 238 C is shown in Figure 2.6. The pathway described in Figure 2.6 is reasonable based on the observed products. However, since not all proposed intermediate structures shown in Figure 2.6 have been identified, it is reasonable to assume that product formation may occur by alternative mechanisms. For example, as discussed in Chapter 1, the diimine is very unstable and is susceptible to nucleophilic attack by species such as H_2O, NH_3, and methanol (Figure 1.2). As shown in Figures 1.2 and 2.6, hydration of the C5=N7 double bond produces the imine alcohol (MW 184). Although not shown in Figures 1.2 or 2.6, imine alcohol formation may also occur by hydration

Figure 2.4. The effect of tip temperature on the positive ion mass spectra of the oxidation products of uric acid at +0.50 V. Flow rate 2.0 mL/min of 0.1 M ammonium acetate. Source temperature 295 C. a) tip temperature 220 C. b) tip temperature 240 C.

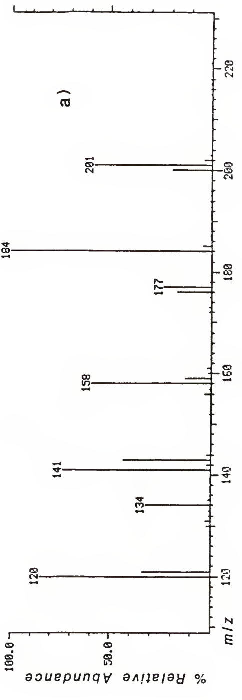
a)
% Relative Abundance
100.0
50.0
m/z
120
140
160
180
200
220
120
134
141
158
177
184
201

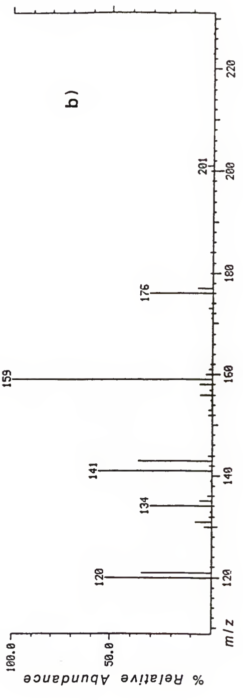
b)
% Relative Abundance
100.0
50.0
m/z
120
140
160
180
200
220
120
134
141
159
176
201

Figure 2.5. The effect of tip temperature on the negative ion mass spectra of the oxidation products of uric acid at +0.50 V. Flow rate 2.0 mL/min of 0.1 M ammonium acetate. Source temperature 295 C. a) tip temperature 220 C. b) tip temperature 240 C.

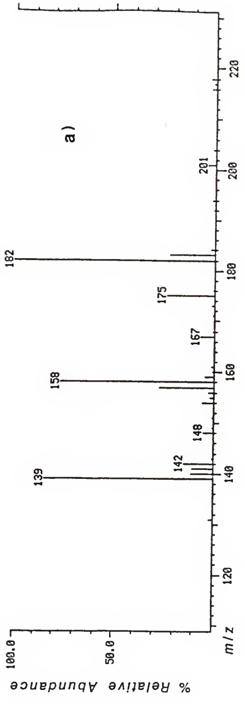
a)
% Relative Abundance
100.0
50.0
m/z
120
140
160
180
200
220
139
142
148
158
167
175
182
201

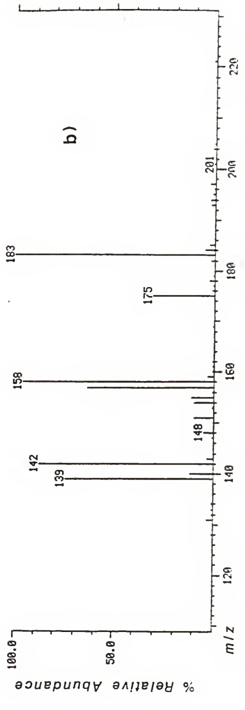
b)
% Relative Abundance
100.0
50.0
m/z
120
140
160
180
200
220
139
142
148
158
175
183
201

Figure 2.6. Electrochemical oxidation pathway of uric acid. The molecular weights are shown for those intermediates and products which have been identified by EC/TSP/MS and EC/TSP/MS/MS.

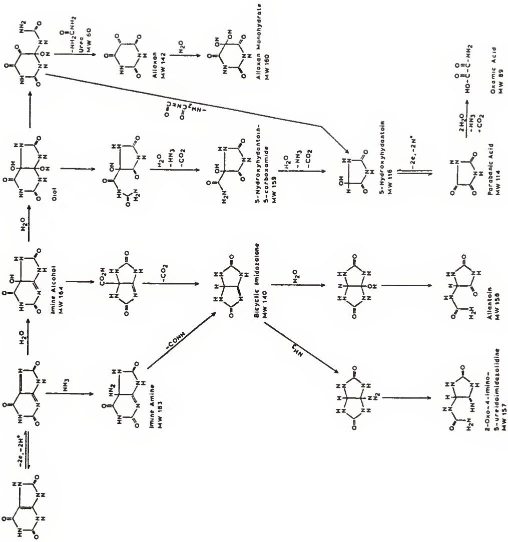
-2e, -2H⁺
H2O
H2O
NH3
Imine Amine
MW 183
-CONH
Imine Alcohol
MW 164
-CO2
Bicyclic Imidazolone
MW 140
H2O
NH3
Allantoin
MW 158
2-Oxo-4-imino-
5-ureidoimidazolidine
MW 157
Diol
H2O
-NH3
-CO2
5-Hydroxyhydantoin-
5-carboxamide
MW 159
5-Hydroxyhydantoin
MW 116
-2e, -2H⁺
Parabanic Acid
MW 114
2H2O
-NH3
-CO2
Oxamic Acid
MW 89
-NH2CNH2
Urea
MW 60
Alloxan
MW 142
H2O
Alloxan Monohydrate
MW 160
-NH2CN=C=O

Table 1. Summary of the positive and negative ions observed in the thermospray mass spectra of the electrochemical oxidation products of uric acid.

POSITIVE IONS

m/z	Identity
45	$[CO_2+H]^+$
61	[Urea+H]$^+$
120	[Urea+Acetamide+H]$^+$
121	[Urea+Urea+H]$^+$
134	[5-Hydroxyhydantoin+NH_4]$^+$
141	[Bicyclic imidazolone+H]$^+$
143	[Alloxan+H]$^+$
158	[2-Oxo-4-imino-5-ureidoimidazolidine+H]$^+$
159	[Allantoin+H]$^+$
169	[Uric acid+H]$^+$
176	[Allantoin+NH_4]$^+$
177	[5-Hydroxyhydantoin-5-carboxamide+NH_4]$^+$
184	[Imine amine+H]$^+$
200	[Bicyclic imidazolone+acetamide+H]$^+$
201	[Imine amine+NH_4]$^+$

NEGATIVE IONS

m/z	Identity
88	[Oxamic acid-H]$^-$
113	[Parabanic acid-H]$^-$
115	[Alloxan monohydrate-CO_2-H]$^-$
139	[Bicyclic imidazolone-H]$^-$
141	[Alloxan-H]$^-$
156	[2-Oxo-4-imino-5-ureidoimidazolidine-H]$^-$
157	[Allantoin-H]$^-$
158	[5-hydroxyhydantoin-5-carboxamide-H]$^-$
167	[Uric acid-H]$^-$
175	[Alloxan monohydrate-CO_2+acetate]$^-$
182	[Imine amine-H]$^-$
183	[Imine alcohol-H]$^-$
201	[Alloxan+acetate]$^-$

of the N3=C4 double bond. In addition, many of the structures shown in Figure 2.6 can exist as oxo-hydroxy tautometers although only one tautometer is shown. Therefore, the structures and pathways shown in Figure 2.6 are reasonable, not absolute.

A positive ion corresponding to the imine alcohol $[M+H]^+$ at m/z 185 is not observed in Figure 2.4. However, as can be seen in Figure 2.5 and Table 1, the imine alcohol does produce an intense $[M-H]^-$ ion at m/z 183. Attack on the diimine intermediate by one molecule of ammonia will, in analogy, produce the amination intermediate (imine amine) (MW 183). Ions such as 184^+ and 182^-, corresponding to the imine amine, can be observed in both the positive ion and negative ion thermospray mass spectra of the oxidation products of uric acid at tip temperatures less that 230 C. As shown in Figures 2.4 and 2.5, pseudo-molecular ions of these intermediates produced by nucleophilic attack by mobile phase components on the quinonoid diimine following the electrooxidation of uric acid are formed during the thermospray process.

As can be seen in the negative ion mass spectra in Figure 2.5, the intermediates formed as a result of hydration and amination reactions with the quinonoid diimine of uric acid have very different optimum tip temperatures. At a tip temperatures of 240 C, the base peak in the negative ion EC/TSP mass spectrum is m/z 183, corresponding to the $[M-H]^-$ of the imine alcohol (hydration) intermediate. However, when the tip temperature is lowered to 231 C, the base peak in the negative ion EC/TSP mass spectrum is m/z 182, corresponding to the imine amine (amination) intermediate. The formation of amination intermediates and products during the thermospray process of electrochemically generated species will be discussed in further detail in Chapter 4.

In order to fully characterize the intermediates and products formed following an electrochemical reaction, both the positive ion and negative ion mass spectra must be considered. This is especially true for compounds formed which produce only an $[M+H]^+$ or $[M-H]^-$ ion. Still other compounds can undergo both reactions. As shown in Figure 2.4, Figure 2.5, and Table 1, the latter case is ideal for the identification of unknown reaction intermediates because the molecular weight is confirmed.

As can be seen in Figure 2.6, the formation of parabanic acid from 5-hydroxyhydantoin requires a second oxidation step. Because the quinonoid diimine must undergo several hydration reactions followed by ring opening before 5-hydroxyhydantoin is produced, the production of parabanic acid from 5-hydroxyhydantoin requires each of these intermediates to remain near or at the electrode surface in order for the second oxidation to occur. During off-line bulk electrolysis of uric acid, the formation of parabanic acid is observed because of long electrolysis times in a closed system. However, in a flowing system, because the material is continuously swept out of the electrochemical cell by the mobile phase, parabanic acid will not be produced unless the hydration reactions and ring openings occur on a very short time scale. Adsorption was considered to play a role in the detection of parabanic acid, and the mass chromatograms were examined to determine if any significant time delay existed between the detection of the $[M-H]^-$ ion of the imine alcohol at m/z 183 and the $[M-H]^-$ ion of parabanic acid at m/z 113. The mass chromatograms revealed no significant time delay between the mass spectrometric detection of the negative ions at m/z 183 and m/z 113. This information and time resolution measurements indicate that neither species is adsorbed. Therefore, it is difficult to explain how parabanic acid is produced by direct oxidation.

The identified products which are listed in Table 1 include allantoin, 5-hydroxyhydantoin-5-carboxamide, parabanic acid, and alloxan monohydrate, all of which were identified in previous off-line studies (37,47) as the final electrochemical oxidation products of uric acid. The positive ions at m/z 159 $[M+H]^+$ and m/z 176 $[M+NH_4]^+$ shown in Figure 2.4, and the negative ion at m/z 157 $[M-H]^-$ shown in Figure 2.5 are due to allantoin (MW 158). As can be seen in Figure 2.6, the ions 139^- and 141^+ must result from the imine alcohol (hydration) intermediate (MW 184) or the imine amine (amination) intermediate (MW 183) which has undergone ring contraction to produce the bicyclic imidazolone (MW 140). Hydration of the bicyclic imidazolone intermediate (MW 140) accompanied by ring opening produces allantoin. The ions 158^+ and 156^- indicate amination reactions can also occur with the bicyclic imidazolone (Figure 2.6) to form 2-oxo-4-imino-5-ureidoimidazolidine (MW 157) with a structure similar to allantoin.

The results tabulated in Table 1 include those ions identified when the lower m/z limit was decreased from 120 to 35. Additional ions such as 61^+, 45^+, and 88^- are detected with the lower scan limit (not shown in Figures 2.4 and 2.5). The positive ion at m/z 61 corresponds to the $[M+H]^+$ of urea. Urea (MW 60) is produced during the formation of alloxan. The 121^+ ion has been identified by MS/MS as a proton-bound dimer of urea. Proton-bound dimers have been detected in TSP/MS (31,32) and their formation has been observed to be dependent on the analyte concentration. The negative ion at m/z 88 has been identified as $[NH_2COCO_2]^-$, the $[M-H]^-$ ion of oxamic acid (MW 89), which results from thermal decomposition of parabanic acid (Table 1).

Table 1 also shows several acetamide adduct ions which have been identified. Smith et al. (32) noted intense $(M+60)^+$ ions for several amino acids studied by TSP/MS, but could not deduce their origin. It is known (83) that acetamide is formed during the dehydration of ammonium acetate; hence the formation of such adduct ions is not surprising. Although the acetamide reagent ion m/z 60^+ is produced during the thermospray process, the formation of acetamide adducts, as with any adducts, will depend on the basicity of the analyte and the conditions in the TSP source.

The ions 143^+ and 141^- (Table 1) have been identified as $[M+H]^+$ and $[M-H]^-$ of alloxan (MW 142). Although only alloxan monohydrate (MW 160) could be obtained as a standard, the presence of alloxan was inferred from the fragmentation pattern in the daughter spectrum. Alloxan monohydrate (MW 160) is produced from the hydration of alloxan and is the only product identified thus far that does not yield an $(M+H)^+$ or an $(M-H)^-$ ion (Table 1); instead it is decarboxylated to produce a $(M-CO_2-H)^-$ ion at m/z 115 and a $(M-CO_2+CH_3COO)^-$ ion at m/z 175. When authentic alloxan monohydrate is analyzed by TSP/MS, the sample is completely decarboxylated to produce the negative ions at m/z 115 and 175. Because neither an $(M+H)^+$ nor an $(M-H)^-$ ion is observed, these ions are most likely the result of thermal decomposition occurring inside the thermospray vaporizer probe or source, rather than a (gas-phase) mass spectrometric fragmentation of the $[M-H]^-$ or $[M+CH_3COO]^-$ ion. In addition, it is unlikely that a weakly held hydrogen-bonded acetate adduct would remain intact if acetate attachment occurred prior to decarboxylation (mass spectrometric fragmentation).

Mass Spectrometric Hydrodynamic Voltammograms

Another important use of on-line EC/TSP/MS is the monitoring of individual species (reactants, intermediates, and products) as a function of electrode potential. Although similar information may be obtained by on-line UV-VIS spectrophotometry (spectroelectrochemistry) (47), MS/MS is much more likely to permit unambiguous monitoring and identification of individual species.

Figure 2.7 illustrates the mass spectrometric hydrodynamic voltammograms of uric acid obtained by EC/TSP/MS. As shown by the cyclic voltammogram obtained under normal conditions in stationary solution at a small electrode (ca. 0.05 cm^2), oxidation of uric acid begins to occur at ca. +0.0 V and proceeds at a maximum rate at ca. +0.40 V. Electrochemical oxidation of uric acid in a flowing stream through a porous electrode, as monitored on-line by mass spectrometry, is shown in Figure 2.7. The oxidation process can be followed by monitoring the intensity of the $[M-H]^-$ ion of uric acid at m/z 167 as a function of the electrode potential. The intensity of the 167^- ion, in agreement with the response shown by cyclic voltammetry, decreases due to the oxidation of uric acid as the electrode potential becomes more positive than +0.0 V vs. Pd. The intensity of the ion corresponding to the imine alcohol intermediate ($[M-H]^-$ m/z 183, Figure 2.7) of uric acid oxidation, which can also be monitored by mass spectrometry, increases with increasing

Figure 2.7. Mass spectrometric hydrodynamic voltammograms of uric acid; m/z 167= $[M\text{-}H]^-$ of uric acid and m/z 183 = $[M\text{-}H]^-$ of imine alcohol. Flow rate of 0.1 M ammonium acetate mobile phase 2.0 mL/min. Tip temperature 240 C and source temperature 290 C. Cyclic voltammogram of 300 μM uric acid on rough pyrolytic graphite. Scan rate of 200 mV s^{-1}. Palladium reference electrode and 0.1 M ammonium acetate supporting electrolyte.

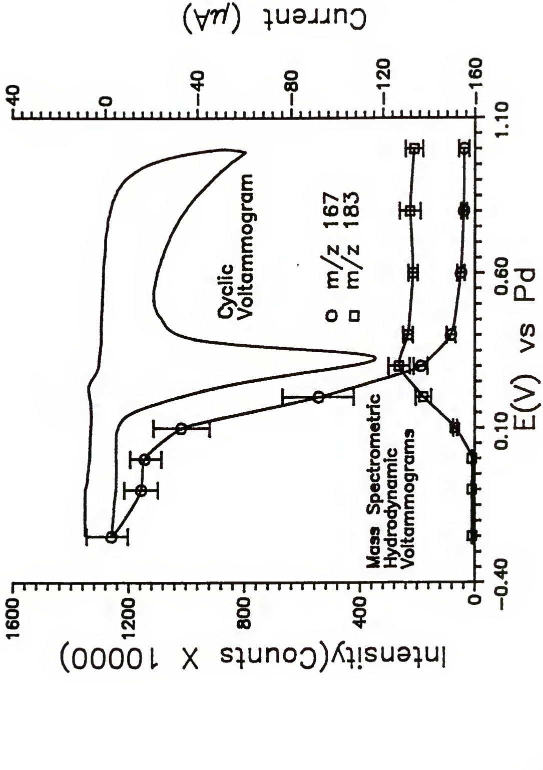
Intensity(Counts X 10000)
1600
1200
800
400
0
Current (μA)
40
0
−40
−80
−120
−160
−0.40
0.10
0.60
1.10
E(V) vs Pd
Cyclic Voltammogram
○ m/z 167
□ m/z 183
Mass Spectrometric Hydrodynamic Voltammograms

electrode potential. However, a steady-state situation develops for all ion intensities at potentials > +0.40 V due to the hydrodynamic flow of reactant. It has been shown that steady-state behavior will be produced in all forms of hydrodynamic voltammetry operating in the limiting current region (55). Similar hydrodynamic voltammograms are produced in electrochemical HPLC detectors. The design of the cell and the high flow rates (2.0 mL/min) used in these studies will contribute to the steady-state behavior observed. As can be seen in Figure 2.7, at potentials greater than +0.40 V the 167^- ion drops to ~ 15% of its original intensity at -0.10 V, indicating that high coulometric efficiencies (ca. 85%) can be obtained with this system. As expected, the formation of the secondary intermediate, the imine alcohol (MW 184) also reaches a steady-state level at ca. +0.40 V. In theory (55), the plateau region that begins at +0.40 V in the mass spectrometric hydrodynamic voltammogram of uric acid should roughly correspond to the peak potential of ca. +0.40 V vs Pd obtained in a cyclic voltammetric experiment. As can be seen in Figure 2.7, the beginning of the steady-state response obtained in the mass spectrometric hydrodynamic voltammogram is in excellent agreement with the peak potential obtained in cyclic voltammetry.

Time Resolution of EC/TSP/MS

One attractive feature of an on-line electrochemistry/identification system is the opportunity to attain sufficient time resolution to detect short-lived intermediates. The delay time (dead volume) between the electrochemical cell and the mass spectrometer is therefore an important parameter and should be as small as possible. Increased dead volume after the cell will not only degrade the time resolution, but will also decrease the probability of detecting important intermediates.

The delay time of our on-line system was determined by two different methods. A delay time of 500 ms at 2.0 mL/min was determined by summing the volume of tubing after the cell (15 μL). The second method used to determine this delay time involved applying a square wave potential-step from an initial potential of -250 mV to a final potential of +800 mV for a duration of 500 ms. After 500 ms, the potential was stepped back to the initial potential of -250 mV. Figure 2.8 illustrates the effect of this potential-step experiment on the relative intensity of an amination intermediate $[M-H]^-$ at m/z 196 produced during the oxidation of 9-methyluric acid (MW 182). 9-Methyluric acid and uric acid undergo the same oxidation/diimine hydration reactions (37). The sample flow rate was 2.0 mL/min and the intermediate monitored was the partial amination product of the diimine (MW 197). As can be seen in Figure 2.8, the delay time before the mass spectrometer starts to respond to the formation of this secondary intermediate is 520 ms, which agrees very well with the time delay of 500 ms calculated from tubing volume. The peak half width of 500 ms equals the pulse duration. Possible explanations for the observed peak tailing include band broadening and adsorption of the intermediate on the electrode surface.

Figure 2.8. a) Potential-step experiment with 9-methyluric acid. Initial potential -250 mV, step potential +800 mV, and final potential -250 mV. Pulse duration 500 ms. b) Relative intensity of amination intermediate at m/z 196^- obtained during a potential step experiment. Flow rate of 0.1 M ammonium acetate mobile phase 2.0 mL/min. Tip temperature 230 C and source temperature 290 C.

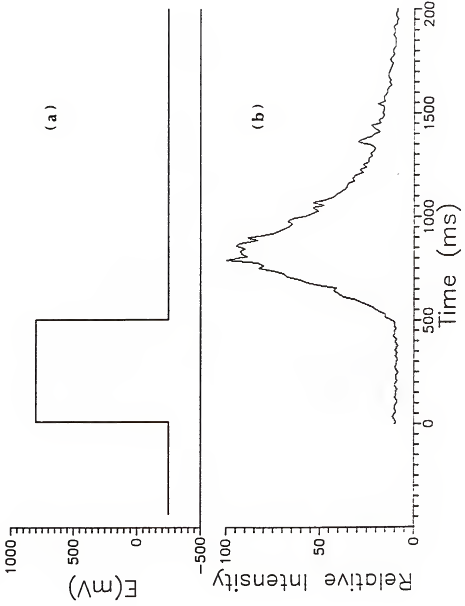
E(mV)
1000
500
0
-500
(a)
Relative Intensity
100
50
0
(b)
0
500
1000
1500
2000
Time (ms)

Identification of Electrochemically Generated Intermediates and Products by Tandem Mass Spectrometry

To obtain structural information about reactants and products during electrochemical oxidation, tandem mass spectrometry (MS/MS) was used to produce structurally significant daughter ions by collisionally activated dissociation (CAD) of selected parent ions. MS/MS provides not only structural information but an additional separation stage which enables co-eluting components in the electrolysis mixture to be identified.

Figure 2.9 illustrates the daughter spectrum of the positive ion at m/z 184 ($[M+H]^+$ of the imine amine in Figure 2.6, the amination product of the diimine) and is an excellent example of the structural information which can be obtained by MS/MS. Neutral losses of 17 (NH_3) are common for $[M+H]^+$ ions of compounds which contain a primary amine. Although this information is important, additional information is obtained when consecutive neutral losses occur. Thus, the 184^+ ion initially fragments to 167^+ (loss of NH_3) which must, therefore correspond to the protonated quinonoid diimine (MW 166) and which is further fragmented to the 124^+ ion (loss of CONH). The parent 184^+ ion can also initially fragment to 141^+ (loss of CONH). Both the 141^+ and 124^+ ions undergo further consecutive fragmentations which were used to elucidate the structure of the parent ion.

The daughter spectra of an $[M+H]^+$ ion and of its complementary $[M-H]^-$ ion are often very different. The differences in fragmentations between $[M+H]^+$ and $[M-H]^-$ ions can be explained in part by the location of the charge and the stability of the ion. The differences can be illustrated by comparing the daughter spectrum of positive ion at m/z 184 described

Figure 2.9 a) Positive ion daughter spectrum of the $[M+H]^+$ ion of the imine amine amination intermediate at m/z 184. Tip temperature 230 C and source temperature 290 C. Collision gas pressure 2.0 mTorr nitrogen. Collision energy -30 eV. b) Negative ion daughter spectrum of the $[M-H]^-$ ion of the imine amine amination intermediate at m/z 182. Tip temperature 230 C and source temperature 290 C. Collision gas pressure 2.0 mTorr nitrogen. Collision energy -30 eV.

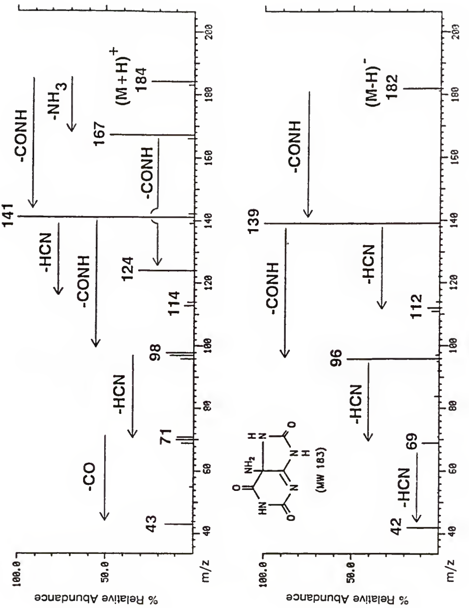
% Relative Abundance
100.0
50.0
m/z
40
60
80
100
120
140
160
180
200
141
167
184
(M+H)$^+$
-CONH
-NH$_3$
-CONH
-HCN
-CONH
124
114
98
-HCN
71
-CO
43
% Relative Abundance
100.0
50.0
m/z
139
182
(M-H)$^-$
-CONH
-CONH
-HCN
112
96
-HCN
69
-HCN
42
(MW 183)

previously, with the daughter spectrum of its complementary $[M-H]^-$ ion at m/z 182 (Figure 2.9). The $[M-H]^-$ ion at m/z 182 initially fragments with a neutral loss of 43 (CONH) to produce the 139^- ion. The 139^- ion undergoes competitive fragmentations to produce the 112^- ion (loss of HCN), the 111^- ion (loss of CO), and the 96^- ion (loss of CONH). The negative daughter ion at m/z 96 undergoes further consecutive fragmentations with two losses of HCN to produce the 42^- ion. As can be seen in Figure 2.9, the positive and negative ion daughter spectra provide structural information which is complementary. For example, only the $[M+H]^+$ ion fragments with a loss of NH_3 indicating the presence of a primary amine. The daughter spectrum of the $[M+H]^+$ ion also clearly shows the presence of three CO groups. This important piece of structural information is confirmed by the daughter spectrum of the $[M-H]^-$ ion.

Other examples of structure elucidation with EC/TSP/MS/MS are summarized in Tables 2 and 3. Each of the identified ions listed in Tables 2 and 3 produces a unique fragmentation pattern which is characteristic of its structure and which provides the necessary structural information to permit structure elucidation of the parent ion. In contrast to previous off-line studies (40,47), fragmentation patterns of the imine amine (Figure 2.9), imine alcohol (Table 3), and the intermediate which results from the addition of methanol (Table 3), provide convincing evidence to support a quinonoid diimine intermediate after a $2e^-,2H^+$ electrooxidation of uric acid. Losses of small neutral molecules such as NH_3, CONH, HCN, CO, or H_2O are common during the CAD of even-electron species such as $[M+H]^+$ and $[M-H]^-$ ions, as can be seen from

Table 2. Positive Ion Daughter Mass Spectra of Identified Oxidation Intermediates and Products of Uric Acid.

$[M+ACETAMIDE+H]^+$ ADDUCT ION OF UREA AT m/z 120

m/z (%RA)	Structure Correlation
120 (4)	parent ion
61 (100)	loss of acetamide from 120^+
60 (36)	loss of urea from 120^+

$[2M+H]^+$ DIMER OF UREA AT m/z 121

m/z (%RA)	Structure Correlation
121 (3)	parent ion
61 (100)	loss of urea from 121^+
44 (6)	loss of NH_3 from 61^+

$[M+H]^+$ ION OF BICYCLIC IMIDAZOLONE AT m/z 141

m/z (%RA)	Structure Correlation
141 (80)	parent ion
98 (10)	loss of CONH from 141^+
71 (15)	loss of HCN from 98^+
70 (12)	loss of CO from 98^+
55 (8)	loss of CONH from 98^+
43 (100)	loss of HCN from 70^+

$[M+H]^+$ ION OF 2-OXO-4-IMINO-5-UREIDOIMIDAZOLIDINE AT m/z 158

m/z (%RA)	Structure Correlation
158 (10)	parent ion
141 (50)	loss of NH_3 from 158^+
115 (12)	loss of CONH from 158^+
98 (100)	loss of NH_3 from 115^+
71 (15)	loss of HCN from 98^+
61 (70)	loss of 97 from 158^+
55 (25)	loss of CONH from 98^+
44 (20)	loss of NH_3 from 61^+
43 (15)	loss of CO from 71^+

Table 2 -- continued.

[M+ACETAMIDE+H]$^+$ ADDUCT ION OF BICYCLIC IMIDAZOLONE AT m/z 200

m/z (%RA)	Structure Correlation
200 (3)	parent ion
141 (100)	loss of acetamide from 200$^+$
98 (8)	loss of CONH from 141$^+$
70 (8)	loss of CO from 98$^+$
60 (3)	loss of 140 from 200$^+$
43 (10)	loss of HCN from 70$^+$

[M+NH$_4$]$^+$ ADDUCT ION OF IMINE AMINE AT m/z 201 *

m/z (%RA)	Structure Correlation
201 (1)	parent ion
184 (35)	loss of NH$_3$ from 201$^+$
167 (35)	loss of NH$_3$ from 184$^+$
141 (100)	loss of CONH from 167$^+$
124 (8)	loss of CONH from 167$^+$
114 (5)	loss of HCN from 141$^+$
98 (10)	loss of CONH from 141$^+$
71 (3)	loss of HCN from 98$^+$
70 (5)	loss of CO from 98$^+$
55 (8)	loss of CONH from 98$^+$
43 (4)	loss of CO from 71$^+$

* Produced in amination reactions at tip temperatures < 240 C.

Table 3. Negative Ion Daughter Mass Spectra of Identified Oxidation Intermediates and Products of Uric Acid.

$[M-H]^-$ ION OF OXAMIC ACID AT m/z 88

m/z (%RA)	Structure Correlation
88 (100)	parent ion
44 (70)	loss of CO_2 from 88^-

$[M-H]^-$ ION OF BICYCLIC IMIDAZOLONE AT m/z 139

m/z (%RA)	Structure Correlation
139 (100)	parent ion
96 (25)	loss of CONH from 139^-
69 (25)	loss of HCN from 96^-
42 (60)	loss of HCN from 69^-

$[M-H]^-$ ION OF ALLOXAN AT m/z 141

m/z (%RA)	Structure Correlation
141 (100)	parent ion
98 (40)	loss of CONH from 141^-
42 (20)	loss of 99 from 141^-

$[M-H]^-$ ION OF 5-HYDROXYHYDANTOIN-5-CARBOXAMIDE AT m/z 158

m/z (%RA)	Structure Correlation
158 (50)	parent ion
140 (5)	loss of H_2O from 158^-
115 (100)	loss of CONH from 158^-
97 (15)	loss of H_2O from 115^-
72 (5)	loss of CONH from 115^-
59 (3)	urea anion
42 (20)	loss of 115 from 158^-

Table 3 -- continued.

$[M\text{-}H]^-$ ION OF THE IMINE ALCOHOL AT m/z 183

m/z (%RA)	Structure Correlation
183 (25)	parent ion
140 (100)	loss of CONH from 183^-
112 (8)	loss of CO from 140^-
97 (90)	loss of CONH from 140^-
69 (3)	loss of CO from 97^-
42 (8)	loss of HCN from 69^-

$[M\text{-}H]^-$ ION OF INTERMEDIATE FORMED VIA ADDITION OF METHANOL AT m/z 197

m/z (%RA)	Structure Correlation
197 (50)	parent ion
196 (20)	loss of $H\cdot$ from 197^-
182 (10)	loss of $CH_3\cdot$ from 197^-
165 (8)	loss of CH_3OH from 197^-
154 (100)	loss of CONH from 197^-
153 (10)	loss of CONH from $196^{-\cdot}$
139 (15)	loss of $CH_3\cdot$ from 154^-
127 (15)	loss of HCN from 154^-
126 (15)	loss of CO from 154^-
122 (10)	loss of CH_3OH from 154^-
111 (10)	loss of CONH from 154^-
97 (8)	loss of $CON\cdot$ from $139^{-\cdot}$

$[M\text{+}ACETATE]^-$ ADDUCT ION OF ALLOXAN AT m/z 201

m/z (%RA)	Structure Correlation
201 (1)	parent ion
141 (100)	loss of acetic acid from 201^-
98 (4)	loss of CONH from 141^-
59 (4)	loss of 142 from 201^-
42 (10)	loss of 99 from 141^-

Tables 2 and 3. The fragmentation patterns described in Tables 2 and 3 are only meant to convey the type of structural information which can be obtained using tandem mass spectrometry. Alternate fragmentation pathways may be possible.

The amount (% relative abundance) of the parent ion remaining after the CAD process depends on parameters such as collision gas pressure and collision energy as well as the stability of the parent ion. The conditions used in this study caused almost complete fragmentation (~ 5% parent ion remaining) of hydrogen-bonded adduct ions such as $[M+NH_4]^+$, $[M+CH_3COO]^-$, and $[M+CH_3CONH_3]^+$, resulting in daughter spectra which contained as their base peak the $[M+H]^+$ or $[M-H]^-$ ion with a corresponding neutral loss of the adduct group (Tables 2 and 3).

For those products (alloxan monohydrate, allantoin, urea, and parabanic acid) which were commercially available, MS/MS was used to confirm their presence in the EC/TSP mass spectra. This was accomplished by comparing the daughter spectra of authentic standards with the daughter spectra of electrochemically generated products. These comparisons are shown in Table 4. The agreement between daughter ion abundances of standards and electrochemically generated products was generally ±20% relative abundance, as shown in Table 4.

Table 4. Comparison of Daughter Spectra of Authentic Standards and Electrochemically Generated Products.

Compound	Ion	Authentic Standard	EC Generated Product
Urea			
(MW 60)	$[M+H]^+$	m/z (%RA)*	m/z (%RA)
		61 (100)	61 (100)
		60 (12)	60 (12)
		44 (80)	44 (80)
		43 (5)	43 (5)
Parabanic Acid			
(MW 114)	$[M-H]^-$	m/z (%RA)	m/z (%RA)
		113 (100)	113 (100)
		85 (10)	85 (4)
		42 (65)	42 (60)
Allantoin			
(MW 158)	$[M-H]^-$	m/z (%RA)	m/z (%RA)
		157 (90)	157 (80)
		140 (10)	140 (10)
		114 (95)	114 (100)
		97 (100)	97 (80)
		71 (10)	71 (8)
		59 (12)	59 (20)
		42 (30)	42 (30)
Alloxan Monohydrate			
(MW 160)	$[M-CO_2+Acetate]^-$	m/z (%RA)	m/z (%RA)
		175 (3)	175 (3)
		115 (100)	115 (100)
		97 (3)	97 (3)
		72 (6)	72 (6)
		59 (6)	59 (6)

Conclusions

The main goal of this chapter was to illustrate the feasibility and capabilities of combining electrochemistry on-line with mass spectrometry. In spite of the complexity of the reactions following the electrochemical oxidation of our model compound, uric acid, EC/TSP/MS/MS allows positive identification of intermediates and products. Although the positive and negative ion mass spectra were extremely helpful in final identifications by providing molecular weight information, structural assignments required MS/MS because the soft nature of thermospray ionization causes little fragmentation.

All of the previously reported major products of uric acid and several of the intermediates have been identified and characterized by EC/TSP/MS/MS. The intermediates resulting from partial hydration (imine alcohol, MW 184) and partial amination (imine amine, MW 183) of the quinonoid diimine have been identified by their fragmentation patterns. In addition, the ions 139^- and 141^+ in the EC/TSP/MS spectra must result from either the imine amine or the imine alcohol undergoing ring contraction followed by decarboxylation which produces the bicyclic intermediate. Identification of this bicyclic intermediate confirms that uric acid can follow three different reactions pathways after electrooxidation.

It is important to recognize that it is the unique operating conditions of EC/TSP/MS/MS which make it possible to detect intermediates as well as final products after electrooxidation. First, the thermospray interface permits direct on-line coupling of the solution-phase electrochemical cell directly to the mass spectrometer, permitting short-lived intermediates to be observed. Second, MS/MS makes it possible to determine the structure of each of the mixture components which produce only molecular ions in TSP.

Because the temperature conditions during thermospray change in 500 ms from 25 C to 250 C, the rate constants for the disappearance of intermediates cannot be readily compared to values obtained by room temperature methods such as spectroelectrochemistry. For example, the imine alcohol intermediate (MW 184) has a half-life estimated by spectroelectrochemistry of ca. 2 minutes in solution at 25 C. If this rate constant remained unchanged under the elevated temperatures in EC/TSP/MS and with a time delay of only 500 ms, it would not be possible to observe any final products. Therefore, it can be expected that many if not all rate constants will be different under EC/TSP/MS conditions.

CHAPTER 3
CHARACTERIZATION OF ELECTROCHEMICAL OXIDATION PATHWAYS VIA ON-LINE CHROMATOGRAPHIC SEPARATION

Introduction

This chapter deals with the characterization of electrochemical oxidation pathways of thiol compounds using on-line chromatographic separation, with detection by mass spectrometry or UV-Vis absorption spectrophotometry. The electrochemical oxidation pathways of 6-TP and other structurally similar thiopurines such as 6-thioxanthine (6-TX) and 6-thioguanine (6-TG) have been studied by off-line methods (38,39,48,65).

Because of the complex nature of the redox reactions which involve multiple electron transfers and following reactions, unambiguous information about reaction pathways of these compounds has not emerged using traditional electrochemical methods. However, when high performance liquid chromatography (HPLC) is used on-line with an electrochemical cell (EC/HPLC), unique insights into reaction pathways can be obtained as a function of electrode potential.

At low potentials, the electrochemical oxidation of thiols usually leads to the corresponding disulfide (76). This has been shown for 6-TP, 6-TX, and 6-TG (38,39,65). The first step in disulfide formation is a one-electron transfer, leading to thiyl radicals (84). Thiopurines such as 6-TX and 6-TG behave differently electrochemically than 6-TP at high potentials of ca. +1.0 V because the electronegative substituents make the purine ring more vulnerable to oxidation.

The chemistry of the thiol group has been well characterized (76,85), due in part to the importance of sulfur in biochemical reactions (58). Modern electrochemical methods are a valuable analytical tool for the determination of sulfur-containing compounds (86-88). Attempts to characterize the electrochemical oxidation pathways of sulfur-containing compounds at low potentials can sometimes lead to complications when the reaction product (disulfide) is insoluble in the medium and covers the electrode (38,39). In other cases, the S-S bond of the disulfides may be unstable in acidic and basic media, resulting in a disproportionation reaction which regenerates the parent thiol in ca. 75% yield (38,89). These complications can hinder accurate coulometric measurements and accurate verification of reaction pathway.

At higher potentials many thiols may be further oxidized to oxygen-containing compounds such as sulfinic (RSO_2H) or sulfonic (RSO_3H) acids (65,84). Unfortunately, these processes are often difficult to observe using coulometry and cyclic voltammetry. Coulometric results can be misleading because unstable sulfinic and sulfonic acids can decompose during long electrolysis times to yield some further electrooxidizable material (65), and cyclic voltammetric peaks are sometimes masked by background discharge at large positive potentials (38,41,65). As will be demonstrated in this chapter, the on-line coupling of high performance liquid chromatography (HPLC) with electrochemistry can provide detailed redox information about two thiols, 6-thiopurine and 2-thiopyrimidine. In addition to detection by thermospray/tandem mass spectrometry

(EC/HPLC/TSP/MS/MS), detection by UV-Vis absorption spectrophotometry (EC/HPLC/UV-Vis) will also be demonstrated.

Experimental

Samples and Reagents

Purine, hypoxanthine, adenine, 6-thiopurine, 2-thiopyrimidine, and 2-hydroxypyrimidine were obtained from Sigma (St. Louis, MO). The reagents were used as received. Bis(6-purinyl) disulfide, sodium purine-6-sulfinate, and sodium purine-6-sulfonate were prepared according to Doerr et al. (89). All compounds except bis(6-purinyl) disulfide were dissolved in 0.1 M ammonium acetate (pH 6.9). Typically, twenty microliters of a 100 ppm solution were injected. Due to the low solubility of bis(6-purinyl) disulfide, a 50 ppm solution was prepared in 0.1 M ammonium acetate/methanol (pH 6.9, 50/50, v/v). The structures and molecular weights of the compounds used in these studies are shown in Figure 3.1.

Spectroelectrochemistry

A Tracor Northern TN 6500 diode array spectrophotometer (Middleton, WI) was used for all spectroelectrochemical experiments. An optically transparent thin-layer spectroelectrochemical cell was constructed (55) by cutting a thin slice of reticulated vitreous carbon (RVC) (ERG, Oakland, CA) and sealing it between two quartz microscope slides. Electrical contact was made to the RVC using conducting TRA-DUCT epoxy (Tra-Con, Medford, MA). To prevent breakage at the edge of the slides, the entire exposed portion of the working electrode was coated with epoxy.

All measurements were versus a SCE reference electrode. The counter electrode in these studies was a platinum wire.

HPLC Procedures

Samples were analyzed by high-performance liquid chromatography using a Microsorb (Rainin, Womack, MA) C-18 reverse-phase column (15-cm X 4.6-mm i.d.) and an Altex (Beckman, San Ramon, CA) bonded cyano phase (CN) column (15-cm X 4.6-mm i.d.). Experiments which required gradient elution were performed with a Rainin MacRabbit HPLC gradient system. Isocratic separations were performed with either the Rainin MacRabbit HPLC system or the LC-2600 ISCO syringe pump. The separation procedure on the C-18 reverse-phase column for the oxidation products of 6-thiopurine required isocratic elution with 0.1 M ammonium acetate/methanol (pH 6.9, 98/2, v/v) for 9 minutes followed by a 2 minute ramp from 2% methanol to 30% methanol with a flow rate of 2.0 mL/min. All UV-Vis detection of the oxidation products of 6-thiopurine was performed at 280 nm. This wavelength was chosen because both reactant and products absorbed strongly in this region. The separation procedure on the CN column for the oxidation products of 2-thiopyrimidine was performed isocratically with 0.1 M ammonium acetate/methanol (pH 6.9, 70/30, v/v) with a flow rate of 1.75 mL/min. All UV-Vis detection of the oxidation products of 2-thiopyrimidine was performed at 258 nm. Although neither 2-thiopyrimidine nor its oxidation products have an absorbance maxima at this wavelength, it corresponded to the region of maximum spectral overlap. The ammonium acetate and methanol solutions were filtered through a 0.45 μm filter

Figure 3.1. Structures and molecular weights of compounds used in chromatographic studies.

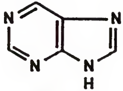

Purine
(MW 120)

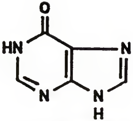

Hypoxanthine
(MW 136)

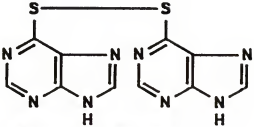

Bis(purinyl) disulfide
(MW 302)

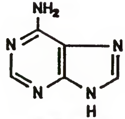

Adenine
(MW 135)

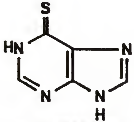

6–Thiopurine
(MW 152)

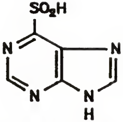

Purine–6–sulfinic acid
(MW 184)

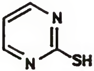

2–Thiopyrimidine
(MW 112)

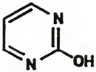

2–Hydroxypyrimidine
(MW 96)

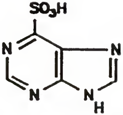

Purine–6–sulfonic acid
(MW 200)

before use. Samples were injected with a Rheodyne (model 7125) injector fitted with a 20μL loop.

Mass Spectrometry

A diagram of the on-line EC/HPLC/TSP/MS/MS system can be seen in Figure 3.2. Details of the electrochemistry/thermospray/tandem mass spectrometry system were described in the experimental section of Chapter 2, and will not be repeated here. Because methanol was used in these studies, the interface was operated in the filament-on mode. At a flow rate of 2.0 mL/min, the typical operating temperatures were tip, 240 C, and source, 290 C. When high concentrations of methanol (30% by volume) were present in the mobile phase, the tip temperature was reduced to 230 C.

Both positive ion and negative ion thermospray mass spectra were obtained by pulsed positive ion/negative ion chemical ionization. Typical conditions for TSP/MS were scan range m/z 120 to 350 in 0.6 s, electron multiplier voltage 1000 V, and preamplifier gain 10^8 VA^{-1}. The lower scan range limit of m/z 120 was normally used to avoid background interference from the ammonium acetate reagent ions. For MS/MS, the scan range and rates varied depending upon the m/z of the parent ion. Collisionally activated dissociation (CAD) studies were carried out using nitrogen as the collision gas (1.9 mTorr) with a collision energy of 30 eV.

Figure 3.2. On-line electrochemistry/high performance liquid chromatography/thermospray/tandem mass spectrometry system.

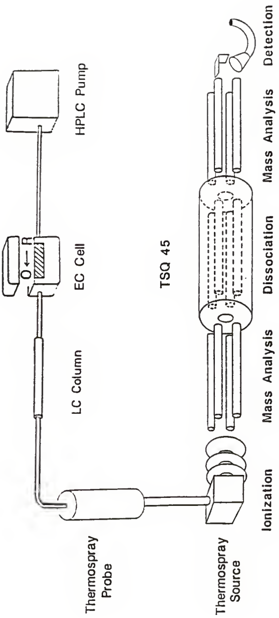
Thermospray Probe
LC Column
EC Cell
O ← R
HPLC Pump
TSQ 45
Thermospray Source
Ionization
Mass Analysis
Dissociation
Mass Analysis
Detection

Detection by UV-Vis Spectrophotometry

6-Thiopurine

High performance liquid chromatography was used on-line with electrochemistry (EC/HPLC) to characterize the oxidation products of 6-TP. Unlike other thiopurines such as 6-TX, purine ring oxidation of 6-TP does not occur even at high potentials because this compound lacks electronegative substituents which make the purine ring vulnerable to oxidation. As a result, in the potential range from +0.0 to 1.0 V vs Pd, only oxidation of the thiol group takes place. Therefore, in order to determine the structures of the oxygen-containing compounds formed when 6-TP is oxidized at high potentials, electrochemically generated products were chromatographically separated and detected with UV-Vis spectrophotometry and TSP/MS.

Figure 3.3 illustrates the on-line EC/HPLC chromatogram of the oxidation products of 6-TP at +0.30 V with UV-Vis detection. At potentials > +0.20 V < +0.50 V vs Pd, a one-electron oxidation of 6-TP occurs resulting in disulfide formation. The peak eluting at 4.5 minutes in Figure 3.3 corresponds to 6-TP, while the peak eluting at ca. 15 minutes has a retention time which is identical to the retention time of the synthesized disulfide. Figure 3.4 illustrates the off-line cyclic voltammogram of 6-TP obtained in stationary solution and shows a single oxidation peak at +0.30 V on the initial sweep to positive potentials. The results shown in Figure 3.3 are in agreement with the cyclic voltammogram shown in Figure 3.4 since disulfide formation is expected at low potentials (65). Although the S-S bond of bis(6-purinyl) disulfide has been shown to be unstable in both acidic and basic media (89), analysis of a fresh solution of synthesized bis(6-purinyl) disulfide by HPLC indicates that the disulfide remains intact during the 15 minute chromatographic procedure used in this study (Figure 3.5). The disulfide does slowly decompose upon standing in pH 7 solution (65,89). Indeed, when a 3 day-old solution of the disulfide was analyzed by HPLC, several new early eluting peaks were observed. However, because the retention times of these early eluting decomposition products did not match the retention times of any of the electrochemically generated products, this work was not pursued. The small peak at ca. 12 minutes in Figure 3.3 has not been identified. However, it is important to note that there is a corresponding peak at ca. 12 minutes in the HPLC/UV-Vis chromatogram of the synthesized disulfide (Figure 3.5).

Electrochemical techniques such as cyclic voltammetry and chronocoulometry rely on monitoring current or charge as a function of potential and time. Unfortunately, these techniques provide little chemical information about the molecular structures of the species which form as a result of electron transfer at the electrode surface. An additional complication is that cyclic voltammetric peaks can sometimes by masked by background discharge. As a result, it is difficult to observe many important reactions which frequently involve multi-electron processes. For example, as shown in Figure 3.3, the cyclic voltammetric peak at ca. +0.30 V corresponds to a one-electron oxidation process which presumably results in the production of a thiyl radical. Recombination of thiyl radicals results in disulfide formation. As can be seen in Figure 3.3, only one oxidation process can be clearly observed in the

Figure 3.3. EC/HPLC/US-Vis chromatogram of the oxidation products of 6-thiopurine at +0.30 V vs. Pd. Reverse-phase C-18 column at a flow rate of 2.0 mL/min with detection at 280 nm. Peak identities are as follows: 1) 6-thiopurine, 2) bis(6-purinyl) disulfide.

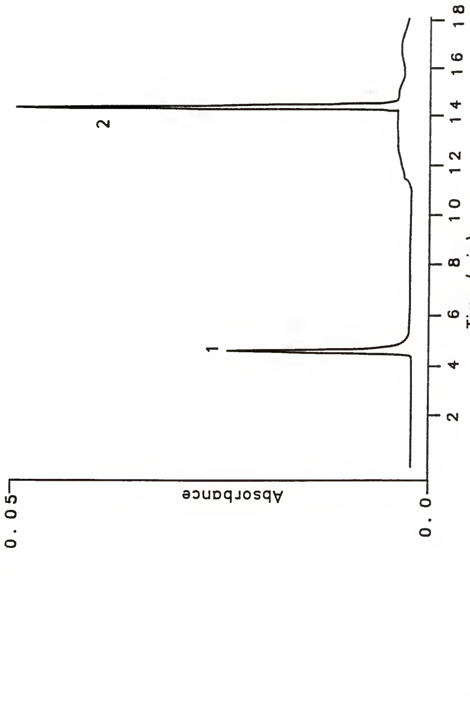
0.05
0.0
Absorbance
Time (min)
2
4
6
8
10
12
14
16
18
1
2

Figure 3.4. Cyclic voltammogram of 90 ppm 6-thiopurine obtained on rough pyrolytic graphite in stationary solution. Scan rate of 200 mV s^{-1}. Palladium reference electrode and 0.1 M ammonium acetate supporting electrolyte.

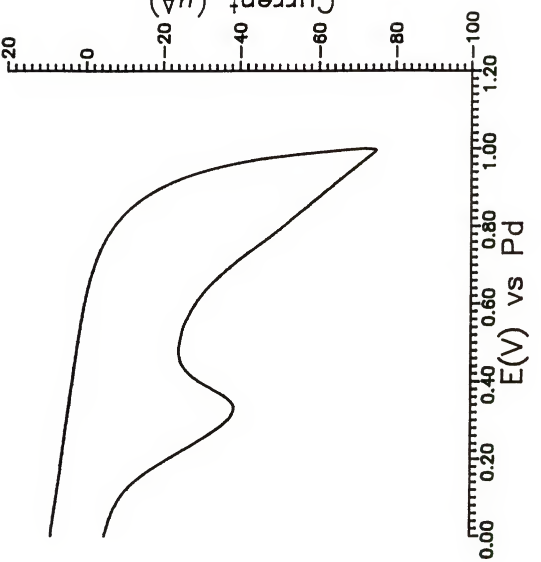
Current (μA)
20
0
-20
-40
-60
-80
-100
E(V) vs Pd
0.00
0.20
0.40
0.60
0.80
1.00
1.20

Figure 3.5. HPLC/US-Vis chromatogram of synthesized bis(6-purinyl) disulfide. Reverse-phase C-18 column at a flow rate of 2.0 mL/min with detection at 280 nm. Peak identities are as follows: 1) 6-thiopurine, 2) bis(6-purinyl) disulfide.

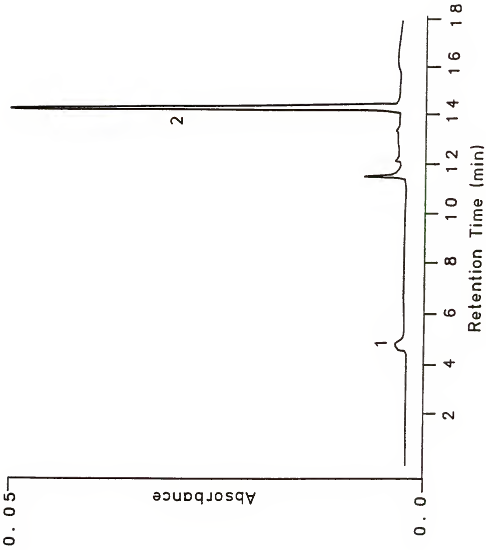
0.05
0.0
Absorbance
1
2
2
4
6
8
10
12
14
16
18
Retention Time (min)

initial sweep to +1.0 V. Indeed, without additional information it would be very difficult to interpret the increase in background as an additional 6-TP oxidation process.

However, using EC/HPLC on-line with UV-Vis spectrophotometry, it is immediately apparent that at potentials > +0.50 V the thiol group of 6-TP can be further oxidized. Figure 3.6 illustrates the on-line EC/HPLC chromatogram of the oxidation products of 6-TP at +0.90 V with UV-Vis detection. Clearly, at least three additional electrochemical processes must occur at potentials > +0.50 V to account for the observed products. The retention times of the synthesized standards of sodium purine-6-sulfinate (RSO_2Na) and sodium purine-6-sulfonate (RSO_3Na) are identical to the retention times of two of the electrochemically generated products. The fact that the electrochemically generated sulfinic and sulfonic acids are hardly retained indicates that these compounds are probably ionized in solution. In addition, a small peak at ca. 3 minutes has been identified as hypoxanthine based on retention time of an authentic sample of hypoxanthine. Loss of the sulfinyl group from sulfinic acids is a fairly general reaction and is analogous to decarboxylation (84). However, these reactions usually occur at high temperatures of 150 C or more (84). Indeed, since the synthesized sulfinate and sulfonate salts are stable in pH 7 solution at room temperature for several hours (65,75,89), the formation of hypoxanthine from simple hydrolysis reactions of either RSO_2Na or RSO_3Na cannot be explained on the time scale of these experiments (ca. 4 minutes). Before successfully synthesizing RSO_2Na according to the method of Doerr (89), it was presumed that the peak at

Figure 3.6. EC/HPLC/UV-VIS chromatogram of the oxidation products of 6-thiopurine at +0.90 V vs Pd. Reverse-phase C-18 column at a flow rate of 2.0 mL/min with detection at 280 nm. Peak identities are as follows: 1) Purine-6-sulfonic acid, 2) purine-6-sulfinic acid, 3) hypoxanthine, 4) purine-6-sulfinamide, 5) bis (6-purinyl) disulfide.

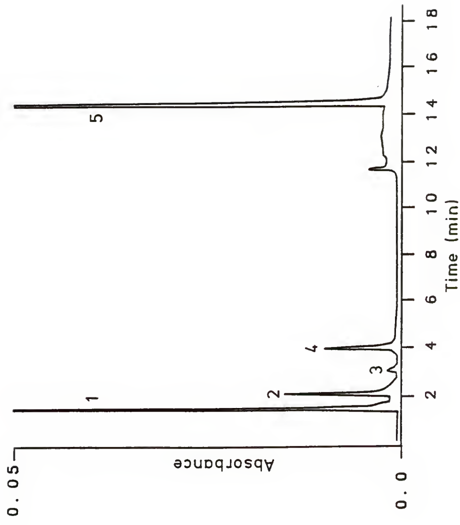
0.05
0.0
Absorbance
1
2
3
4
5
Time (min)
2
4
6
8
10
12
14
16
18

ca. 4 minutes (which has been subsequently identified as purine-6-sulfinamide ($RSONH_2$)) formed a result of a solution-phase reaction between purine-6-sulfinate and the ammonium acetate mobile phase. However, as can be seen in Figure 3.7, the HPLC chromatogram of authentic RSO_2Na in ammonium acetate buffer does not show a peak at this retention time. Therefore, the product with a retention time of 4 minutes probably forms during electrolysis of 6-TP in ammonium acetate buffer (Figure 3.8). Similar on-line electrochemical studies in phosphate buffer do not produce this product. Unfortunately, an authentic sample of $RSONH_2$ could not be obtained and as a result its retention time of ca. 4 minutes could not be verified. The identification of purine-6-sulfinamide by tandem mass spectrometry will be discussed later in this chapter.

Clearly, two different processes occur at potentials > +0.50 V to produce RSO_2H and RSO_3H. In order to form RSO_2H and RSO_3H during the electrooxidation of 6-TP, four and six electrons must be transferred, respectively. It is extremely doubtful that a direct four-electron or six-electron transfer reaction is responsible for the formation of RSO_2H and RSO_3H, respectively, because bis(purinyl) disulfide is still observed at potentials as large as +1.0 V (Figure 3.6).

Figure 3.9 illustrates the results obtained by monitoring the chromatographic peak heights of 6-TP and its oxidation products as a function of electrode potential. Electrooxidation of 6-TP at low potentials produces only 6-TP disulfide (Figure 3.3) via a one-electron oxidation. This process is also responsible for the peak obtained during cyclic voltammetry (Figure 3.4). As can be seen in Figure 3.9, a steady

Figure 3.7. HPLC/UV-Vis chromatogram of synthesized sodium purine-6-sulfinate. Reverse-phase C-18 column at a flow rate of 2.0 mL/min with detection at 280 nm. Peak identities are as follows: 1) Purine-6-sulfonic acid, 2) purine-6-sulfinic acid.

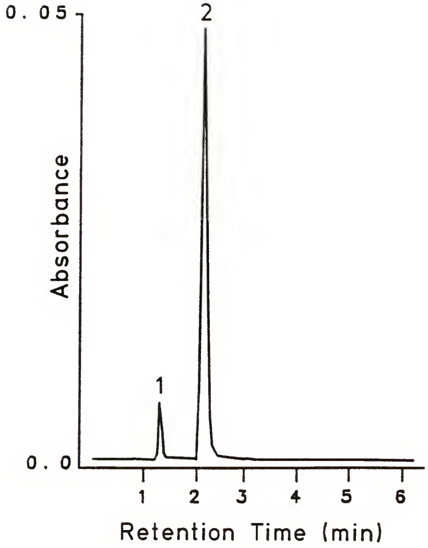
0.05
0.0
Absorbance
1
2
1
2
3
4
5
6
Retention Time (min)

Figure 3.8. Proposed electrochemical oxidation pathway of 6-thiopurine at potentials > +0.50 V vs. Pd.

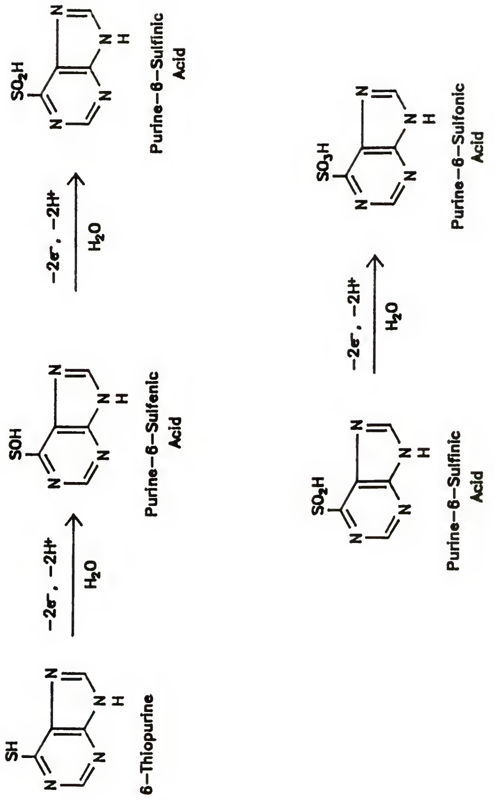
SH
6-Thiopurine
−2e⁻, −2H⁺
H₂O
SOH
Purine-6-Sulfenic Acid
−2e⁻, −2H⁺
H₂O
SO₂H
Purine-6-Sulfinic Acid
SO₂H
Purine-6-Sulfinic Acid
−2e⁻, −2H⁺
H₂O
SO₃H
Purine-6-Sulfonic Acid

state situation occurs for 6-TP oxidation at ca. +0.55 V as a result of this oxidation process. As expected, the production of bis(purinyl) disulfide, the product of this one-electron oxidation process, reaches a maximum at ca. +0.60 V. In theory (55), the plateau region that occurs at +0.55 V in oxidation of 6-TP (Figure 3.9) should roughly correspond to the peak potential obtained in an off-line cyclic voltammetric experiment. However, as can be seen in Figures 3.4 and 3.9, there is some discrepancy between the peak potential of ca. +0.30 V obtained during the off-line cyclic voltammetric experiment and the plateau region of +0.55 V obtained in the on-line EC/HPLC hydrodynamic experiment. This difference can be explained on the basis of adsorption. The response obtained during off-line cyclic voltammetry of 6-TP is due to an adsorption-controlled process (65), whereas in the hydrodynamic experiment diffusing reactants and products are primarily detected because the mobile phase continually flushes out the electrochemical cell during the on-line EC/HPLC experiment. Hence, the discrepancy between the off-line cyclic voltammogram shown in Figure 3.4 and the on-line EC/HPLC/UV-Vis results shown in Figure 3.9 is due to difference in relative sensitivity between the two techniques.

In contrast to off-line cyclic voltammetric results (Figure 3.4), these on-line studies clearly show that at potentials > +0.50 V additional oxidation processes must occur to account for the three products (RSO_2H, $RSONH_2$, and RSO_3H) which are produced during the electrooxidation of 6-TP. As can be seen in Figure 3.9, the processes which account for product formation can be easily separated as a function of electrode potential

Figure 3.9. EC/LC/UV-Vis results of the electrochemical oxidation products of 6-thiopurine. Relationship between product chromatographic peak height and electrode potential.

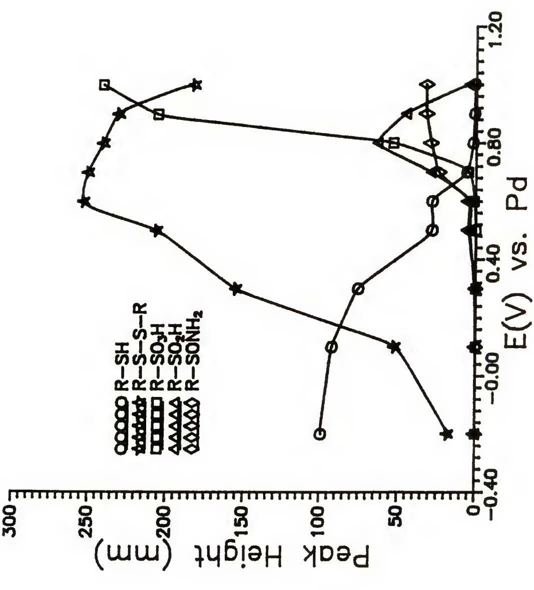
Peak Height (mm)
300
250
200
150
100
50
0
−0.40
−0.00
0.40
0.80
1.20
E(V) vs. Pd
R—SH
R—S—S—R
R—SO$_3$H
R—SO$_2$H
R—SONH$_2$

using on-line EC/LC. It is important to note that these individual processes cannot be observed using cyclic voltammetry or coulometry.

As shown in Figure 3.8, at potentials greater than +0.50 V, a competing two-electron oxidation process may result in the formation of an unstable sulfenic acid (RSOH). Since RSO_2H has been identified, it is reasonable to assume that once RSOH is formed in a two-electron oxidation reaction, at these potentials it could be easily further oxidized to RSO_2H (Figure 3.8). Although this reaction is a net four-electron oxidation process, only two electrons are required to form the primary electrochemical intermediate, RSOH. As can be seen in Figure 3.9, production of RSO_2H reaches a maximum at ca. +0.80 V while production of $RSONH_2$ reaches a steady-state level at +0.80 V.

Additional evidence supporting the formation of RSOH as the primary electrochemical intermediate during 6-TP electrooxidation includes the detection and identification of hypoxanthine and $RSONH_2$. Since hypoxanthine is formed only during electrooxidation of 6-TP at potentials > +0.50 V, it may be the result of a hydration reaction of RSOH during electrooxidation to RSO_2H. Indeed, hypoxanthine also reaches a steady-state level at +0.80 V.

The disappearance of RSO_2H at potentials > +0.80 V and the formation of RSO_3H at potentials where the 6-TP disulfide still forms can still be explained by the same oxidation mechanism. As mentioned previously, at potentials > +0.50 V the RSOH may be further oxidized to RSO_2H. However, at potentials > +0.80 V, it is possible that RSO_2H may be further oxidized to RSO_3H. The results in Figure 3.9 support this since the amount of RSO_3H formed during electrooxidation of 6-TP appears to increase at the expense of RSO_2H formation. In other words, at high potentials RSO_2H which may form in the oxidation of RSOH is immediately oxidized further to RSO_3H. The result is a net six-electron oxidation process. Unlike RSO_2H, production of $RSONH_2$ remains constant at potentials > +0.80 V. Since both products are formed at the same electrode potential (Figure 3.9), they presumably originate from the same precursor, proposed to be RSOH (Figure 3.8). Although a standard of $RSONH_2$ is not available, one possible explanation for the steady-state behavior of $RSONH_2$ is that it may be more stable than RSO_2H towards further oxidation.

As can be seen in Figure 3.9, bis(purinyl) disulfide is formed at potentials as large as +1.0 V. At such large potentials, 6-TP is also proposed to be further oxidized to RSO_2H and RSO_3H in a net four-electron and six-electron oxidation process, respectively. Since the proposed primary electrochemical oxidation intermediate of 6-TP at potentials > +0.50 V, RSOH, is produced by a two-electron oxidation process, it is too difficult explain how the disulfide can be produced via a one-electron oxidation mechanism. However, disulfide formation can be explained on the basis of some recent work by Billmers and Davis (90). In this work, it was suggested that sulfenic acids may be involved in disulfide formation (Equation 3.1).

$$RSOH + RSH \text{ ---->} RSSR + H_2O \qquad (3.1)$$

Disulfide production decreases (Figure 3.9) at potentials > +0.50 V. Unfortunately, it is not possible to distinguish which mechanism is responsible for disulfide formation at such large potentials. The chemistry of sulfenic acids is not well understood due to their unstable and highly reactive nature (74,90,91). Since the principal reactions of sulfenic acids are seldom directly observed, much of their chemistry has been derived indirectly, via rationalization of end reaction products (91).

Thiopurine drugs such as 6-TP are known to be activated by cytochrome P-450 to highly reactive metabolites. Covalent bonding of purine-6-sulfenic acid to liver proteins has been proposed to explain the hepatotoxic effects associated with the drug (74) (Figure 3.10). However, the enzymatic oxidation of 6-TP to its sulfenic acid is difficult to prove due to its reactivity (74). Therefore, alternative techniques such as on-line EC/HPLC/UV-Vis and EC/HPLC/TSP/MS can provide insights into redox and related chemical reactivity of such compounds by providing structural information as well as product identification.

2-Thiopyrimidine

Preliminary characterization of the electrochemical oxidation products of 2-thiopyrimidine (2-TPY) was also performed by EC/HPLC/US-Vis. This work was performed to determine if the oxidation pathway proposed for 6-TP (Figure 3.8) was common for thiols. Unfortunately, the lack of available sulfinate and sulfonate standards of 2-thiopyrimidine severely limited the work. Because of the long chromatographic retention time of the disulfide of 2-TPY on the reverse-phase C-18 column, the chromatographic work was performed on a CN column.

One of the problems associated with monitoring the electrochemical oxidation of 2-TPY with a fixed wavelength detector is that there is very little overlap in the absorbance spectra of 2-TPY and its oxidation

Figure 3.10. Proposed mechanism for the formation of purine-6-sulfenic acid with subsequent binding to liver proteins (74).

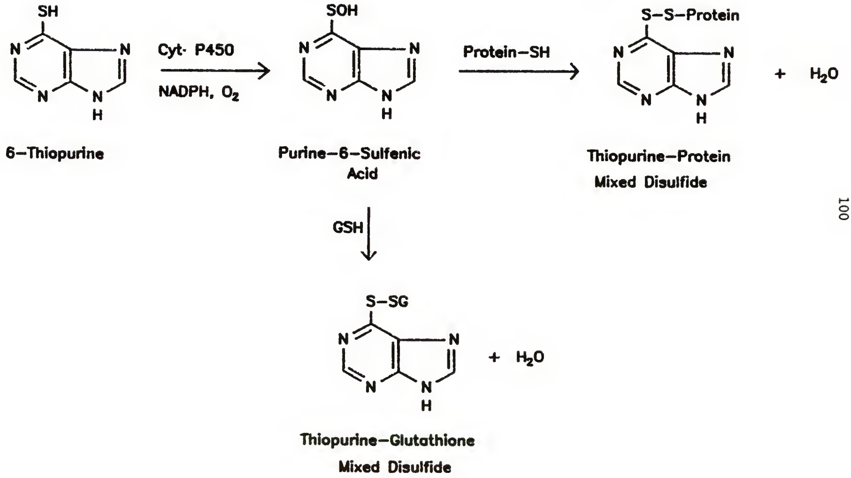
SH
6–Thiopurine
Cyt· P450
NADPH, O_2
SOH
Purine–6–Sulfenic Acid
Protein–SH
S–S–Protein
+ H_2O
Thiopurine–Protein Mixed Disulfide
GSH
S–SG
+ H_2O
Thiopurine–Glutathione Mixed Disulfide

products. This can be seen in Figure 3.11 which illustrates the results of a thin-layer spectroelectrochemical experiment with 2-TPY at +0.90 V. As can be seen in Figure 3.11, before the start of electrolysis, 2-TPY exhibits only one UV peak at 275 nm. As electrolysis proceeds, the UV peak corresponding to 2-TPY at 275 nm decreases while a new UV peak at 237 nm increases. This new UV peak at 237 nm presumably corresponds to the disulfide of 2-TPY. In contrast to the results reported previously for 6-TP, in these studies it is important to note that at the end of electrolysis, 2-TPY and its oxidation product(s) do not absorb strongly in the region (250-260 nm) where the spectra overlap.

Figure 3.12 illustrates the on-line EC/HPLC chromatogram of the oxidation products of 2-TPY at +0.50 V with UV-Vis detection. The peak eluting at ca. 2 minutes in Figure 3.12 corresponds to 2-TPY, while the peak eluting at 3 minutes corresponds to the disulfide of 2-TPY. Figure 3.13 illustrates the off-line cyclic voltammogram of 2-TPY obtained in stationary solution and shows a single oxidation peak at ca. +0.25 V on the initial sweep to positive potentials. The results shown in Figure 3.12 are in agreement with the cyclic voltammogram shown in Figure 3.13 since disulfide formation is expected at low potentials. However, at potentials greater than +0.70 V, several additional oxidation products are observed in the EC/HPLC/UV-Vis chromatogram. As can be seen in Figure 3.14, these small early eluting peaks are not well resolved on the CN column. Since sulfinate and sulfonate standards were not available, it was not possible to confirm the identity of these new peaks. It is important to note that the oxidation processes responsible for the new

Figure 3.11. Thin-layer spectroelectrochemical experiment with 25 ppm 2-thiopyrimidine at +0.90 V vs SCE. Working electrode consisted of reticulated vitreous carbon. Platinum counter electrode. Supporting electrolyte was 0.1 M ammonium acetate buffer, pH 6.9. Curve (1) is 2-thiopyrimidine before electrolysis. Curve (2) is 2 minutes after the start of electrolysis. Curve (3) is the spectrum after 3 minutes and curve (4) is the spectrum obtained after 4 minutes of electrolysis.

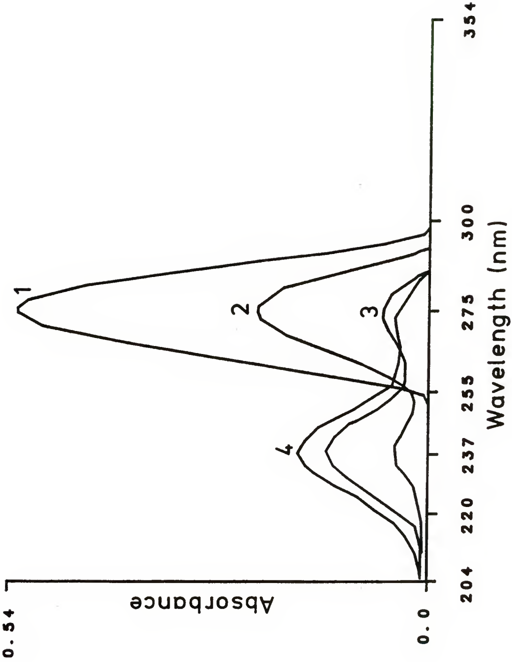
0.54
0.0
Absorbance
204
220
237
255
275
300
354
Wavelength (nm)
1
2
3
4

Figure 3.12. EC/HPLC/US-Vis chromatogram of the oxidation products of 2-thiopyrimidine at +0.50 V vs. Pd. Separation was performed on a bonded CN phase column isocratically with 0.1 M ammonium acetate/methanol (pH 6.9, 70/30, v/v) with a flow rate of 1.75 mL/min. UV-Vis detection at 258 nm. Peak identities are as follows: 1) 2-thiopyrimidine, 2) 2-thiopyrimidine disulfide.

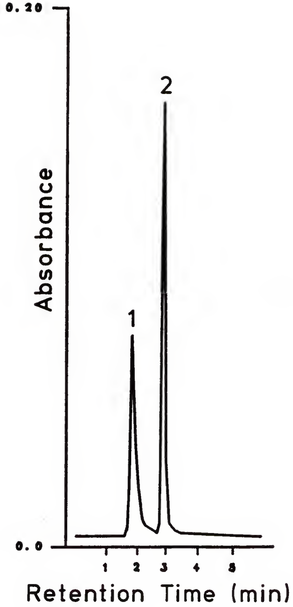
0.20
0.0
Absorbance
1
2
1
2
3
4
5
Retention Time (min)

Figure 3.13. Cyclic voltammogram of 50 ppm 2-thiopyrimidine obtained on rough pyrolytic graphite in stationary solution. Scan rate of 200 mV s^{-1}. Palladium reference electrode and 0.1 M ammonium acetate supporting electrolyte.

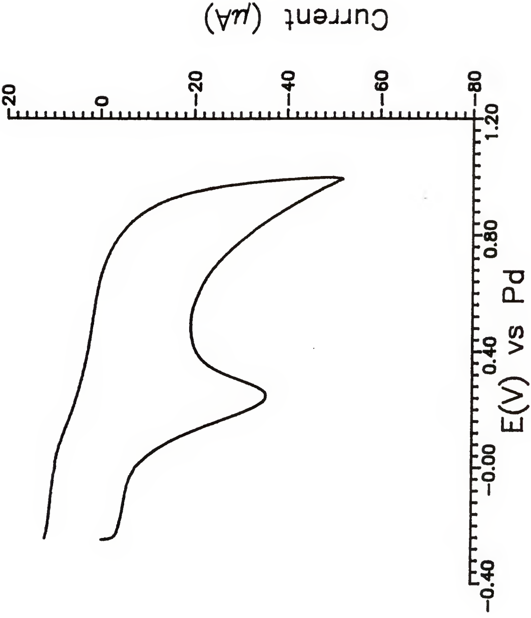
Current (μA)
20
0
−20
−40
−60
−80
1.20
0.80
0.40
−0.00
−0.40
E(V) vs Pd

Figure 3.14. EC/HPLC/US-Vis chromatogram of the oxidation products of 2-thiopyrimidine at +0.90 V vs. Pd. Separation was performed isocratically with 0.1 M ammonium acetate/methanol (pH 6.9, 70/30, v/v) with a flow rate of 1.75 mL/min. UV-Vis detection at 258 nm. Early eluting peak are unidentified oxidation products. Peak 1 is 2-thiopyrimidine disulfide.

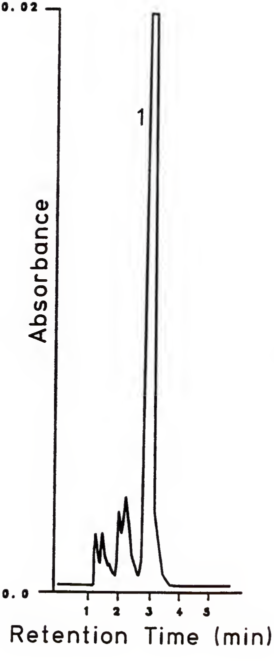
0.02
0.0
Absorbance
1
1
2
3
4
5
Retention Time (min)

chromatographic peaks shown in Figure 3.14 are not observed in the cyclic voltammogram shown in Figure 3.13.

Detection by TSP/MS was only slightly more informative and will be discussed later in the chapter. Although the information obtained about the electrochemical oxidation of 2-TPY is far from complete, it indicates that the thiol group of 2-TPY may be further oxidized.

Detection by Thermospray/Mass Spectrometry

6-Thiopurine

Based on the electrochemical results and the known chemistry of 6-TP [65,10], EC/TSP/MS results with 6-TP were expected to indicate dimer formation by producing intact molecular-type ($[M+H]^+$ and $[M-H]^-$) ions of the disulfide. The results obtained by on-line EC/TSP/MS (no chromatographic column in place) of 6-TP were initially confusing because of the unusual products which were detected and identified. Table 5 lists the ions identified in the EC/TSP mass spectra of 6-TP. The formation of purine, adenine, and hypoxanthine (Table 5) during the electrooxidation of 6-TP must clearly involve substitution reactions prior to mass analysis. Attempts to determine the location of these reactions will be discussed in Chapter 4.

Tandem mass spectrometry was used to confirm the presence of purine, adenine, and hypoxanthine in the EC/TSP mass spectra by comparing the daughter spectra of authentic standards with the daughter spectra of electrochemically generated products. The agreement between daughter ion abundances of standards and electrochemically generated products was

Table 5. Oxidation Products of 6-Thiopurine at +0.70 V Determined by EC/TSP/MS.

Positive Ions m/z	Negative Ions m/z	Structure Correlation
121	-	Purine $[M+H]^+$
136	134	Adenine $[M+H]^+$, $[M-H]^-$
-	194	Adenine $[M+CH_3COO]^-$
137	135	Hypoxanthine $[M+H]^+$, $[M-H]^-$
154	195	Hypoxanthine $[M+NH_4]^+$, $[M+CH_3COO]^-$
153	151	6-thiopurine $[M+H]^+$, $[M-H]^-$
170	-	6-thiopurine $[M+NH_4]^+$
184	182	purine-6-sulfinamide $[M+H]^+$, $[M-H]^-$

generally ±10% relative abundance. The comparison of results is shown in Table 6. Also included in Table 6 is the negative ion daughter mass spectrum of the $[M-H]^-$ ion of $RSONH_2$ at m/z 182. Although the neutral losses which occur during the CAD process of even-electron species such as $[M+H]^+$ and $[M-H]^-$ ions provide important information, additional structural information can be obtained when consecutive neutral losses occur. For example, the 182^- ion initially fragments with a neutral loss of 63 to the 119^- ion (loss of SONH). The 119^- ion corresponds to the $[M-H]^-$ion of purine (MW 120). Additional structural information about the purine ring is obtained because the 119^- ion is further fragmented to the 92^- ion (loss of HCN). The initial loss of the entire modified sulfur moiety provides structural proof to identify this electrochemically generated compound. Also included in Table 6 is the 62^- fragment ion $[SON]^-$ which corresponds to neutral loss of the entire purine molecule.

As discussed previously, electrooxidation of 6-thiopurine in pH 7 ammonium acetate buffer at potentials greater than +0.50 V results in the

Table 6. Comparison of Daughter Spectra of Authentic Standards and Electrochemically Generated Oxidation Products of 6-thiopurine.

Compound	Ion	Authentic Standard	EC Generated Product
Purine (MW 120)	[M+H]$^+$	m/z (%RA)* 121(100) 94(35) 67(10) 52(2)	m/z (%RA) 121(100) 94(36) 67(7) 52(2)
Adenine (MW 135)	[M+H]$^+$	m/z (%RA) 136(100) 119(73) 94(5) 92(5)	m/z (%RA) 136(100) 119(63) 94(1) 92(5)
Hypoxanthine (MW 136)	[M+H]$^+$	m/z (%RA) 137(100) 119(21) 110(23) 82(3) 55(2)	m/z (%RA) 137(100) 120(5) 119(20) 110(26) 94(10) 82(3) 55(2)
Purine-6-sulfinamide (MW 183)	[M-H]$^-$	No standard available	m/z (%RA) 182(13) 119(100) 92(2) 62(2)

* % Relative Abundance

Figure 3.15. EC/HPLC/TSP positive ion mass chromatograms of the oxidation products of 6-thiopurine at +0.60 V. Flow rate 2.0 mL/min., tip temperature 240 C, and source temperature 300 C.

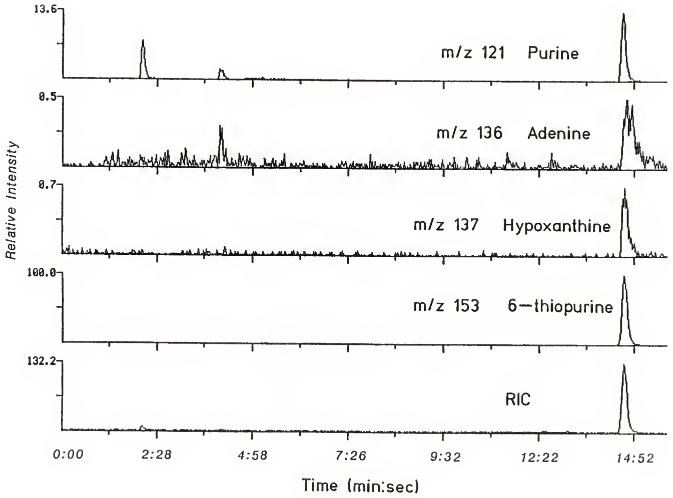
13.6
0.5
0.7
100.0
132.2
Relative Intensity
m/z 121 Purine
m/z 136 Adenine
m/z 137 Hypoxanthine
m/z 153 6—thiopurine
RIC
0:00
2:28
4:58
7:26
9:32
12:22
14:52
Time (min:sec)

formation of purine-6-sulfinic acid (RSO_2H), purine-6-sulfinamide ($RSONH_2$), and purine-6-sulfonic acid (RSO_3H). The on-line EC/HPLC/TSP/MS results obtained for the electrochemical oxidation products of 6-thiopurine at +0.60 V can be seen in Figure 3.15. The positive ion mass chromatograms obtained in an EC/HPLC/TSP/MS experiment (Figure 3.15) are in agreement, when both the retention time and relative intensity are compared, with the positive ion mass chromatograms obtained for the authentic 6-TP disulfide standard (Figure 3.16). Although thermospray is known as a soft ionization technique, as can be seen in Figures 3.15 and 3.16, the disulfide can decompose during the thermospray ionization process producing purine, 6-TP, adenine, and hypoxanthine. However, small amounts of the intact disulfide can sometimes be observed when the thermospray interface is operated in the filament-on mode or if the pH is lowered.

In addition to the peak corresponding to the disulfide of 6-TP at ca. 15 minutes in the EC/HPLC/TSP mass chromatograms in Figure 3.15, two smaller peaks with much shorter retention times (2 and 4 minutes) are also observed. As discussed in a previous section of this chapter, these peaks have been identified as RSO_2H and $RSONH_2$, respectively. Unfortunately, purine-6-sulfinic acid decomposes to purine during the thermospray process (Figure 3.15). Because the thermospray interface operates at high temperatures (240 C), loss of the sulfinyl group from purine-6-sulfinic acid was not unexpected since this is a fairly general reaction for sulfinic acids at temperatures of 150 C or more (84). In addition, the structurally similar $RSONH_2$, which has a retention time of ca. 4 minutes can also decompose to produce purine and small amounts of adenine (Figure 3.15).

Figure 3.17 illustrates the positive ion mass chromatograms obtained in an EC/LC/TSP/MS experiment of 6-TP at +0.90 V. As can be seen in Figure 3.17, the peak at ca. 1 minute produces weak $[M+H]^+$ ions at m/z 201 and m/z 137. These ions correspond to RSO_3H (MW 200) and its decomposition product, hypoxanthine (MW 136), respectively. As can be seen in Figure 3.18, when a sample of synthesized RSO_3Na is analyzed by LC/TSP/MS, in addition to producing a weak $[M+H]^+$ ion at m/z 201, thermospray-induced decomposition produces $[M+H]^+$ ions of adenine (MW 135) and hypoxanthine at m/z 136 and m/z 137, respectively. The second peak, at ca. 2 minutes in Figures 3.15 and 3.17, has been identified as RSO_2H by comparing the retention time of this electrochemically generated product to that of an authentic standard of RSO_2H. As can be seen in Figures 3.15 and 3.17, the electrochemically generated RSO_2H undergoes thermospray-induced decomposition to produce an ion at m/z 121 which corresponds to the $[M+H]^+$ of purine (MW 120). Authentic purine has a retention time of ca. 6 minutes. The third peak at ca. 3 minutes in Figure 3.17 produces only one ion at m/z 137 which corresponds to the $[M+H]^+$ of hypoxanthine. This information is in agreement, when both the retention time and mass spectrum of the peak at ca. 3 minutes are compared, with the positive ion mass chromatogram obtained for authentic hypoxanthine. As can be seen in Figure 3.17, the fourth peak, at ca. 4 minutes, produces a weak $[M+H]^+$ ion at m/z 184 and has been identified as $RSONH_2$ (MW 183). In addition, $RSONH_2$ decomposes to produce purine at m/z 121 and hypoxanthine at m/z 137. Even at potentials as high as +1.0 V, electrooxidation of 6-TP produces bis(purinyl) disulfide. The disulfide which elutes at ca. 15 minutes produces a weak $[M+H]^+$ ion at m/z 303.

Figure 3.16. HPLC/TSP positive ion mass chromatograms of synthesized bis(purinyl) disulfide). Flow rate 2.0 mL/min., tip temperature 240 C, and source temperature 300 C.

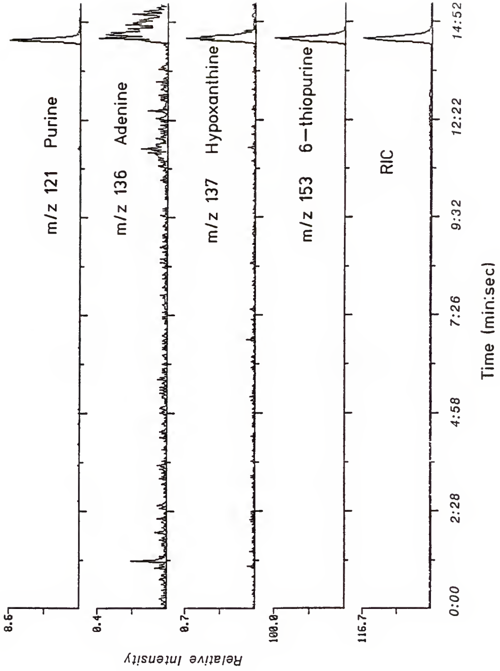
m/z 121 Purine
m/z 136 Adenine
m/z 137 Hypoxanthine
m/z 153 6—thiopurine
RIC
0.6
0.4
0.7
100.0
116.7
Relative Intensity
0:00
2:28
4:58
7:26
9:32
12:22
14:52
Time (min:sec)

Figure 3.17. EC/HPLC/TSP positive ion mass chromatograms of the oxidation products of 6-thiopurine at +0.90 V vs Pd. Flow rate 2.0 mL/min., tip temperature 240 C, and source temperature 300 C. Peak identities are as follows: (1) m/z 201 = $[M+H]^+$ ion of purine-6-sulfonic acid, (2) m/z 121 = $[M+H]^+$ ion of purine, a decomposition product of purine-6-sulfinic acid, (3) m/z 137 = $[M+H]^+$ ion of hypoxanthine, (4) m/z 184 = $[M+H]^+$ ion of purine-6-sulfinamide, (5) m/z 303 = $[M+H]^+$ ion of 6-thiopurine disulfide.

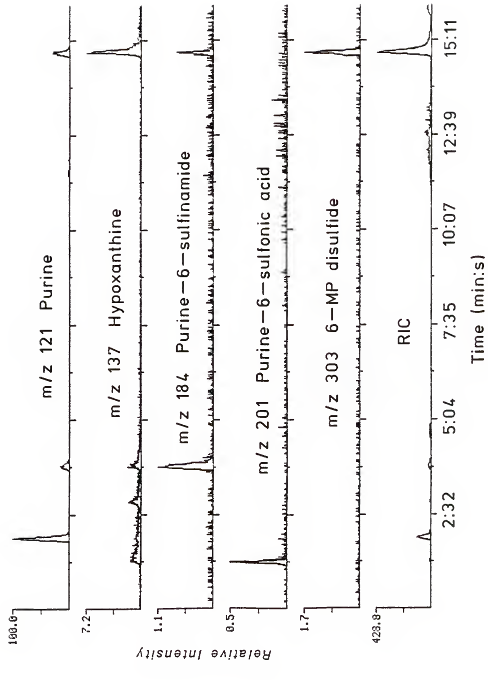
m/z 121 Purine
m/z 137 Hypoxanthine
m/z 184 Purine−6−sulfinamide
m/z 201 Purine−6−sulfonic acid
m/z 303 6−MP disulfide
RIC
100.0
7.2
1.1
0.5
1.7
423.8
Relative Intensity
2:32
5:04
7:35
10:07
12:39
15:11
Time (min:s)

Figure 3.18. HPLC/TSP positive ion mass chromatograms of the thermospray-induced decomposition products of sodium purine-6-sulfonate. Flow rate 2.0 mL/min., tip temperature 240 C, and source temperature 300 C.

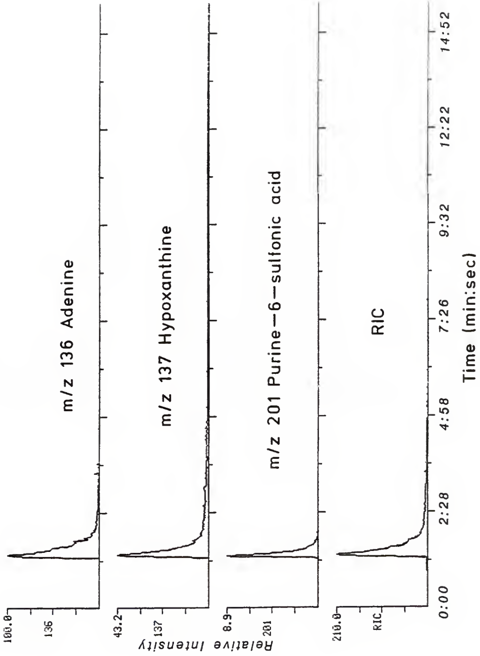
m/z 136 Adenine
m/z 137 Hypoxanthine
m/z 201 Purine—6—sulfonic acid
RIC
Relative Intensity
100.0
136
43.2
137
8.9
201
210.0
RIC
0:00
2:28
4:58
7:26
9:32
12:22
14:52
Time (min:sec)

As shown in Figure 3.17, the positive ion mass chromatograms of 6-TP at +0.90 V indicates that an ion at m/z 121 is produced during the thermospray process of three different chromatographic peaks. Because the MS/MS data shown in Table 6 were obtained in the flow injection mode (i.e. no chromatography), it was considered possible that one of the chromatographic peaks which produces a positive ion at m/z 121 in Figure 3.17 did not correspond a $[M+H]^+$ ion of purine. However, as shown in Figure 3.19, on-line EC/HPLC/TSP/MS/MS provides convincing evidence that purine is indeed formed during the thermospray process of RSO_2H, $RSONH_2$, and bis(purinyl) disulfide.

Mass Spectrometric Hydrodynamic Voltammograms

Figure 3.20 illustrates the mass spectrometric hydrodynamic voltammogram of 6-TP obtained by EC/TSP/MS (no chromatography). As can be seen by noting the intensity of the $[M+H]^+$ ion of 6-TP at m/z 153 in Figure 3.20, oxidation begins at potentials > +0.20 V and reaches a steady-state level at ca. +0.50 V. Since this work was performed in a flow-injection mode, the peak contains a mixture of 6-TP and its oxidation products. As can be seen in Figure 3.19, at +0.50 V the 153^+ ion drops to ca. 70% of its original intensity at +0.10 V. This result is apparently inconsistent with the previous claim of ca. 80% conversion efficiency mentioned in Chapter 2. However, as shown previously in Figures 3.15 and 3.16, bis(purinyl) disulfide, the main product of 6-TP oxidation at these potentials, disproportionates to regenerate 6-TP during thermospray ionization. Hence the intensity of 6-TP during this steady-state region is a combination of unreacted starting material and 6-TP resulting from disproportionation of the disulfide. The mass spectrometric results are in agreement with the off-line cyclic voltammogram also shown in Figure 3.20, since steady-state behavior is expected for both reactants and products when operating in the limiting current region due to the hydrodynamic flow of reactant in the electrolysis cell. However, as can be seen in Figure 3.20, there is an offset between the peak potential obtained in the off-line cyclic voltammogram and the steady-state behavior obtained in the on-line mass spectrometric hydrodynamic voltammogram of 6-TP. As discussed previously, this offset is due to the adsorption of 6-TP on the electrode surface during cyclic voltammetry.

As can be seen in the mass spectrometric hydrodynamic voltammograms of 6-TP (Figure 3.20), at ca. +0.65 V, a second oxidation process appears to occur. This process can be followed by noting the decrease in the intensity of the $[M+H]^+$ ion of 6-TP at m/z 153. A corresponding peak for this second oxidation process is noticeably absent in the off-line cyclic voltammogram (Figure 3.20). This second oxidation process has a dramatic effect on the intensities of the decomposition products purine, hypoxanthine, and adenine (Figure 3.21). As the electrode potential is increased, the intensities of the decomposition products, purine and hypoxanthine, reach a maximum at ca. +0.70 V. This is in agreement with the EC/HPLC/UV-Vis and EC/HPLC/TSP/MS results discussed previously. At potentials greater than ca. +0.70 V, the intensities of purine and hypoxanthine decrease while the formation of adenine is favored. By noting the intensities of the ions in Figure 3.21, it appears that a third oxidation process occurs at ca. +0.70 V since adenine formation is favored. Such behavior would be expected if further electrochemical

Figure 3.19. EC/HPLC/MS/MS mass chromatograms of the oxidation products of 6-thiopurine at +0.90 V. Daughter ions of 121^+. Collision energy 25 eV and nitrogen collision gas pressure 1.9 mTorr. Flow rate 2.0 mL/min., tip temperature 240 C, and source temperature 300 C.

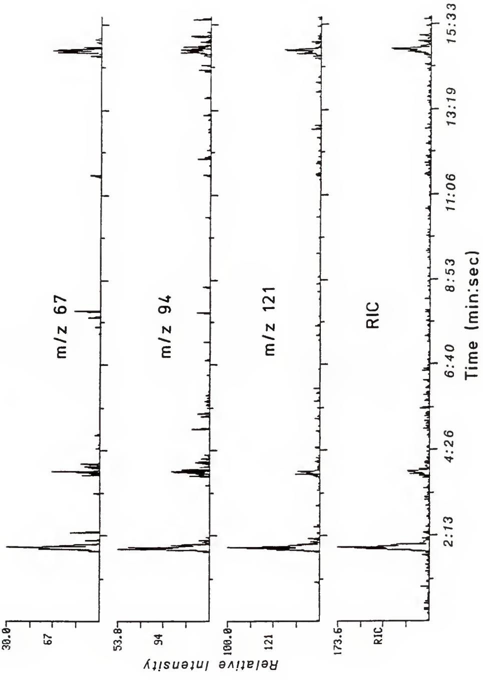
m/z 67
m/z 94
m/z 121
RIC
30.0
67
53.8
94
100.0
121
173.6
RIC
Relative Intensity
2:13
4:26
6:40
8:53
11:06
13:19
15:33
Time (min:sec)

Figure 3.20. Mass spectrometric hydrodynamic voltammogram of 6-thiopurine. Flow rate 2.0 mL/min of 0.1 M ammonium acetate mobile phase. Results obtained by loop injection (i.e. no chromatography). Error bars indicate standard deviation of triplicate measurements. Tip temperature 240 C and source temperature 300 C. Cyclic voltammogram of 90 ppm 6-thiopurine on rough pyrolytic graphite. Scan rate 200 mV s^{-1}. Palladium reference electrode and 0.1 M supporting electrolyte.

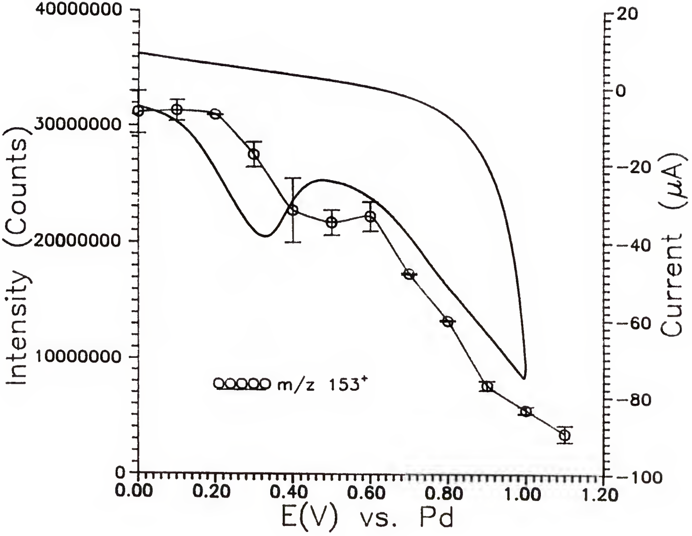
40000000
30000000
20000000
10000000
0
Intensity (Counts)
20
0
−20
−40
−60
−80
−100
Current (μA)
0.00
0.20
0.40
0.60
0.80
1.00
1.20
E(V) vs. Pd
m/z 153⁺

Figure 3.21. Mass spectrometric hydrodynamic voltammograms of the oxidation products of 6-thiopurine. Flow rate 2.0 mL/min of 0.1 M ammonium acetate mobile phase. Results obtained by loop injection (i.e. no chromatography). Error bars indicate standard deviation of triplicate measurements Tip temperature 240 C and source temperature 300 C.

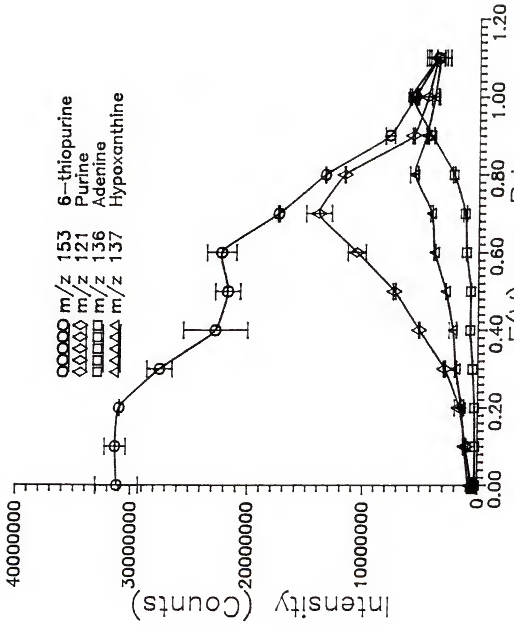
m/z 153 6–thiopurine
m/z 121 Purine
m/z 136 Adenine
m/z 137 Hypoxanthine
Intensity (Counts)
40000000
30000000
20000000
10000000
0
0.00
0.20
0.40
0.60
0.80
1.00
1.20
E(V) vs. Pd

oxidation of 6-TP results in the formation of products which do not readily undergo the same substitution reactions as the products formed at lower potentials. Indeed, this latter observation is consistent with the EC/HPLC/UV-Vis and EC/HPLC/TSP/MS results discussed previously, since the main electrochemical product at large positive potentials, purine-6-sulfonic acid, preferentially decomposes to adenine during the thermospray process (Figure 3.18).

2-Thiopyrimidine

Preliminary characterization of the electrochemical oxidation products of 2-thiopyrimidine by EC/HPLC/UV-Vis indicated disulfide formation occurs at low potentials (Figure 3.12). Figure 3.22 illustrates the EC/HPLC/TSP mass chromatograms of 2-TPY at +0.60 V. As can be seen in Figure 3.22, an intense $[M+H]^+$ ion of 2-TPY disulfide is observed at m/z 223. Unlike the disulfide of 6-TP (Figure 3.16), most of the electrochemically generated 2-TPY disulfide remains intact during the thermospray process. However, as can be seen in Figure 3.22, cleavage of the S-S bond is presumably responsible for the formation of small amounts of 2-TPY (MW 112) (Figure 3.22). It is important to note that thermospray-induced decomposition of 2-TPY disulfide does not result in the formation of 2-hydroxypyrimidine or pyrimidine. Because the chromatographic separation procedure used in the on-line EC/HPLC/TSP/MS studies (0.1 M ammonium acetate/methanol, 60/40, v/v) was different than that in the on-line EC/HPLC/UV-Vis studies (0.1 M ammonium acetate/methanol, 70/30, v/v), the retention times of the standards and electrochemically generated products

Figure 3.22. EC/HPLC/TSP positive ion mass chromatograms of the oxidation products of 2-thiopyrimidine at +0.50 V. Flow rate 1.75 mL/min., tip temperature 228 C, and source temperature 300 C. The chromatographic separation procedure was isocratic (0.1 M ammonium acetate/ methanol, 60/40, v/v).

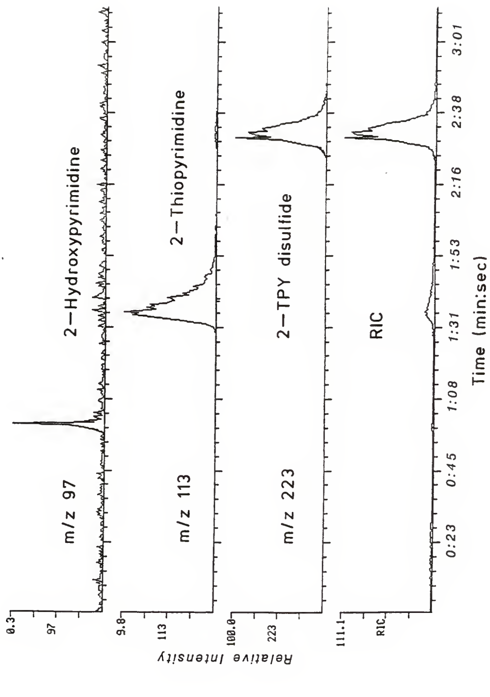
2—Hydroxypyrimidine
m/z 97
2—Thiopyrimidine
m/z 113
2—TPY disulfide
m/z 223
RIC
0.3
97
9.8
113
100.0
223
111.1
RIC
Relative Intensity
0:23
0:45
1:08
1:31
1:53
2:16
2:38
3:01
Time (min:sec)

are ca. 30 s shorter for the EC/HPLC/TSP/MS studies (Figures 3.12 and 3.22).

Also shown in Figure 3.22 is the positive ion mass chromatogram of m/z 97, $[M+H]^+$ of 2-hydroxypyrimidine (MW 96). As discussed previously in this chapter, electrochemically generated sulfinic and sulfonic acids can decompose during the thermospray process. However, as can be seen in Figure 3.23, electrochemically generated 2-hydroxypyrimidine has the same retention time as the authentic standard. Unfortunately, a combination of factors hinders the interpretation of this result. First, the large percentage of methanol in the mobile phase results in very short retention times. As a result, it is entirely possible that a pyrimidine sulfinic or sulfonic acid could have the same retention time as 2-hydroxypyrimidine. Most importantly, the lack of available pyrimidine sulfinic and sulfonic acid standards makes absolute identification impossible.

Analogous to 6-TP, at large positive potentials the thiol group of 2-TPY can be oxidized to oxygen-containing compounds. This process can be seen in Figure 3.24 which illustrates the EC/HPLC/TSP positive ion mass chromatograms of the oxidation products of 2-TPY at +1.1 V. The ions at 97^+ and 223^+ correspond to $[M+H]^+$ of 2-hydroxypyrimidine and 2-TPY disulfide, respectively. The presence of 2-hydroxypyrimidine was confirmed by comparing the daughter mass spectrum of the electrochemically generated product to the daughter mass spectrum of authentic 2-hydroxypyrimidine. As can be seen in Figure 3.24 electrooxidation at +1.1 V produces several new products as evidenced by the mass chromatograms. The new ions at 144^+ and 159^+ presumably correspond to the $[M+H]^+$ of pyrimidine-2-sulfinamide ($RSONH_2$) and pyrimidine-2-sulfonamide (RSO_2NH_2),

Figure 3.23. HPLC/TSP positive ion mass chromatograms of a two component mixture of 2-hydroxypyrimidine and 2-thiopyrimidine. Flow rate 1.75 mL/min., tip temperature 228 C, and source temperature 300 C. The chromatographic separation procedure was isocratic (0.1 M ammonium acetate/ methanol, 60/40, v/v).

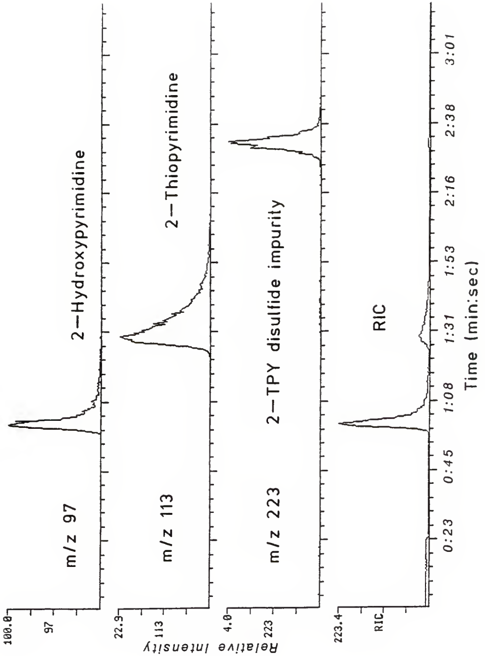
m/z 97
2—Hydroxypyrimidine
m/z 113
2—Thiopyrimidine
m/z 223
2—TPY disulfide impurity
RIC
100.0
97
22.9
113
4.0
223
223.4
RIC
Relative Intensity
0:23
0:45
1:08
1:31
1:53
2:16
2:38
3:01
Time (min:sec)

Figure 3.24. EC/HPLC/TSP positive ion mass chromatograms of the oxidation products of 2-thiopyrimidine at +1.1 V. Flow rate 1.75 mL/min., tip temperature 228 C, and source temperature 300 C. The chromatographic separation procedure was isocratic (0.1 M ammonium acetate/ methanol, 60/40, v/v).

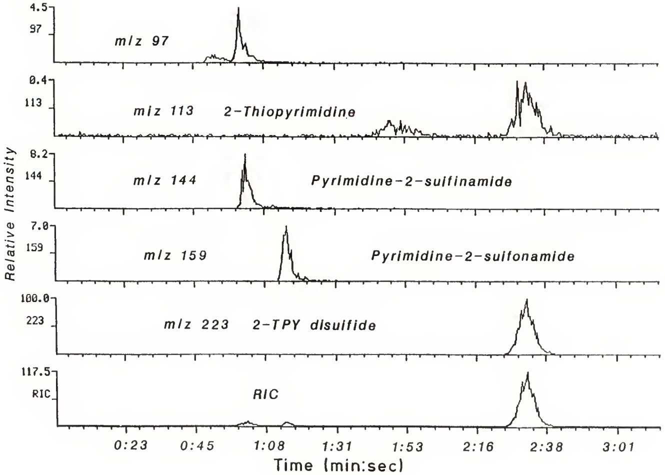
4.5
97
m/z 97
0.4
113
m/z 113
2-Thiopyrimidine
8.2
144
m/z 144
Pyrimidine-2-sulfinamide
7.0
159
m/z 159
Pyrimidine-2-sulfonamide
100.0
223
m/z 223
2-TPY disulfide
117.5
RIC
RIC
Relative Intensity
0:23
0:45
1:08
1:31
1:53
2:16
2:38
3:01
Time (min:sec)

respectively. Although not shown in Figure 3.24, the molecular weights of these compounds were confirmed since $[M+NH_4]^+$ adduct ions of $RSONH_2$ and RSO_2NH_2 are also observed at m/z 161 and m/z 176, respectively.

As shown in Figure 3.24, the 97^+ ion and the 144^+ ion may originate from two different products since the peaks in the mass chromatograms are slightly separated in time. The EC/HPLC/UV-Vis studies of 2-thiopyrimidine at +0.90 V (Figure 3.14), show at least four unresolved compounds elute before 2-TPY disulfide. The EC/HPLC/TSP/MS results shown in Figure 3.24 indicate that three different products (not including 2-TPY and 2-TPY disulfide) are present in the mass chromatograms. Hence, it would appear that one or more of the electrochemical oxidation products of 2-TPY is not amenable to thermospray ionization under the conditions used.

Mass Spectrometric Hydrodynamic Voltammograms

Figure 3.25 illustrates the mass spectrometric hydrodynamic voltammograms of 2-TPY obtained by EC/TSP/MS (no chromatography). Behavior similar to that shown for 6-TP is observed. Oxidation begins at ca. +0.10 V and reaches a steady-state level at potentials > +0.50 V. The oxidation process can be monitored by noting the intensity of the of the $[M+H]^+$ ion of 2-TPY at m/z 113. As can be seen in Figure 3.25, at potentials greater than +0.50 V the 113^+ ion drops to ca. 15% of its original intensity at -0.10 V, comparable to the conversion efficiency obtained for uric acid (Chapter 2).

As is illustrated in Figure 3.25, at ca. +0.50 V, a second oxidation process appears to occur. The $[M+H]^+$ ion of 2-TPY at m/z 113 cannot be

Figure 3.25. Mass spectrometric hydrodynamic voltammograms of the oxidation products of 2-thiopyrimidine. Flow rate 2.0 mL/min of 0.1 M ammonium acetate mobile phase. Results obtained by loop injection (i.e. no chromatography). Tip temperature 240 C and source temperature 300 C.

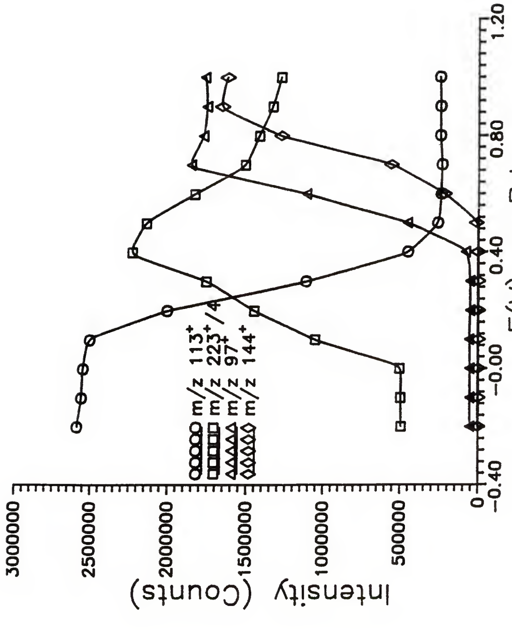
Intensity (Counts)
3000000
2500000
2000000
1500000
1000000
500000
0
−0.40
−0.00
0.40
0.80
1.20
E(V) vs Pd
m/z 113+
m/z 223+/4
m/z 97+
m/z 144+

used to monitor this process since it reaches a steady-state level at potentials > +0.50 V. However, a second oxidation process must occur at potentials > +0.50 V, because the 223^+ ion corresponding to 2-TPY disulfide decreases while the 97^+ ion (2-hydroxypyrimidine) and 144^+ ion (pyrimidine-2-sulfinamide) increase with increasing potential. A corresponding peak for this second oxidation process is noticeably absent in the off-line cyclic voltammogram (Figure 3.13).

The third oxidation process, which is responsible for the formation of pyrimidine-2-sulfonamide, cannot be observed in Figure 3.25 since a positive ion corresponding to pyrimidine-2-sulfonamide at m/z 159 is not observed during EC/TSP/MS. This ion is only observed by EC/HPLC/MS at potentials > +0.80 V. One possible explanation for this phenomenon is the competitive nature of thermospray ionization. Since chemical ionization reactions appear to be the predominant ionization mechanism during the thermospray process (23-33), the relative proton affinities of the species in the electrolysis mixture will largely determine which compounds are ionized. As can be seen in Figure 3.25, 2-TPY disulfide is ionized very efficiently by thermospray. Hence, when 2-TPY disulfide and pyrimidine-2-sulfonamide are present in a mixture, it is possible that 2-TPY disulfide may be preferentially ionized. However, when HPLC is used to chromatographically separate these two compounds, there is no longer a competitive process and both species can be ionized.

Conclusions

Electrochemistry has been used on-line with high performance liquid chromatography with spectrophotometric and mass spectrometric detection.

On-line thermospray/tandem mass spectrometry provided structural information which was necessary for product identification. New insights into redox reactions of two thiols, 6-thiopurine and 2-thiopyrimidine, were provided by this unique instrument combination. In spite of the complexity of the reactions following the electrochemical oxidation of thiols, EC/TSP/MS/MS and EC/HPLC/TSP/MS allows positive identification of many of the products.

At low potentials, the electrochemical oxidation of 6-thiopurine and 2-thiopyrimidine proceeds via a one-electron oxidation resulting in disulfide formation. However, at potentials > +0.50 V, further oxidation of the thiol group of 6-TP results in the formation of oxygen-containing compounds which have been identified as purine-6-sulfinic acid, purine-6-sulfinamide, purine-6-sulfonic acid. The oxygen-containing compounds which form during the oxidation of 2-TPY have been tentatively identified as pyrimidine-2-sulfinamide and pyrimidine-2-sulfonamide. Since the disulfides of 2-TPY and 6-TP continue to form at potentials as large +1.0 V, it is highly unlikely that more than two electrons are directly transferred to form the observed products. It is proposed that purine-6-sulfenic acid and pyrimidine-2-sulfenic acid are formed at potentials > +0.50 V. Further oxidation of these unstable sulfenic acids presumably results in the formation of the observed products. Unfortunately, due to the reactive nature of sulfenic acids, it is difficult to observe these processes directly.

CHAPTER 4
CHARACTERIZATION OF SOLUTION-PHASE AND GAS-PHASE REACTIONS IN ON-LINE ELECTROCHEMISTRY/THERMOSPRAY/TANDEM MASS SPECTROMETRY

Introduction

This chapter deals with attempts to characterize the location of the chemical reactions which occur after on-line electrooxidation. As mentioned in Chapter 2, some of the reactions which follow the initial electron transfer at the electrode are affected by the vaporizer tip temperature of the thermospray probe and the composition of the thermospray buffer. Although tandem mass spectrometry played an important role in the identification of intermediates and products produced during electrooxidation of uric acid and 6-thiopurine, MS/MS did not provide any information concerning the location of the reactions responsible for these products.

Gas-phase studies, solution-phase studies, and on-line high performance liquid chromatography (HPLC) were used to determine the location of the decomposition reactions of bis(purinyl) disulfide under thermospray conditions. Gas-phase studies were performed by modifying a standard Vestec thermospray interface to allow the introduction of nucleophilic gases such as ammonia, methanol, and methylamine to the thermospray source. The solution-phase studies were limited to monitoring the change in ion intensity of the molecular ions of reaction products as a function of vaporizer tip temperature and source temperature. Finally, on-line EC/HPLC/TSP/MS studies, already reported in Chapter 3, were employed.

Experimental

Samples and Reagents

Purine, hypoxanthine, adenine, 6-thiopurine, methylamine (30% solution in water), and uric acid were obtained from Sigma. Methylamine (high purity) and ammonia (high purity) were obtained from Matheson. Methanol, ammonium acetate, and acetic acid were obtained from Fisher Scientific. The reagents were used as received. Typically, twenty microliters of a 80 ppm solution were injected. Methanol was not part of the normal mobile phase and was only added during experiments to determine if new intermediates and products formed as a result of methanolysis reactions. For these experiments, > 15% of methanol by volume was required before methanolysis intermediates and products were observed.

Mass Spectrometry

Two temperatures were monitored in these experiments: the vaporizer exit temperature (tip temperature) and the source block temperature. In the tip temperature profile studies, the tip temperature was varied while the source temperature was held constant at 290 C. At a flow rate of 2.0 mL/min, the typical operating temperatures were tip, 240 C, and source, 290 C. Details of the electrochemistry/thermospray/tandem mass spectrometry system were described in the experimental section of Chapter 2, and will not be repeated here.

In order to introduce various reagent gases capable of acting as nucleophiles into the thermospray source (Figure 4.1), the discharge electrode was removed and a gas-tight fitting was put in its place. Methanol, NH_3, and methylamine were introduced directly into the thermospray source via a variable leak valve (Granville-Phillips) at indicated pressures between 0.35 and 0.42 Torr above the normal operating source pressure at a flow rate of 2.0 mL/min.

Both positive ion and negative ion thermospray mass spectra were obtained by pulsed positive ion/negative ion chemical ionization (PPINICI). Typical conditions for TSP/MS were scan range m/z 120 to 350 in 0.3 s, electron multiplier voltage 1000 V, and preamplifier gain 10^8 VA^{-1}. The lower scan range limit of m/z 120 was normally used to avoid background interference from the ammonium acetate reagent ions. For MS/MS, the scan range and rates varied depending upon the m/z of the parent ion. Collisionally activated dissociation (CAD) studies were carried out using nitrogen as the collision gas (1.8 mTorr) with a collision energy of 25-30 eV.

Tip Temperature and Source Temperature Studies

Oxidation of Uric Acid

Under the conditions employed in these studies, a maximum solvent-buffer ion intensity is obtained at a tip temperature of ca. 240 C for a flow rate of 2.0 mL/min. This tip temperature also produces the most intense reconstructed ion current for samples in EC/TSP/MS. However, as mentioned in Chapter 2, ions have been identified which have maximum

Figure 4.1. Modified Vestec thermospray source. Reagent gases introduced in the oriface normally holding the discharge electrode. Source pressure monitored by replacing vapor temperature sensor with thermogauge.

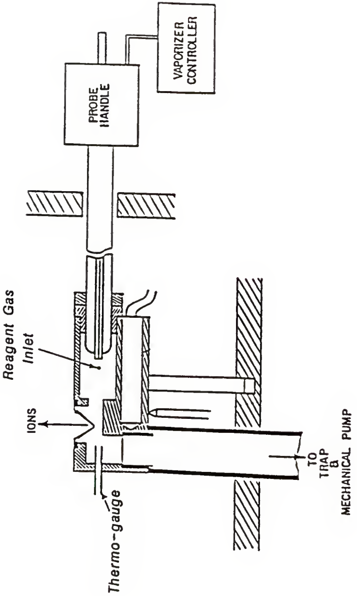
Reagent Gas Inlet
IONS
Thermo-gauge
TO TRAP & MECHANICAL PUMP
PROBE HANDLE
VAPORIZER CONTROLLER

responses at lower tip temperatures. At tip temperatures lower than 240 C, additional ions such as 158^+, 184^+, and 182^- are observed in the EC/TSP mass spectra of uric acid which correspond to intermediates and products formed from amination reactions.

As can be seen in Figure 4.2, the imine double bonds of the primary diimine intermediate make it very susceptible to nucleophilic attack by species such as H_2O, NH_3, methanol, and methylamine. Attack by one molecule of water produces the hydration intermediate (MW 184); attack by one molecule of ammonia will, in analogy, produce the amination intermediate (MW 183). During the thermospray process, some of the ammonium acetate buffer (0.1 M, pH 6.9) will be converted to ammonia and acetic acid. Hydration reactions of intermediates following the electrochemical oxidation of uric acid (Figure 4.2) are well known (37); therefore, the formation of amination intermediates and products under EC/TSP/MS conditions is not surprising, although it has not been previously reported.

As can be seen in Figure 4.3, the intermediates formed as a result of hydration and amination reactions with the quinonoid diimine (Figure 4.2) of uric acid have very different optimum tip temperatures. At tip temperatures > 240 C, the base peak in the negative ion EC/TSP mass spectrum is m/z 183, corresponding to the $[M-H]^-$ of the imine alcohol (hydration) intermediate. However, when the tip temperature is lowered to 231 C, the base peak in the negative ion EC/TSP mass spectrum is m/z 182 corresponding to the imine amine (amination) intermediate. Figure 4.4 illustrates the tip temperature dependence of hydration and amination reactions of another intermediate, the bicyclic imidazolone. The positive

Figure 4.2. Formation of the primary oxidation intermediate of uric acid, which further reacts by nucleophilic addition.

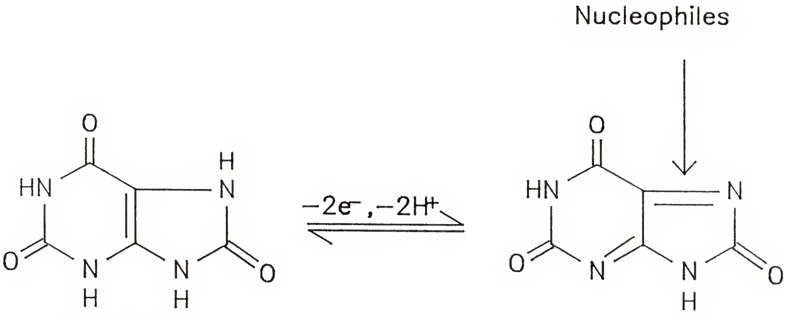

Uric Acid
(MW 168)

Diimine

Figure 4.3. Effect of tip temperature on the $[M-H]^-$ ions of the imine alcohol (hydration) and imine amine (amination), intermediates of uric acid oxidation at +0.50 V. Flow rate of 0.1 M ammonium acetate mobile phase 2.0 mL/min. Source temperature 290 C.

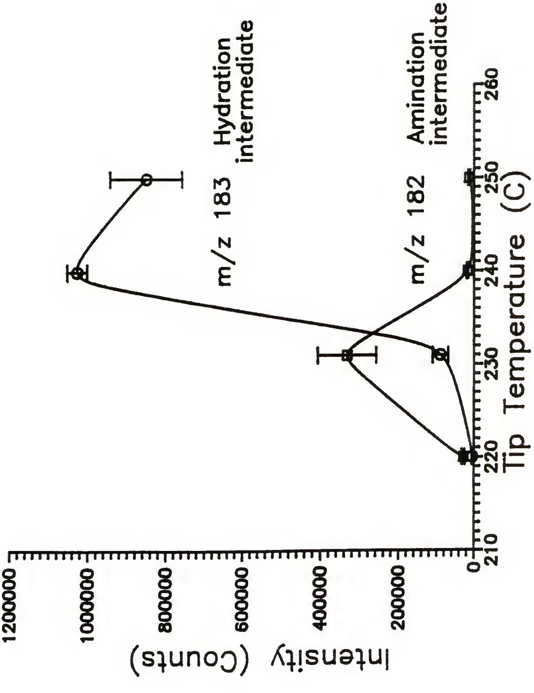
Intensity (Counts)
1200000
1000000
800000
600000
400000
200000
0
210
220
230
240
250
260
Tip Temperature (C)
m/z 183 Hydration intermediate
m/z 182 Amination intermediate

Figure 4.4. Effect of tip temperature on the $[M+H]^+$ ions of allantoin (hydration) and 2-oxo-4-imino-5-ureidoimidazolidine (amination), products of uric acid oxidation at +0.50 V. Flow rate of 0.1M ammonium acetate mobile phase 2.0 mL/min. Source temperature 290 C.

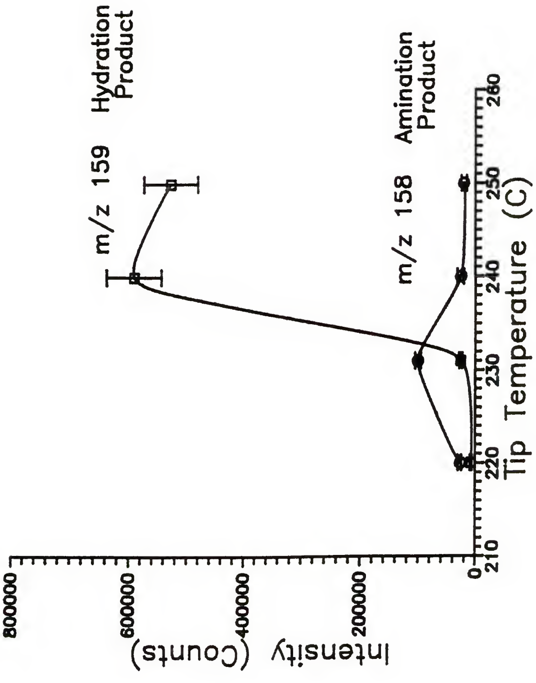
m/z 159
Hydration Product
m/z 158
Amination Product
Intensity (Counts)
800000
600000
400000
200000
0
210
220
230
240
250
260
Tip Temperature (C)

$[M+H]^+$ ion at m/z 158 results from an amination reaction to form 2-oxo-4-imino-5-ureidoimidazolidine, while the positive ion at m/z 159 results from a hydration reaction of the bicyclic imidazolone to form allantoin, the expected final oxidation product of uric acid. The relative mass spectral abundances of the ions corresponding to the amination products (Figures 4.3 and 4.4) vary dramatically over a 20 C range in tip temperature from 230 C to 250 C, indicating that the amination reactions may occur inside the vaporizer probe.

Since vaporizer tip temperature studies (Figures 4.3 and 4.4) indicated differences in tip temperature behavior between the hydration and amination intermediates and products of uric acid, studies were performed to determine if these ions exhibited similar behavior as a function of source temperature. Figure 4.5 illustrates the source temperature profiles of the $[M-H]^-$ ions of the hydration and animation intermediates at m/z 183 and m/z 182, respectively. As can be seen in Figure 4.5, the ion signals due to both intermediates increase with increasing source temperature. It is clear from Figure 4.5 that low source temperatures interfere with the efficient ionization of sample molecules, possibly by disrupting the normal vaporization and chemical ionization processes.

One possible explanation for decreased ionization efficiency at low source temperatures is due to condensation of the vapor on the relatively cool walls of the thermospray source. Indeed, previous studies have shown that low source temperatures may result in increased sample decomposition due to this effect (29). As shown in Figure 4.5, the ion signals reach a maximum at ca. 270 C. Any further increases in source temperature up

Figure 4.5. Effect of source temperature on the $[M-H]^-$ ions of the imine alcohol (hydration) and imine amine (amination), intermediates of uric acid oxidation at +0.50 V. Flow rate of 0.1 M ammonium acetate mobile phase 2.0 mL/min. Source temperature 290 C.

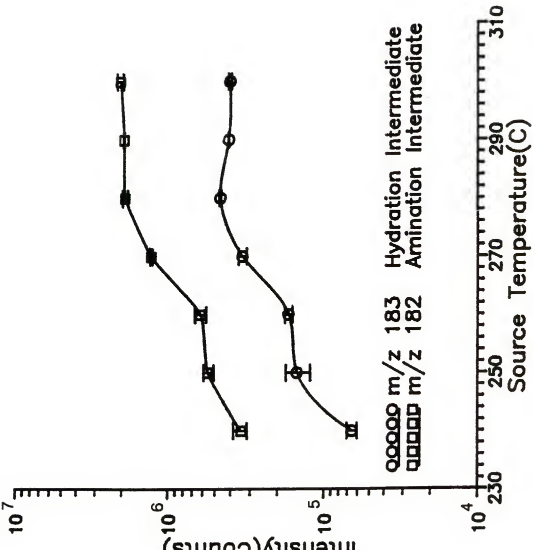
Intensity(Counts)
10^7
10^6
10^5
10^4
230
250
270
290
310
Source Temperature(C)
○○○○○ m/z 183 Hydration Intermediate
□□□□□ m/z 182 Amination Intermediate

to 300 C does not result in an increase in ion signal for either the hydration or the amination intermediate. Although not shown in Figure 4.5, the positive ions at m/z 159 and m/z 158 corresponding to the $[M+H]^+$ of allantoin (hydration product) and 2-oxo-4-imino-5-ureidoimidazolidine (amination product) have similar source temperature profiles. Indeed, all the intermediates and products of uric acid oxidation have virtually identical source temperature profiles.

Oxidation of 6-Thiopurine

In order to help determine the whether the decomposition reactions of bis(purinyl) disulfide occurred in solution prior to analysis by thermospray or during the thermospray vaporization process, some of the data discussed in Chapter 3 using high performance liquid chromatography (HPLC) to separate electrochemically generated products prior to analysis by thermospray/tandem mass spectrometry (EC/HPLC/TSP/MS/MS) will be reviewed. It was postulated that if the decomposition products of the disulfide were formed in solution immediately after electrooxidation, then it should be possible to correlate the retention times of these products with the retention times of the authentic standards. If, on the other hand, these products were formed later, in the thermospray probe or in the source, their retention times should instead be the same as the retention time of the electrochemically generated disulfide which eventually leads to their formation.

Figure 4.6 illustrates the HPLC/TSP positive ion $[M+H]^+$ mass chromatograms of a four-component mixture of authentic purine (MW 120),

Figure 4.6. HPLC/TSP/MS positive ion mass chromatograms of 4-component purine mixture using a reverse-phase C-18 column at a flow rate of 2.0 mL/min (details provided in Chapter 3). Tip temperature 240 C, source temperature 290 C.

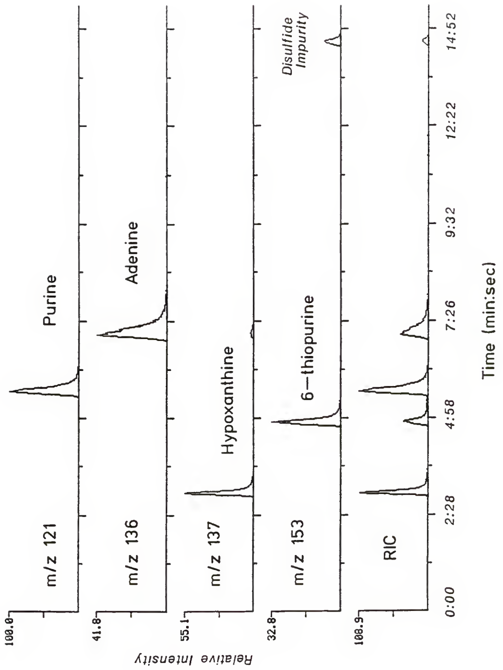

Relative Intensity
100.0
41.8
55.1
32.8
108.9
m/z 121
m/z 136
m/z 137
m/z 153
RIC
Purine
Adenine
Hypoxanthine
6—thiopurine
Disulfide
Impurity
0:00
2:28
4:58
7:26
9:32
12:22
14:52
Time (min:sec)

adenine (MW 135), hypoxanthine (MW 136), and 6-TP (MW 152) which are chromatographically separated in ca. 8 minutes. The small peak at ca. 14 minutes (Figure 4.6) is due to trace amounts of the 6-TP disulfide, an impurity in the 6-TP standard. The retention time of this small peak at ca. 14 minutes is identical to the retention time of the synthesized disulfide.

As was discussed in Chapter 3, when a sample of synthesized 6-TP disulfide is analyzed by HPLC/TSP/MS, decomposition reactions occur during the thermospray vaporization process which result in the formation of 6-thiopurine, adenine, hypoxanthine, and purine. The fact that all four products originate from a single peak with a retention time of ca. 14 minutes reveals that decomposition of the disulfide occurs somewhere during the thermospray ionization process. This is clear from the comparison of the retention times of the authentic purine standards (Figure 4.6) with the retention times of the decomposition products arising from the disulfide (Figure 3.16).

Some ions produced during the vaporization process of 6-TP oxidation products do not follow the tip temperature profiles of the authentic standards. In these studies, we have identified the ions which show different responses. These ions have been identified as decomposition products of purine-6-sulfinate, purine-6-sulfinamide, purine-6-sulfonate, and bis(purinyl) disulfide.

Figure 4.7 compares the tip temperature profiles of authentic adenine and hypoxanthine with the tip temperature profiles of electrochemically generated adenine and hypoxanthine. At ca. +0.50 V, the main product of 6-TP oxidation is the disulfide. As can be seen in Figure 4.7, the

Figure 4.7. Effect of tip temperature on the decomposition products of 6-thiopurine oxidation at +0.50 V. Comparison of the $[M+H]^+$ ions of hypoxanthine and adenine produced during the decomposition of bis(purinyl) disulfide and authentic standards of hypoxanthine and adenine. Flow rate of 0.1M ammonium acetate mobile phase 2.0 mL/min. Source temperature 290 C.

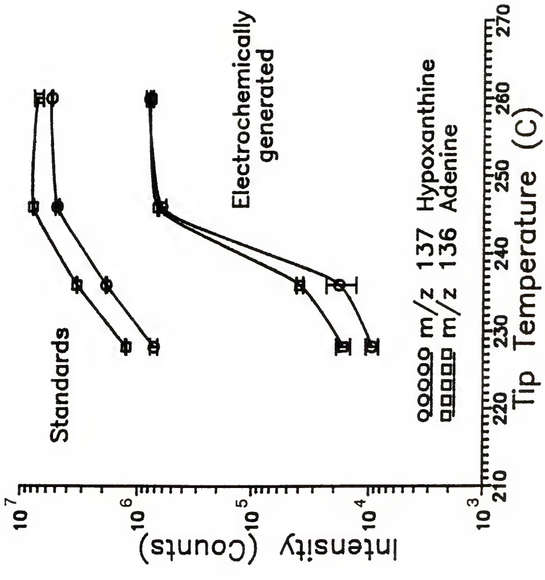
Intensity (Counts)
10^7
10^6
10^5
10^4
10^3
210
220
230
240
250
260
270
Tip Temperature (C)
Standards
Electrochemically generated
○○○○○ m/z 137 Hypoxanthine
□□□□□ m/z 136 Adenine

profiles differ dramatically at tip temperatures lower than 240 C due to the decreased efficiency with which bis(purinyl) disulfide decomposes and undergoes amination and hydration reactions. The decreased intensity of products at lower tip temperatures indicates that the decomposition reactions of the disulfide which result in the formation of adenine and hypoxanthine occur inside the vaporizer probe.

Unlike the tip temperature studies, source temperature studies did not reveal any significant differences between the profiles of the electrochemically generated products and the authentic standards. It is important to point out that no additional decomposition products are observed in any of the studies when the lower m/z scan limit is reduced from m/z 120 to m/z 25.

Mobile-Phase and Gas-Phase Studies

Methylamine

Methylamine was chosen as a model nucleophile in these experiments because its chemical properties and reactivity are similar to those of ammonia and it is not present in the normal thermospray buffer. When a mixture of 0.1 M methylamine (CH_3NH_2) and 0.1 M ammonium acetate (pH 6.9) is used as a buffer during the electrooxidation of 6-TP at +0.50 V, a new product, N6-methyladenine (MW 149), is observed in the positive and negative ion EC/TSP mass spectra. Figure 4.8 illustrates positive ion $[M+H]^+$ mass chromatograms of the decomposition products of 6-TP oxidation. As can be seen in Figure 4.8, the $[M+H]^+$ ion of N6-methyladenine at m/z 150 is produced when methylamine is present in the buffer in addition to

Figure 4.8. EC/TSP/MS positive ion mass chromatograms of the products of 6-thiopurine oxidation at +0.50 V. Triplicate loop injections of 60 ppm 6-thiopurine (no chromatography) with a mobile phase consisting of 0.1 M methylamine/ammonium acetate at a flow rate of 2.0 mL/min. Tip temperature 240 C, source temperature 290 C.

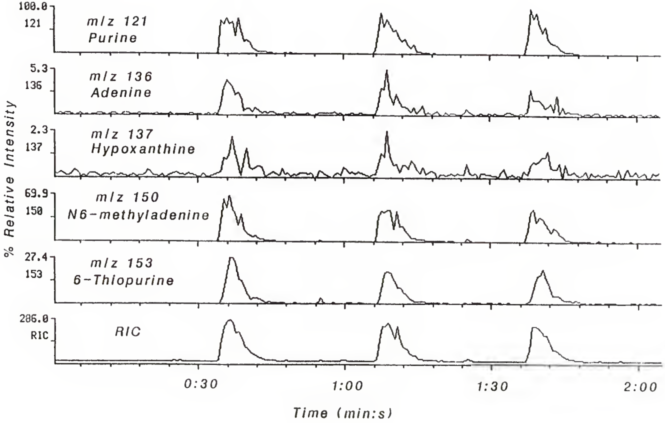
100.0
121
m/z 121
Purine
5.3
136
m/z 136
Adenine
2.3
137
m/z 137
Hypoxanthine
69.9
150
m/z 150
N6-methyladenine
27.4
153
m/z 153
6-Thiopurine
286.0
RIC
RIC
% Relative Intensity
0:30
1:00
1:30
2:00
Time (min:s)

the normal decomposition products of the disulfide discussed previously. N6-methyladenine is formed as a result of the bis(purinyl) disulfide undergoing reactions with methylamine in analogy to the reaction with NH_3 which forms adenine. Although not shown in Figure 4.8, the $[M-H]^-$ ion of N6-methyladenine at m/z 148 can be also observed in the negative ion mass spectrum.

To determine if the reaction with methylamine can occur inside the thermospray source, methylamine (0.4 torr) was introduced into the thermospray source while 0.1 M ammonium acetate was used as the buffer. Under these conditions, no gas-phase reactions between methylamine and the electrochemical oxidation products of 6-TP are observed. Specifically, N6-methyladenine was not detected (Table 7). Hence, it appears that methylamine must be present in the solution phase (buffer solution) to react and form N6-methyladenine.

Ammonia

Additional results supporting the conclusion that the reactions occurred in the solution phase and not in the gas phase were obtained using 0.1 M acetic acid (pH ~ 2.8) as the buffer while introducing ammonia (0.4 torr) into the thermospray source. In this way, ammonia was present only in the thermospray source (gas phase) and was not part of the solution phase. When acetic acid buffer is introduced into the thermospray source via the vaporizer probe, it reacts with ammonia inside the thermospray source and undergoes an acid-base reaction to form the primary reagent ions (NH_4^+ and CH_3COO^-) which are responsible for chemical ionization of the analyte. Although the production of the reagent ions in this manner is different than that in the normal thermospray process, many of the chemical ionization reagent ions are the same. Under the conditions employed in this study, adenine is not observed following electrooxidation of 6-thiopurine in acetic acid buffer at +0.50 V. However, hypoxanthine and purine are still observed in addition to small amounts of the intact disulfide (Table 7). For comparison purposes, the decomposition products obtained under normal thermospray conditions using 0.1 M ammonium acetate buffer are also included in Table 7.

Table 7. Products Formed in Solution-Phase and Gas-Phase Studies During Electrooxidation of 6-thiopurine.

	Reagent Gas Added to Source	Buffer Composition	Products
1)	none	0.1 M NH_4OAC	purine, hypoxanthine, 6-thiopurine, and adenine
2)	none	0.1 M NH_4OAC/CH_3NH_2	purine, hypoxanthine, 6-thiopurine, adenine, and N6-methyl adenine
3)	CH_3NH_2	0.1 M NH_4OAC	purine, hypoxanthine, 6-thiopurine, and adenine
4)	NH_3	0.1 M HOAC	purine, hypoxanthine, 6-thiopurine, and bis(purinyl) disulfide

Table 7 summarizes the results obtained in the solution-phase and gas-phase studies of the oxidation products of 6-thiopurine. As can be seen in Table 7, decomposition of the disulfide results in the formation of purine, hypoxanthine, and adenine when the normal thermospray buffer (0.1 M NH_4OAC) is used. When methylamine is present in the buffer, reactions occur and result in the formation of N6-methyladenine. However, when methylamine is added to the gas phase, N6-methyladenine is not detected.

Additional evidence of solution-phase reactions was obtained when acetic acid was used as the buffer and ammonia was introduced into the thermospray source. As can be seen in Table 7, when ammonia was introduced into the thermospray source, adenine was not detected.

Conclusions

When high performance liquid chromatography (HPLC) was used on-line with electrochemistry to separate stable oxidation products prior to analysis by thermospray/tandem mass spectrometry, it was apparent that many of the products observed in on-line EC/TSP/MS result from chemical reactions of unstable compounds with components of the mobile phase during the thermospray process.

Unlike the tip temperature studies, source temperature studies did not indicate the presence of temperature-dependent chemical reactions. Most importantly, since no gas-phase reactions were observed, it appears that these reactions may occur mainly in the solution phase. Therefore, the reactions responsible for the formation of hypoxanthine, N6-methyladenine, and adenine probably occur inside the vaporizer probe during the thermospray vaporization process, rather than in the thermospray ion source.

CHAPTER 5
CHARACTERIZATION OF THERMOSPRAY/TANDEM MASS SPECTROMETRY FOR STUDYING ENZYMATIC OXIDATION PATHWAYS

Introduction

This chapter describes studies to characterize the enzymatic oxidation pathway of uric acid on-line with thermospray/tandem mass spectrometry. The main objective was to determine the capability of TSP/MS/MS to monitor on-line enzymatic reactions. For this purpose, the peroxidase-catalyzed reaction of uric acid was investigated on-line with TSP/MS/MS.

The premise of using electrochemical methods to provide useful and unique insights into the pathways and mechanisms of enzymatic redox reactions of biologically important molecules has been described in Chapter 1. The oxidation pathway of uric acid was first characterized by EC/TSP/MS/MS in Chapter 2 to serve as a model for the enzymatic work. Indeed, Dryhurst and co-workers has shown considerable similarity between the pathways of the electrochemical and peroxidase-catalyzed oxidation of uric acid (37,40,46,47,60,62,92) using off-line methods. In these studies, electrochemical measurements were successfully combined off-line with spectroelectrochemistry, gel-permeation chromatography, liquid chromatography, and gas chromatography/mass spectrometry to provide a complete picture of the reaction products. However, these techniques could provide only limited information about intermediates and the solution reactions which followed the initial electrochemical or enzymatic oxidation. As will be demonstrated in this chapter, combining enzymes on-line with mass spectrometry allows rapid identification of intermediates and products produced in enzymatic-catalyzed reactions.

Experimental

Samples and Reagents

Uric acid, hydrogen peroxide, and type VIII horseradish peroxidase (EC 1.11.1.7) were obtained from Sigma (St. Louis, MO). The reagents were used as received. In all enzymatic studies, uric acid was dissolved in, and then injected into, a mobile phase which consisted of aqueous 0.1 M ammonium acetate (pH ~ 5.0) and 50 μM hydrogen peroxide. Twenty microliters of a 50 ppm solution were injected.

Enzyme Binding Procedure

In order to prepare the enzyme reactor, forty milligrams of type VIII horseradish peroxidase were dissolved in 50 mL of 0.1 M phosphate buffer (pH ~7) and were recirculated through a Hydropore-EP Affinity (Rainin) column (10-cm X 4.6-mm i.d.) for twenty-four hours at a flow rate of 0.1 mL/min. The Hydropore-EP Affinity stationary phase consists of a modified hydrocarbon spacer arm attached to a silica support (Figure 5.1). The enzyme, which contains primary amine functional groups, can react with the epoxide moiety located on the end of the spacer arm to form a covalent bond with the stationary phase. Upon completion of the binding procedure, the column was flushed with 50 mL of 0.1 M phosphate buffer (pH ~7) and

Figure 5.1. Diagram of enzyme coupling to stationary phase by reaction with epoxide.

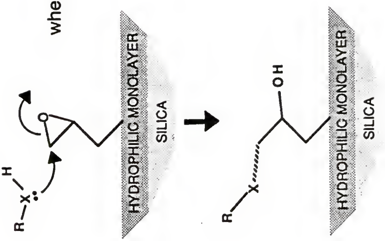

where X = -NH_2 or -SH

stored in phosphate buffer at 10 C. The enzyme solution, ammonium acetate buffer, and phosphate buffer solutions were filtered through a 0.45 μm filter before use.

In the standard UV-Vis assay for determining the activity of horseradish peroxidase, the enzyme catalyzed the oxidation of pyrogallol to purpurogallin in the presence of H_2O_2. The low solubility of the product does not interfere with the UV-Vis assay. However, because of possible contamination of the column due to precipitation of the low solubility purpurogallin product, this assay was not used to determine the activity of the enzyme covalently bonded to the column. During a month-long period after the column was prepared using the binding procedure, uric acid was oxidized with no apparent decrease in enzyme activity. The enzymatic conversion efficiency was determined by monitoring the $[M-H]^-$ ion of uric acid; after a reaction time of 2 minutes with 50 μM H_2O_2 (flow rate through column 0.75 mL/min), the intensity of the $[M-H]^-$ ion decreases to ~ 15% of its original intensity.

Mass Spectrometry

The thermospray interface was operated in the filament-on mode, in contrast to the previous studies in Chapter 2, which did not employ a filament. As discussed in Chapters 1 and 2, the inner diameter of the stainless steel capillary inside the vaporizer probe appears to play an important role in the vaporization and subsequent ionization processes of uric acid. The diameter of the capillary may be reduced by partial clogging due to the deposition of involatile residue from the mobile phase or uric acid which itself has low solubility. Unfortunately, the mass spectrometric signal due to the $[M-H]^-$ ions of uric acid decreases after prolonged use (6 hours) of the vaporizer probe, possibly due to widening of the capillary orifice. Therefore, the filament-on mode was used to improve sensitivity for uric acid. Since this process cannot be precisely controlled, daily variations (30%) in the intensity of the ions corresponding to uric acid can occur. At a flow rate of 2.0 mL/min, the operating temperatures were tip, 238 C, and source, 290 C. Both positive ion and negative ion thermospray mass spectra were obtained by pulsed positive ion/negative ion chemical ionization (PPINICI). Typical conditions for TSP/MS were scan range m/z 120 to 350 in 0.3 s, electron multiplier voltage 1000 V, and preamplifier gain 10^8 VA^{-1}.

Uric Acid

Previous off-line studies of the enzymatic oxidation of uric acid have shown that several types of horseradish peroxidase are capable of catalyzing the oxidation of uric acid (92). However, it has been shown that at pH 5, type VIII horseradish peroxidase exhibited the highest activity towards uric acid (92). In the enzyme studies, an enzyme reactor with the covalently bonded horseradish peroxidase was placed on-line with TSP/MS (Figure 5.2). The primary goal of these studies was to assess the capability of TSP/MS to monitor the intermediates and products of the enzymatic reaction on-line.

The amount of time the substrate, uric acid, reacts with the enzyme can be varied by changing the flow rate of the mobile phase through the enzyme reactor. Since thermospray is a flow-rate dependent technique, a tee was placed after the enzyme column and make-up flow from another HPLC

Figure 5.2. Diagram of on-line enzyme/thermospray/tandem mass spectrometry system.

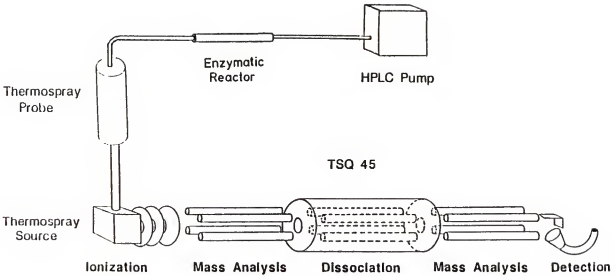
Thermospray
Probe
Enzymatic
Reactor
HPLC Pump
TSQ 45
Thermospray
Source
Ionization
Mass Analysis
Dissociation
Mass Analysis
Detection

pump was used so that the thermospray interface always operated at a combined flow rate of 2.0 mL/min (Figure 5.3). Figure 5.4 illustrates the intensities of the $[M-H]^-$ ions of uric acid (MW 168), imine amine intermediate (MW 183), and the final product allantoin (MW 157) as a function of enzymatic reaction time. The data at zero time were obtained without the enzyme reactor. The intensity of the $[M-H]^-$ ion of uric acid at m/z 167 decreases as the enzymatic reaction time increases as a result of increasingly complete enzymatic conversion. Consequently, as the reaction time increases the intensities of the ions corresponding to intermediates (e.g., imine amine, $[M-H]^-$ m/z 182, Figure 5.4) and product (e.g., allantoin, $[M-H]^-$ m/z 157, Figure 5.4) of uric acid oxidation increase. Because it was considered possible for uric acid to undergo non-enzymatic oxidation in the presence of H_2O_2, the H_2O_2 oxidation of a structurally similar compound, 9-methyl uric acid, was also examined. As discussed previously, ions corresponding to uric acid are often difficult to observe. Therefore, 9-methyl uric acid was chosen because it produces a more intense and reproducible thermospray signal. The enzymatic and electrochemical properties of 9-methyl uric acid are very similar to those of uric acid (46,62,93). The addition of 50 μM H_2O_2 to a solution of 50 ppm 9-methyl uric acid did not cause any detectable oxidation during a 30 minute time period at room temperature, or during the thermospray process.

To characterize the intermediates and products formed in the enzymatic oxidation, both the positive ion and negative ion thermospray mass spectra were examined. As discussed in Chapter 2, this is because certain species will have favorable proton affinities to produce only an $[M+H]^+$ ion or an

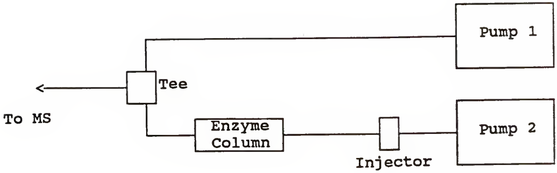

Figure 5.3. Diagram of 2-pump system used to vary flow rate through the enzyme column. Constant flow rate of 2.0 mL/min entered the mass spectrometer.

Figure 5.4. Mass spectrometric monitoring of reactant, intermediate, and product produced during the peroxidase-catalyzed oxidation of uric acid; m/z 167 = $[M-H]^-$ of uric acid, m/z 182 = $[M-H]^-$ of imine amine, m/z 157 = $[M-H]^-$ of allantoin. Error bars indicate standard deviation of triplicate measurements. Mobile phase pH 5.0, 0.1 M ammonium acetate (50 μM H_2O_2) at a total flow rate of 2.0 mL/min. Tip temperature 238 C, source temperature 300 C.

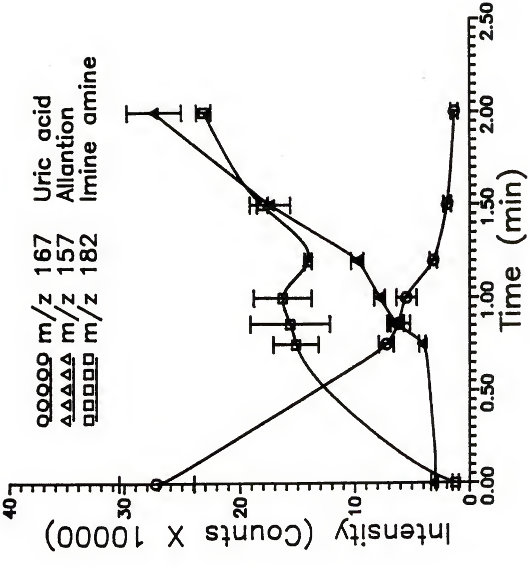
OOOOO m/z 167 Uric acid
ΔΔΔΔΔ m/z 157 Allantion
□□□□□ m/z 182 Imine amine
0.00
0.50
1.00
1.50
2.00
2.50
Time (min)
0
10
20
30
40
Intensity (Counts X 10000)

$[M\text{-}H]^-$ ion via gas-phase proton transfer reactions with the ammonium acetate buffer. Figures 5.5a and 5.5b illustrate typical electrochemistry/thermospray positive ion and negative ion mass spectra of the oxidation intermediates and products of uric acid.

The positive and negative ion mass spectra of the enzymatic oxidation intermediates and products obtained when the uric acid substrate residence time in the reactor is ca. 1 min (flow rate 1.5 mL/min through reactor) are shown in Figures 5.6a and 5.6b. Comparison of the mass spectra obtained from the peroxidase-catalyzed and the electrochemical oxidation of uric acid shows that the intermediates and products formed in the enzymatic oxidation are the same as those formed in the electrochemical oxidation. However, the positive ion mass spectrum of the enzymatic oxidation products contains two as yet unidentified ions (130^+, 131^+) which are not present in the electrochemical mass spectrum.

Although most of the same ions are present in both the electrochemical and enzymatic mass spectra, their relative abundances are different. The product/intermediate intensity ratios $134^+/184^+$ ($[\text{5-hydroxyhydantoin}+NH_4]^+$/$[\text{imine amine}+H]^+$) and $175^-/182^-$ ($[\text{alloxan monohydrate}-CO_2+\text{acetate}]^-$/$[\text{imine amine}-H]^-$) are an indication of the degree of completeness of the reactions which follow the initial oxidation process (Figure 2.6). For example, the electrochemical oxidation is characterized by a $134^+/184^+$ intensity ratio of 0.30 and a $175^-/182^-$intensity ratio of 0.25 (Figures 5.5a and 5.5b). However, in the enzymatic oxidation the $134^+/184^+$ intensity ratio is 1.8 while the $175^-/182^-$ intensity ratio is 0.45 (Figures 5.6a and 5.6b). These intensity ratios indicate that the hydration reactions of the oxidation

Figure 5.5. Positive ion (a) and negative ion (b) spectra of the electrochemical oxidation intermediates and products of uric acid. Tip temperature 238 C and source temperature 290 C. Flow rate 2.0 mL/min. Peaks marked by an asterisk have been identified in Table 1.

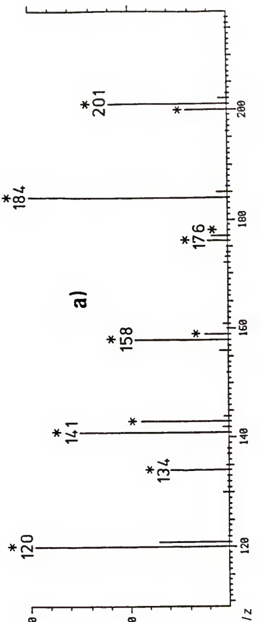
a)
% Relative Abundnace
100.0
50.0
m/z
120
140
160
180
200
*120
*134
*141
*
*158
*
*176
*
*184
*201
*

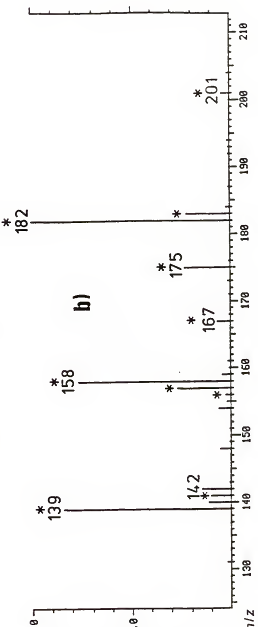
b)
% Relative Abundance
100.0
50.0
m/z
130
140
150
160
170
180
190
200
210
*139
142
*
*158
*
*
*167
*175
*182
*
*201

Figure 5.6. Positive ion (a) and negative ion (b) spectra of the enzymatic oxidation intermediates and products of uric acid. Enzyme-substrate reaction time of 1 min. Flow rate through reactor 1.5 mL/min. Total flow rate 2.0 mL/min. Tip temperature 238 C and source temperature 290 C. Peaks marked by an asterisk have been identified in Table 1.

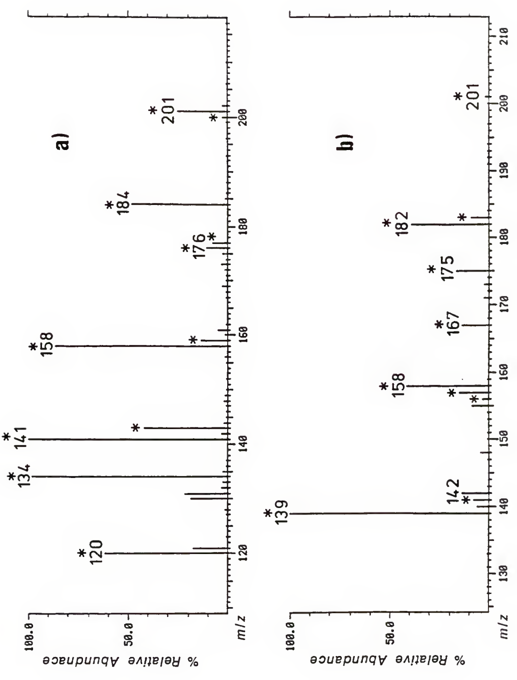
a)
% Relative Abundnace
100.0
50.0
m/z
120
140
160
180
200
*120
*134
*141
*
*158
*
*176
*
*184
*201
*
b)
% Relative Abundance
100.0
50.0
m/z
130
140
150
160
170
180
190
200
210
*139
142
*
*158
*
*
*167
*175
*182
*
*201

intermediates (Figure 2.6) have proceeded to a greater extent in the enzymatic oxidation, leading to greater intensities of the final products. The enzymatically generated intermediates have a much longer residence time in solution (reaction time of 1 min. at a flow rate of 1.5 mL/min through reactor) than the electrochemical intermediates (500 ms) and this accounts for the different intensity ratios. For example, during the 1 min. enzymatic reaction period, some of the imine alcohol and imine amine (Figure 2.6) can decay to the bicyclic imidazolone as well as to the final products. Greater relative abundances of the 139^- and the 141^+ ions in Figures 5.6a and 5.6b which correspond to the $[M-H]^-$ and $[M+H]^+$ of the bicyclic imidazolone indicate this in fact occurs.

Unfortunately, the peak detected following enzymatic oxidation is much broader (peak width ca. 14 s) because of dispersion after a 1 min. reaction than is the peak following electrochemical oxidation (peak width ca. 4 s). In addition, the make-up flow added at the tee dilutes the reaction mixture as it exits the enzyme reactor. These two factors contribute to the low intensities observed in the on-line enzymatic studies and prevent acquisition of reasonable daughter mass spectra by MS/MS.

Conclusions

Because of the similarities observed in the previous off-line studies of the electrochemical and peroxidase-catalyzed oxidation of uric acid, it was anticipated that on-line EC/TSP/MS/MS would serve as a useful model in the present work. It is clear from the information described in this chapter that EC/TSP/MS/MS data served as a useful model for the on-line enzyme/TSP/MS work. Products and intermediates formed as a result of the enzymatic oxidation of uric acid were monitored as the enzyme-substrate reaction time was varied. In the enzymatic oxidation of uric acid with peroxidase and H_2O_2, the same intermediates and products were observed as in the electrochemical oxidation. The primary intermediate can follow three distinct reaction pathways to produce the identified final products. The final enzymatic and electrochemical oxidation products which were observed in these studies were urea, CO_2, alloxan, alloxan monohydrate, allantoin, 5-hydroxyhydantoin-5-carboxamide, and parabanic acid.

Since the electrochemical and enzymatic thermospray mass spectra are virtually identical, both reactions must follow similar reaction pathways. Therefore, it is reasonable to postulate that the structures of the intermediates and products elucidated by EC/TSP/MS/MS reflect those of the enzymatically generated compounds of the same m/z ratio. Hence, the observation of the imine alcohol and the imine amine intermediates during the peroxidase-catalyzed oxidation supports the formation of a diimine intermediate after the enzymatic oxidation of uric acid. This work clearly shows that enzymatic reactors coupled on-line with TSP/MS can provide useful information about both intermediates and products formed during an enzymatic reaction.

CHAPTER 6
CONCLUSIONS AND FUTURE WORK

This thesis reports the first on-line coupling of electrochemistry with tandem mass spectrometry. It also represents the first time that electrochemical and enzymatic redox reactions have been studied by such on-line techniques. The significance of this work is three-fold: first and foremost, this on-line technique offers for the first time the ability to directly monitor reactants, short-lived intermediates, and products of electrochemical and enzymatic reactions as a function of reaction conditions, with high selectivity for individual components; second, the use of MS/MS provides structural confirmation of the intermediates and products produced; third, coupling via a thermospray interface permits on-line analysis of involatile compounds. In addition, it was determined that nucleophilic reactions of reactive species (e.g. intermediates and unstable compounds) in the thermospray process occur in the solution phase in the heated capillary, not in the gas phase in the ion source.

Uric acid served as a model compound and was used to demonstrate the feasibility and capabilities of this approach. The EC/TSP mass spectra of uric acid reveal a complete picture of intermediates and products formed upon electrooxidation. Due to the soft nature the thermospray ionization process, the EC/TSP mass spectra of uric acid contained mainly $[M+H]^+$ and $[M-H]^-$ ions of intermediates and products. The mass spectra of electrolysis mixtures are therefore easily interpreted to provide molecular weight information. Indeed, if the interface produced abundant fragment ions for the individual mixture components, the mass spectra of the electrolysis mixtures would be almost impossible to interpret. Although molecular weight information is important, lack of structural information severely limits compound identification by TSP/MS. As a result, tandem mass spectrometry played an important role in product identification. MS/MS was used to confirm the presence of products by comparing the daughter spectra of authentic standards to the daughter spectra of electrochemically generated products. In addition, the capabilities of the triple quadrupole mass spectrometer were used to elucidate the structures of intermediates and previously unknown products.

All of the previously reported major products of uric acid oxidation and several of the previously proposed intermediates have been identified and characterized by EC/TSP/MS/MS. The intermediates resulting from the addition of water, ammonia, and methanol to the primary electrochemical intermediate of uric acid (diimine) have been identified by their MS/MS fragmentation patterns. This work provides convincing evidence that the primary electrochemical intermediate of uric acid oxidation has a diimine structure. In addition, identification of the bicyclic intermediate confirms that uric acid can follow three different reactions pathways after electrooxidation.

The use of high performance liquid chromatography (HPLC) to separate electrochemical oxidation products prior to detection by mass spectrometry and by UV-Vis absorption spectrophotometry has also been demonstrated. It was shown that unique insights into reaction pathways of thiols could be obtained as a function of electrode potential. In contrast to off-line cyclic voltammetric results, which show a single voltammetric oxidation peak, the on-line EC/HPLC studies clearly show that several additional oxidation processes occur during the oxidation of thiols which account for the new products observed at high potentials. These individual processes cannot be observed using cyclic voltammetry or coulometry; however, using on-line EC/HPLC, the processes responsible for product formation can be easily separated as a function of electrode potential.

It was also shown that product formation was affected by the vaporizer tip temperature of the thermospray probe and the composition of the thermospray buffer. These reactions are not affected by changes in the thermospray source temperature or gas composition in the ion source. In addition, it was shown that unstable compounds which undergo decomposition reactions during thermospray ionization can form additional products. Either hydration or amination reactions of the initial electrochemical oxidation intermediates or products can occur with pH 7 ammonium acetate buffer. This has been shown for uric acid and the oxidation products of 6-thiopurine.

Methylamine was added to the normal ammonium acetate buffer and products resulting from reactions between unstable electrochemically generated compounds and methylamine were observed. When modifications allowed methylamine to be introduced as a gas into the thermospray source, products resulting from reactions between unstable electrochemically generated compounds and methylamine were not observed. This and similar gas-phase studies indicate that many of the decomposition products observed during on-line EC/TSP/MS are the result of solution-phase chemical reactions occurring primarily inside the thermospray probe.

The utility of combining enzymes on-line with thermospray/mass spectrometry was also demonstrated. Products and intermediates formed as a result of an enzymatic-catalyzed reaction were monitored on-line with mass spectrometry. The enzymatic and electrochemical oxidation pathways of uric acid determined on-line with thermospray/tandem mass spectrometry were compared. In the enzymatic oxidation of uric acid with peroxidase and H_2O_2, the same intermediates and products were observed as in the electrochemical oxidation. Since the ion intensities of the intermediates and products of the enzymatic-catalyzed reaction were much lower than those obtained electrochemically, the EC/TSP/MS/MS data were used as a model for the enzymatic studies. It was also shown that products and intermediates formed as a result of the enzymatic-catalyzed reaction of uric acid could be monitored on-line as the enzyme-substrate reaction time was varied.

Possible future directions of this project include using thermospray probes equipped with replaceable vaporizer tips of various diameters. The use of such probes may reduce the large day-to-day variations in analyte signals. Using small diameter tips will result in the production of smaller droplets. As a result, the new probes may improve the sensitivity and reproducibility of this method.

With the appropriate stable isotopic standards, future work could also include quantitation of electrochemical and enzymatically generated oxidation products. Future work should also include optimizing chromatographic conditions to separate the oxidation products of 2-

thiopyrimidine prior to detection by UV-Vis absorption spectrophotometry and thermospray/mass spectrometry, since the on-line EC/HPLC studies of 2-thiopyrimidine were not complete.

A long-range future project could center on the design and construction of a continuous flow FAB probe to incorporate a three-electrode assembly on the FAB probe tip. One version of the may modified probe tip might consist of three concentric rings of platinum, electrically isolated from one another by a press-fit teflon sleeve. The inner ring or disk would serve as the working electrode while the middle platinum ring would be used as a pseudo-reference electrode. The outer ring would act as a counter electrode. Such a method would allow the detection of reactive intermediates and products under controlled electrochemical conditions. Because the working electrode acts as the FAB target, the system should have excellent time resolution. As an instrumental method, it can provide unique insight into the reactivity of xenobiotics which require activation.

Finally, the on-line EC/TSP/MS/MS and enzyme/TSP/MS/MS methods developed here have potential for fundamental and analytical studies other than investigation of the oxidation of purines. Clearly, these techniques could be employed to provide insights into metabolic pathways of other drugs and pesticides. Furthermore, this approach should prove useful in helping us to better understand basic electrochemical and enzymatic processes such as thermodynamics, kinetics, and adsorption effects.

LITERATURE CITED

1. Bruckenstein, S.; Gadde, R.R. J. Am. Chem. Soc. 1971, 93, 793.

2. Bruckenstein, S.; Petek, M. J. Electroanal. Chem. 1973, 42, 397.

3. Bruckenstein, S.; Gadde, R.R. J. Electroanal. Chem. 1974, 50, 163.

4. Bruckenstein, S.; Grambow, L. Electrochimica Acta 1977, 22, 377.

5. Bolzan, A.E.; Iwasita, T.; Vielstich, W. J. Electrochem. Soc. 1987, 134, 3052.

6. Pinnick, W.J.; Lavine, B.K.; Weisenberger, C.R.; Anderson, L.R. Anal. Chem. 1980, 52, 1102.

7. McFadden, W.H. "Techniques Combined Gas Chromatography/Mass Spectrometry"; John Wiley and Sons: New York, 1973.

8. Brockman, T.J.; Anderson, L.B. Anal. Chem. 1984, 56, 207.

9. Blakely, C.R.; Carmody, J.J.; Vestal, M.L. J. Am. Chem. Soc. 1980, 102, 5931.

10. Hambitzer, G.; Heitbaum, J. Anal. Chem. 1986, 58, 1067.

11. Getek, T.A. "Proceedings of the 35th ASMS Conference on Mass Spectrometry and Allied Topics" 1987, 443.

12. Volk, K.J.; Lee, M.S.; Yost, R.A.; Brajter-Toth, A. Anal. Chem. 1988, 60, 720.

13. Getek, T.A.; Korfmacher, W.A. "Proceedings of the 36th ASMS Conference on Mass Spectrometry and Allied Topics" 1988, 452.

14. Bartmess, J.E.; Phillips, L.R. Anal. Chem. 1987, 59, 2014.

15. Kim, H.Y.; Pilosof, D.; Dyckes, D.F.; Vestal, M.L. J. Am. Chem. Soc. 1984, 106, 7304.

16. Stachowiak, K.; Wilder, C.; Vestal, M.L.; Dyckes, D.F. J. Am. Chem. Soc. 1988, 110, 1758.

17. Voyksner, R.D.; Pack, T. "Proceedings of the 36th ASMS Conference on Mass Spectrometry and Allied Topics" 1988, 1138.

18. Barber, M.; Bordoli, R.S.; Sedgwick, R.D.; Tyler, A.N. J. Chem. Soc. Chem. Commun. 1981, 325.

19. Smith, L.A.; Caprioli, R.M. Biomed. Mass Spectrom. 1984, 11, 392.

20. Caprioli, R.M.; Fan, T.; Cottrell, J.S. Anal. Chem. 1986, 58, 2949.

21. Caprioli, R.M.; DaGue, G.; Fan, T.; Morre, W.T. Biochem. Biophys. Res. Comm. 1987, 146, 291.

22. Caprioli, R.M.; Fan, T. Biochem. Biophys. Res. Comm. 1986, 141, 1058.

23. Caprioli, R.M. "Proceedings of the 36th ASMS Conference on Mass Spectrometry and Allied Topics" 1988, 549.

24. Blakely, C.R.; McAdams, M.J.; Vestal, M.L. J. Chromatogr. 1980, 158, 261.

25. Blakely, C.R.; Carmody, J.J.; Vestal, M.L. Anal. Chem. 1980, 52, 1636.

26. Blakely, C.R.; Carmody, J.J.; Vestal, M.L. Clin. Chem. 1980, 26, 1467.

27. Covey, T.R.; Bruins, A.P.; Henion, J.D. Org Mass Spectrom. 1988, 23, 178.

28. Voyksner, R.D. Org. Mass Spectrom. 1987, 22, 513.

29. Lee, M.S. Ph.D. Dissertation, University of Florida, Gainesville, 1987.

30. Bursey, M.M. Anal. Chem. 1985, 57, 2597.

31. Alexander, A.J.; Kebarle, P. Anal. Chem. 1986, 58, 470.

32. Smith, R.W.; Parker, C.E.; Johnson, D.M.; Bursey, M.M. J. Chromatogr. 1987, 394, 261.

33. Parker, C.E.; Smith, R.W.; Gaskell, S.J.; Bursey, M.M. Anal. Chem. 1986, 58, 1661.

34. McLean, M.A.; Flory, D.A.; Vestal, M.L. "Proceedings of the 36th ASMS Conference on Mass Spectrometry and Allied Topics" 1988, 1229.

35. Geerdink, B.; Maris, F.A.; DeJong, G.J.; Frei, R.W.; Brinkman, U.A. J. Chromatogr. 1987, 394, 51.

36. McFadden, W.H.; Lammert, S.A. J. Chromatogr. 1987, 385, 201.

37. Dryhurst, G. "Electrochemistry of Biological Molecules"; Academic Press: New York, 1977.

38. McKenna, K.; Brajter-Toth, A. J. Electroanal. Chem. 1987, 233, 49.

39. Kraske, P.J.; Brajter-Toth, A. J. Electroanal. Chem. 1986, 207, 101.

40. Goyal, R.N.; Brajter-Toth, A.; Dryhurst, G. J. Electroanal. Chem. 1982, 131, 181.

41. Childers-Peterson, T.E.; Brajter-Toth, A. J. Electroanal. Chem. 1988, 239, 161.

42. Childers-Peterson, T.E.; Brajter-Toth, A. Anal. Chim. Acta. 1987, 202, 167.

43. Astwood, D.; Lippincott, T.; Deysher, M.; D'Amico, C.; Szurley, E.; Brajter-Toth, A. J. Electroanal. Chem. 1983, 159, 295.

44. Miner, D.J.; Rice, J.R.; Riggin, R.M.; Kissinger, P.T. Anal. Chem. 1981, 53, 2258.

45. Andrews, P.A.; Pan, Su-Shu; Bachur, N.R. J. Am. Chem. Soc. 1986, 108, 4158.

46. Dryhurst, G.; Kadish, K.M.; Scheller, F.; Renneberg, R. "Biological Electrochemistry"; Academic Press: New York, 1982.

47. Brajter-Toth, A.; Dryhurst, G. J. Electroanal. Chem. 1981, 122, 205.

48. Dryhurst, G.; Niki, K. "Redox Chemistry and Interfacial Behavior of Biological Molecules"; Plenum Press: New York, 1988.

49. Hawley, M.D.; Tatawawadi, S.V.; Piekarski, S.; Adams, R.N. J. Am. Chem. Soc. 1967, 89, 447.

50. Adams, R.N. Anal. Chem. 1976, 48, 1126A.

51. McCreery, R.L. J. Pharm. Sci. 1977, 66, 357.

52. Neptune, M.; McCreery, R.L. J. Org. Chem. 1978, 43, 5006.

53. Sackett, P.H.; McCreery, R.L. J. Med. Chem. 1979, 22, 1447.

54. Cheng, H.Y.; Sackett, P.H.; NcCreery, R.L. J. Med. Chem. 1978, 21, 948.

55. Kissinger, P.T.; Heineman, W.R. "Laboratory Techniques in Electroanalyticl Chemistry"; Marcell Dekker, Inc.: New York, 1984.

56. Adams, R.L. "Electrochemistry at Solid Electrodes"; Marcell Dekker, Inc.: New York, 1969.

57. Panzer, R.E.; Elving, P.J. J. Electrochem. Soc. 1972, 119, 864.

58. Lehninger, A.L. "Biochemistry"; Worth Publisher, Inc.: New York, 1975.

59. Stanbury, J.B.; Wyngaarden, J.B.; Fredrickson, D.S. "The Metabolic Basis of Inherited Disease"; McGraw-Hill: New York, 1972.

60. Owens, J.L.; Marsh, H.A.; Dryhurst, G. J. Electroanal. Chem. 1978, 91, 231.

61. Bentley, R.; Neuberger, A. Biochem. J. 1952, 52, 694.

62. Wrona, M.Z.; Dryhurst, G. Biochim. Biophys. Acta 1979, 570, 371.

63. Dryhurst, G.; Elving, P.J. J. Electrochem. Soc. 1968, 115, 1014.

64. Goyal, R.N.; Dryhurst, G. J. Electroanal. Chem. 1982, 135, 75.

65. Dryhurst, G. J. Electrochem. Soc. 1969, 116, 1097.

66. Hansen, B.H.; Dryhurst, G. J. Electroanal. Chem. 1971, 32, 405.

67. Conway, A.C.; Goyal, R.N.; Dryhurst, G. J. Electroanal. Chem. 1981, 123, 243.

68. Hansen, B.H.; Dryhurst, G. J. Electroanal. Chem. 1971, 30, 417.

69. Elion, G.B.; Callahan, S.; Rundles, R.W. Cancer Res. 1963, 23, 1207.

70. Bergmann, F.; Levene, L. Biochim. Biophys. Acta 1976, 429, 672.

71. Goth, A. "Medical Pharmacology"; C.V. Mosby Co.: St. Louis, 1976.

72. Hyslop, R.M.; Jardine, I. J. Pharmacol. Exp. Ther. 1981, 218, 621.

73. Abraham, R.T.; Benson, L.M.; Jardine, I. J. Pharmacol. Exp. Ther. 1985, 234, 670.

74. Abraham, R.T.; Benson, L.M.; Jardine, I. J. Med. Chem. 1983, 26, 1523.

75. Jemmens, V.J.; Moore, D.E. J. Chem. Soc. Perkin Trans. II 1984, 209.

76. Patai, S. "The Chemistry of the Thiol Group", Part 2; John Wiley & Sons: New York, 1974.

77. Rudewicz, P.; Straub, K.M. Anal. Chem. 1986, 58, 2928.

78. Perchalski, R.J.; Yost, R.A.; Wilder, B.J. Anal. Chem. 1982, 54, 1466.

79. Dryhurst, G. Bioelectrochem. and Bioenerg. 1985, 14, 251.

80. Blakley, C.R.; Vestal, M.L. Anal. Chem. 1983, 55, 750.

81. Linberg, C.; Paulson, J. J. Chromatogr. 1987, 394, 117.

82. Voyksner, R.D.; Haney, C.A. Anal. Chem. 1985, 57, 991.

83. Pine, S.H.; Hendrickson, J.B.; Gram, D.J.; Hammond, G.S. "Organic Chemistry", 4th Ed.; McGraw-Hill: New York, 1980.

84. Swelim, A.; Khodair, I.A.; El-Sheikh, F. Int. J. Sulfur Chem. B 1971, 6, 195.

85. Pryor, W.A. "Mechanisms of Sulfur Reactions"; McGraw-Hill Book Co.: New York, 1962.

86. Belal, F.; Anderson, J.L. Analyst(London) 1985, 110, 1493.

87. Allison, L.A.; Shoup, R.E. Anal. Chem. 1983, 55, 8.

88. Johnson, D.C.; Weber, S.G.; Bond, A.M.; Wightman, R.M.; Shoup, R.E.; Krull, I.S. Anal. Chim. Acta 1986, 180, 187.

89. Doerr, I.L.; Wempen, I.; Clarke, D.A.; Fox, J.J. J. Org. Chem. 1961, 26, 3401.

90. Davis, F.A.; Billmers, R.L. J. Am. Chem. Soc. 1981, 103, 7016.

91. Davis, F.A.; Jenkins, R.H.; Rizvi, S.Q.; Yocklovich, S.G. J. Org. Chem. 1981, 46, 3467.

92. Marsh, H.A.; Dryhurst, G. J. Electroanal. Chem. 1979, 95, 81.

93. Wrona, M.Z.; Owens, J.L.; Dryhurst, G. J. Electroanal. Chem. 1979, 105, 295.

BIOGRAPHICAL SKETCH

Kevin John Volk was born in Chicago, Illinois, on September 1, 1962. Kevin lived in a pleasant, west suburb of Chicago called Westchester until the age of 15. The Volk family moved to Orlando, Florida, in 1978. He graduated from Lake Brantley High School in 1980.

In the fall of 1980, Kevin enrolled at the University of Central Florida (UCF) in Orlando. He spent two summers performing undergraduate research under the direction of Dr. Michael Hampton. In the fall of 1981, he joined the University of Central Florida Karate Club and for the next year served as vice-president of the organization. While at UCF, he developed a strong interest in analytical chemistry and earned a Bachelor of Science degree in 1985.

In August 1985, Kevin began his graduate work in analytical chemistry under the direction of Dr. Richard A. Yost and Dr. Anna Brajter-Toth. On July 19, 1986, Kevin married Linda Sagues, whom he had met while attending UCF. In 1988, he received a graduate fellowship from Merck Sharp & Dohme. Upon completion of his graduate studies, he will begin work at CIBA-GEIGY in Ardsley, New York.

I certify that I have read this study and that in my opinion it conforms to acceptable standards of scholarly presentation and is fully adequate, in scope and quality, as a dissertation for the degree of Doctor of Philosophy.

Richard A. Yost, Chairman
Associate Professor of Chemistry

I certify that I have read this study and that in my opinion it conforms to acceptable standards of scholarly presentation and is fully adequate, in scope and quality, as a dissertation for the degree of Doctor of Philosophy.

Anna Brajter-Toth
Associate Professor of Chemistry

I certify that I have read this study and that in my opinion it conforms to acceptable standards of scholarly presentation and is fully adequate, in scope and quality, as a dissertation for the degree of Doctor of Philosophy.

James D. Winefordner
Graduate Research Professor of Chemistry

I certify that I have read this study and that in my opinion it conforms to acceptable standards of scholarly presentation and is fully adequate, in scope and quality, as a dissertation for the degree of Doctor of Philosophy.

James A. Deyrup
Professor of Chemistry

I certify that I have read this study and that in my opinion it conforms to acceptable standards of scholarly presentation and is fully adequate, in scope and quality, as a dissertation for the degree of Doctor of Philosophy.

Raymond J. Bergeron

Raymond Bergeron
Professor of Medicinal Chemistry

This dissertation was submitted to the Graduate Faculty of the Department of Chemistry in the College of Liberal Arts and Sciences and to the Graduate School and was accepted as partial fulfillment of the requirements for the degree of Doctor of Philosophy.

August 1989

Dean, Graduate School